Sensory Integration Model Inspired by the Superior Colliculus For Multimodal Stimuli Localization

Kiran Kumar Ravulakollu

University of Sunderland

A thesis submitted in partial fulfillment of the requirements of the University of Sunderland for the degree of Doctor of Philosophy

October 2012

Faculty of Applied Sciences
Department of Computing, Engineering and Technology
University of Sunderland
Sunderland
United Kingdom

Acknowledgements

I would like to acknowledge a number of people, who provided me moral and physical motivation along with support in successful completion of the thesis.

First, I would like to thank my primary director of studies Prof. Stefan Wermter who has provided a constant guidance and support during the research and development of this project. Stefan is very helpful in shaping the idea into a research area and constantly monitored the progress through-out the process. His initiation for publications assisted to realize their importance for a bright start.

My supervisor late Dr. Harry Erwin had been an immense treasure for biological inspiration in this project. His clarifications and discussions had given an insight in the area which later helped in modeling the project. I would like to convey my deep regards for his support during the research and development of the project.

I would like to thank my director of studies Dr. Kevin Burn for giving me the opportunity to continue under his supervision during the writing-up state. His motivation and constant encouragement has extended my confidence in successful completion of this research project.

I would also like to thank a number of fellow researchers in the group in particular Dr. Jindong Liu, Dr. Michael Knowles, Mr. Simon Farrand and Dr. Chi-Yung Yan who has shared their experience on several areas that let me able to find insights at conceptual level and execute the motivation behind the approach.

I would like to thank my brother Dr. Ravi Shankar Ravulakollu for his moral and financial support and also for believing in me without which I wouldn't have fulfilled my dream. I also take the opportunity to thank my family, for their undivided patience and understanding. I feel deeply sorry to them since my research has always proceeded over their requirements. Hereafter, my contributions to family will be equal to my career.

Finally, I would like to acknowledge the continued support of my friends. In particular, I thank Dhinesh Gollapudi, Kiran Kumar Vangara and Bharath Kumar Musunuru who have believed in me and gave necessary motivation along with constant support during the times necessary. Their sponsorship at times needed for my publication is much appreciated. I also thank all my near and dear friends who supported me directly or indirectly for everything during the research and development.

Abstract

Sensory information processing is an important feature of robotic agents that must interact with humans or the environment. For example, numerous attempts have been made to develop robots that have the capability of performing interactive communication. In most cases, individual sensory information is processed and based on this, an output action is performed. In many robotic applications, visual and audio sensors are used to emulate human-like communication. The Superior Colliculus, located in the mid-brain region of the nervous system, carries out similar functionality of audio and visual stimuli integration in both humans and animals.

In recent years numerous researchers have attempted integration of sensory information using biological inspiration. A common focus lies in generating a single output state (i.e. a multimodal output) that can localize the source of the audio and visual stimuli. This research addresses the problem and attempts to find an effective solution by investigating various computational and biological mechanisms involved in the generation of multimodal output. A primary goal is to develop a biologically inspired computational architecture using artificial neural networks. The advantage of this approach is that it mimics the behaviour of the Superior Colliculus, which has the potential of enabling more effective human-like communication with robotic agents.

The thesis describes the design and development of the architecture, which is constructed from artificial neural networks using radial basis functions. The primary inspiration for the architecture came from emulating the function top and deep layers of the Superior Colliculus, due to their visual and audio stimuli localization mechanisms, respectively. The integration experimental results have successfully demonstrated the key issues, including low-level multimodal stimuli localization, dimensionality reduction of audio and visual input-space without affecting stimuli strength, and stimuli localization with enhancement and depression phenomena. Comparisons have been made between computational and neural network based methods, and unimodal verses multimodal integrated outputs in order to determine the effectiveness of the approach.

List of Contents

Glossary

AANN	:	Auto Associative Neural Network
AI	:	Artificial Intelligence
ANN	:	Artificial Neural Network
BN	:	Bayesian Network
CANN	:	Compounded Artificial Neural Network
DImg	:	Difference Image
DSP	:	Digital Signal Processing
EA	:	Evolutionary Algorithms
GCC	:	Generalized Cross Correlation
HSFr	:	Horizontal Scale Frame
IC	:	Inferior Colliculus
ILD	:	Interaural Level Difference
ITD	:	Interaural Time Difference
LED	:	Light Emitting Diode
SC	:	Superior Colliculus
RGB	:	Red-Green-Blue
TDNN	:	Time Delay Neural Network
TDOA	:	Time Difference On Arrival
TOA	:	Time Of Arrival

List of Tables

List of Figures

List of Equations

Chapter 1

Introduction

1.1. Overview

The human brain performs numerous stimuli-based information-processing operations in order to enable a person to interact with the environment. Of these, sensory information processing is a significant task. Each part of the brain has its own vital activities such as sensing or response, or both in certain cases. As a result many researchers are involved in decoding brain processing states, which controls and co-ordinates human interaction with the environment.

This research attempts to develop an understanding of the co-ordination involved in sensing the visual and audio stimuli that provide a mutual and controlled motor response to those stimuli. In particular, the Superior Colliculus, located in the mid-brain of the human nervous system, is one such location which performs multimodal information processing. This thesis aims to develop an integration model inspired by the Superior Colliculus, so that audio and visual stimuli can be integrated to provide an efficient and controlled motor response.

1.2. Motivation

Humans and animals can effectively localize any visual or audio stimuli generated within range. This is a key feature for interaction, either with the environment, or with other humans or animals as stated in Appendix-A. There are several potential applications of intelligent robotics involving human-robot interaction where it would be desirable to have this feature. For example, in situations where a robot must respond to human instructions (such as “ASIMO” in a ‘tour guide’ robotic

application (Koide, 2004)), the simultaneous, rather than sequential, arrival of stimuli for both audio and visual information often takes place where significant noise is present (the so-called 'cocktail party' effect (Elhilali, 2006)).

The equivalent human or animal response in such scenarios is effective and spontaneous. If a robotic agent is able to provide a similar response by attending to an individual requesting attention, it has the potential of making the interaction more human-like. One way of providing such efficiency would be by mimicking the biological processes carried out for integration. The Superior Colliculus (SC) region of the brain is responsible for providing audio-visual integration, as well as response generation. Hence, a computational architecture inspired by the SC has the potential to provide an effective platform for generating similar behaviour.

In terms of development, the use of 'sensor fusion' methods such as the Kalman filter will provide an effective engineering-based integrated output according to the given inputs. However, an engineering or computational approach will provide the solution only for the defined platform. When it comes to using such engineering-based agents, any irregularities in the defined input data set will not be addressed. To eliminate this, a platform independent approach is proposed. The aim is to develop an effective multisensory integration model inspired by the SC using a neural network platform, so that the simultaneous arrival of audio and visual stimuli will result in the effective localization of the source.

1.3. Research Question

Is it possible to create a computational architecture inspired by the Superior Colliculus of the mid-brain, using artificial neural networks, which enables the efficient integration of audio and visual stimuli arriving simultaneously at an agent, in order to localize the source of the stimuli?

1.4. Aim and Objectives

The project aim is to design and develop an architecture for multisensory integration that is inspired by the functionalities of the SC when processing audio and visual information.

The specific objectives are:

1. To understand the biological way of multimodal functionalities of the SC.
2. To review the literature on modelling the SC.
3. To review different approaches to audio and visual extraction and integration.
4. To examine neural network approaches to integration.
5. To develop and design an architecture suitable for multimodal integration for a robotic platform.
6. To test and evaluate the performance of the architecture.

1.5. Research Contribution

The main contribution lies in the reduction of dimensional space (audio and visual) to an integrated single space by using neural networks for processing stimuli integration mechanisms. The novelty lies in the form of the architecture and its ability to handle low intensity stimuli and generate an efficient and accurate integrated output, even in the presence of low audio and visual signals.

1.6. Thesis Structure

The remainder of this thesis is organized as follows:

Chapter 2 is an overview of the SC and multimodality. Following a brief introduction to the SC from a biological perspective, stimulus processing in the SC is studied. How the SC exhibits multimodal behaviour is detailed in relation to stimuli processing and motor response. A review of existing literature in

understanding multimodal behaviour in different contexts is provided. Along with a theoretical analysis, computational implementation aspects of the SC are also discussed in order to identify the feasibility of considering multimodal behaviour.

Chapter 3 details the methodology of the research carried out. It describes two different types of stimuli processing: unimodal and multimodal for audio and visual stimuli, along with a design strategy towards implementation. Starting with a briefing on existing literature concerning available design aspects of multimodal integration mechanisms, the architecture is proposed in order to generate a unique model that can perform integration of audio and visual stimuli. The architecture is based on a defined design strategy, which identifies the stimuli localization aspects. The importance of the learning mechanism and its use in the integration model is also discussed.

Chapter 4 deals with the implementation of the model. Starting with the reasons behind developing a neural network platform, various issues that are significant when building a neural network with learning criteria and its implementation, including the advantages, are discussed. Along with theoretical aspects of the audio and visual integration model, the practical and implementation constraints, along with the biological inspiration for the model are also discussed.

Chapter 5 describes experimental work carried out with the model. It starts with the motivation behind the experimental setup and environment along with data collection of both unimodal and multimodal sensory audio and visual stimuli. This includes data set analysis, preparation of data sets and stability of the integrated outcome. Later the data sets are used to train the integration network, followed by verification with the test data.

Chapter 6 presents a detailed analysis of the experimental results. It includes a critical analysis of training and testing, and unimodal and integration results are compared. A detailed performance evaluation is also undertaken.

Chapter 7 details the main conclusions resulting from the work, in the context of the research hypothesis and initial objectives. There is also a discussion of suggested future work.

Chapter 2

Literature Review

2.1. Introduction

Throughout the history of technology, there has been a constant transformation of biological inspirations to sustain modern requirements. This research of sensory stimuli processing, concerned with audio and visual information, has been inspired by information processing within the human nervous system, including the brain. When it comes to receiving visual and audio stimuli, the eyes and ears are the most widely used primary sensory organs. In this chapter, research into understanding the biological way of processing visual and audio stimuli in the human brain is described in the form of a detailed literature review on existing work of various researchers active in this area. The emphasis is on the region of the brain called the Superior Colliculus (SC). Also discussed is the feasibility of a conceptual transformation of the SC into a computational method.

2.2. Biological Overview of the Superior Colliculus

In this section, a motivation was provided detailing the need for biological inspiration. During the process, the purpose for the SC was identified by answering several questions raised during the research. Later an investigation into the SC based on neuro-science aspects is detailed.

2.2.1. The Biological Motivation:

An early motivation behind the research was to investigate ways to integrate sensory stimuli such that the outcome or resultant could be in the form of a combined response. Questions that arose include:

- What is the need to have a combined response for sensory stimuli?
- How is the combined response different from the individual responses?
- How can this combined response be more useful than the individual responses?

During research into autonomous intelligent robotics and industrial robots, there is always a requirement for sensors to acquire data from the environment as the robot performs its task. Every sensor is designed for its own specific purpose of information receiving and transmitting to a designated receiver. Later, using this response, the agent will perform the desired operation like movement etc. However in certain cases, the final action from the agent may not only depend on the response of a single sensor, but on the response of a group of sensors. For example, the control of an autonomous-guided robotic vehicle may require:

- visual information from both the front and side views;
- balancing the vehicle at the desired speed;
- noise from a rear or side vehicle to be recognized and localized;

In the above-mentioned scenario, use of a visual sensor and audio sensor, and balancing with gyro information, will be necessary to handle the acceleration and braking of the vehicle effectively. In such a case rather than a centralized network, a distributed network with individual processing units for dedicated functionalities will reduce overload of the network. During such circumstances sensory stimuli integration prior to the intended action is always an advantage when it comes to performance and accuracy of the system. Hence there is an advantage of integrating the sensory stimuli to reduce the processing time and time of response. Since the research is concerned with audio and visual stimuli, a small region of the human brain that performs a similar mechanism is of direct interest and relevance.

When it comes to audio and visual information, there are two different kinds of response that are observed while studying the stimuli response mechanisms. Study of these mechanisms is essential as they represent the efficiency of the integration. They are:

- Voluntary response.
- Involuntary response.

In the human brain, involuntary responses are sudden and unplanned, and are frequently observed during action-response mechanisms. However the Superior Colliculus is one region of the human brain that is responsible for generating voluntary responses in terms of eye movements called *saccades* as an extension to head movements. In order to have a clear understanding of saccades, it is important to have a detailed and clear knowledge of the SC and its working mechanism.

2.2.2. Neuroscience aspects of the Superior Colliculus

The SC forms the rostral bumps located on either side of the dorsal aspects of the mid brain of the human as shown in figure 2.1. This forms a part of the roof of the midbrain. Unlike the Inferior Colliculus, which is audio centred, the SC is vision centred, with a reflexive mechanism as its central functionality.

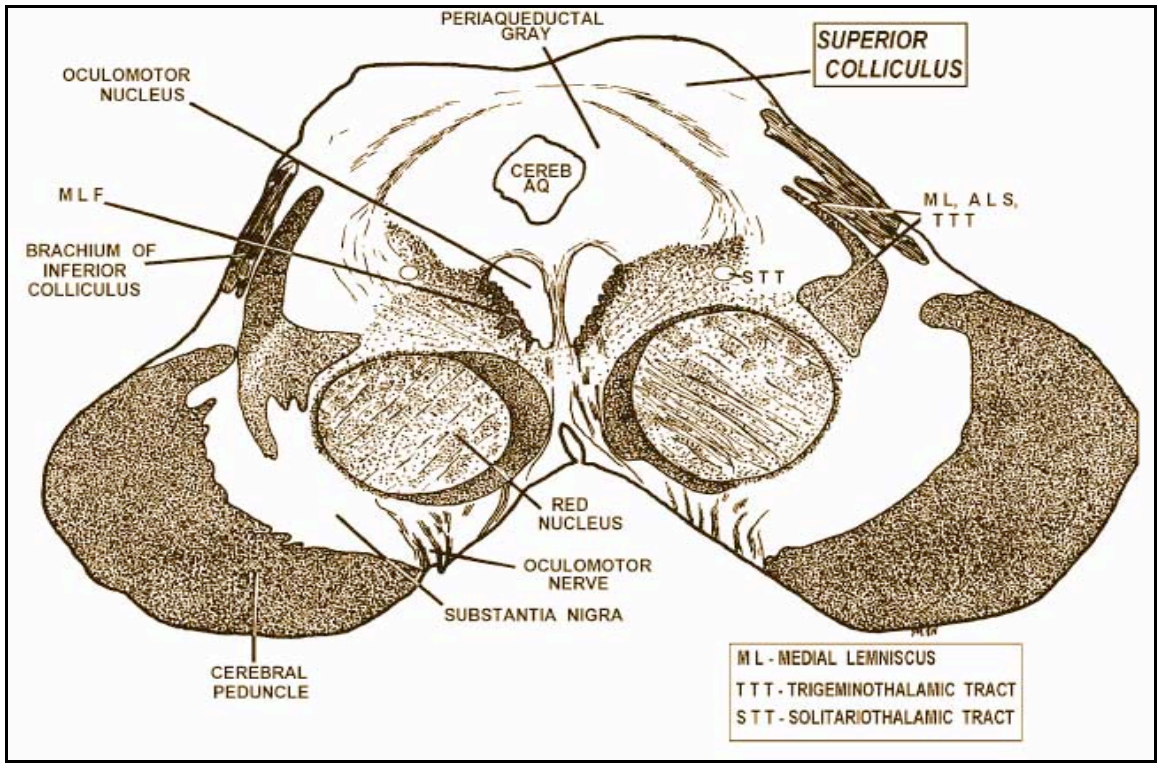

Figure 2.1 ***Superior Colliculus region in the mid-brain:*** *Superior Colliculus located in the mid-brain region of the human brain. Image Courtesy of Medical Neurosciences 731*

The SC is a layered structure containing I-VII layers that can gather information from visual organs and extend to other layers, which can generate responses to perform centre activities such as saccade (section 2.3, page 10) generation (Juan, 2008) is shown in figure 2.2.

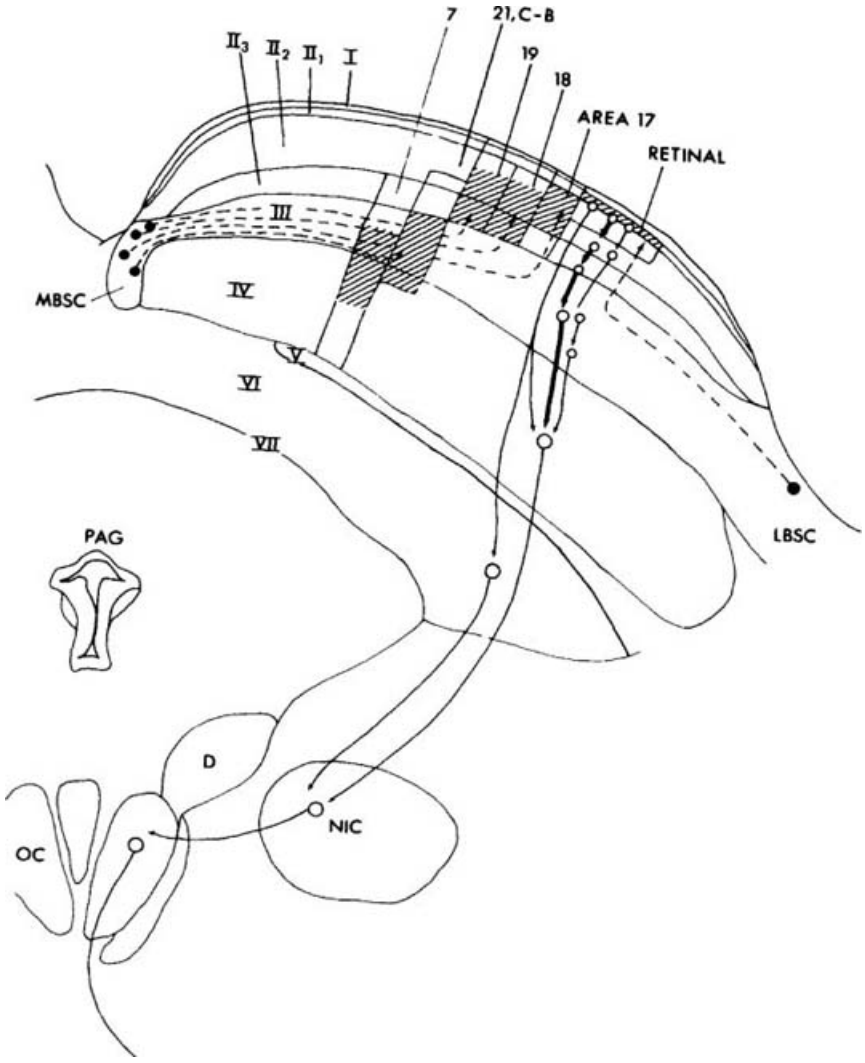

Figure 2.2: ***Schematic drawing of cat superior colliculus showing possible neuronal linkages in visuomotor transform:*** *Thick arrows, major path; boxes outline representative slices of terminal fields from optic (retinal) tract and corticotectal tracts from areas 17, 18, 19, 21, C-B, and 7; shaded areas, major foci of degeneration after lesions to these areas. MBSC, medial brachium of superior colliculus; LBSC, lateral brachium of superior colliculus; NIC, interstitial nucleus of Cajal and adjacent reticular formation; C-B, Clare-Bishop area; D, nucleus of*

Darkshevitch; OC, oculomotor nuclei; PAG, periaquiductal gray matter. Roman numerals represent the seven-collicular laminae (layers) of the Superior Colliculus signifying the arrangement inside the superior colliculus. (Source: From Ingle and Sprague 123.)

The neuro-science interpretation of the SC is that the top, or superficial, layers are in direct contact with the optical tract, as shown in figure 2.3. Through this tract visual information is transmitted into the SC from the eyes. This visual information is received through the retina and visual cortex regions of the human eye. Due to this direct contact, the SC is the primary receiver of visual stimuli. This means that the SC is involved in the generation of involuntary or reflexive responses that are caused by visual stimuli. However, since the deep layers are in contact with the Inferior Colliculus (IC) (audio processing unit) and Somatosensory system (sense of touch), the SC responds to visual, audio and somatosensory stimuli.

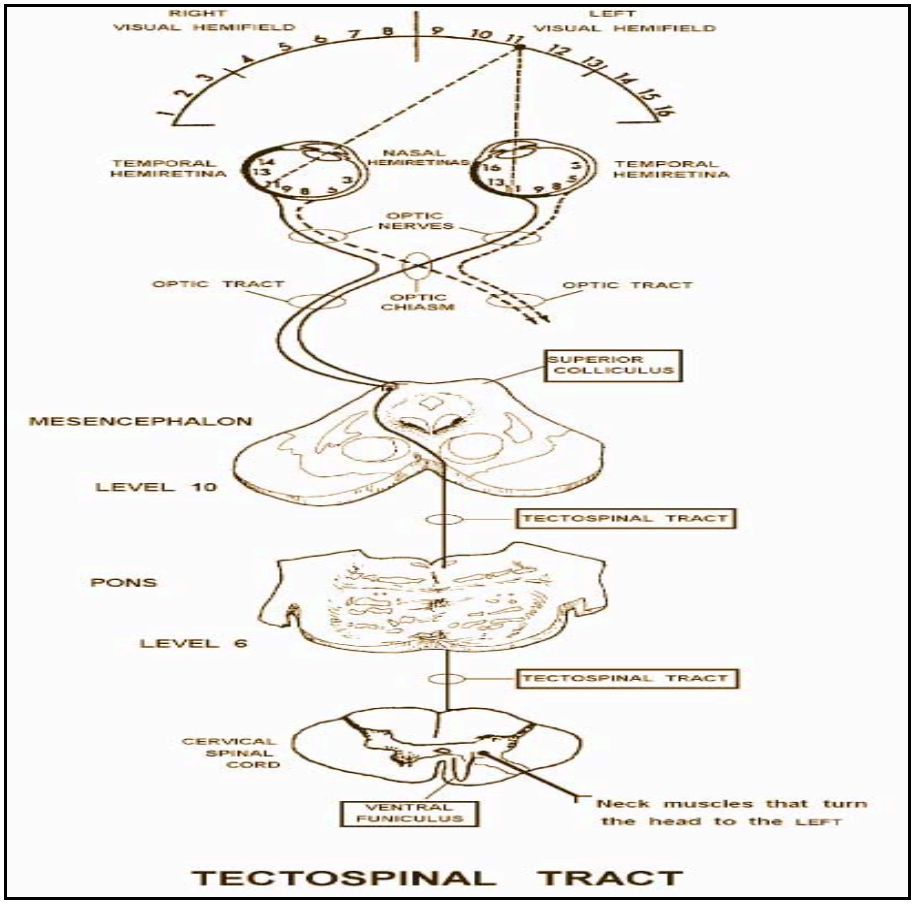

Figure 2.3 ***Control flow of the Superior Colliculus connectivity:*** *Control flow diagram representing an internal connectivity of superior colliculus towards receiving visual stimuli directly*

from optic tract along with an extension towards spinal cord for motor action. Image Courtesy by Medical Neurosciences 731

Therefore, the SC cannot be considered as a vision-only centred processing unit. This is due to its intermediate and deep layers, which are in contact with many other stimuli processors and sensory modalities, together with motor response units. For this reason the SC can receive sensory stimuli from various regions of the brain and can also receive and transmit motor responses. Hence it is sensitive to audio, visual and somatosensory (touch) stimuli. If the strategic alignment of layers and their influence on the stimuli is considered, it is understood that the deep layers play a major role in the motor response generated by the SC. However this influence is not completely exclusive. The SC extends towards the spinal cord through tectospinal tracts. Due to this extension, the SC is able to co-ordinate reflexive movements such as eye and head movements.

A neuroscience study of the SC reveals that the localization of audio and visual stimuli is carried out in the mid-brain region of the nervous system. As established earlier, the SC actions can be both voluntary and involuntary. However, voluntary actions are usually influenced by other regions of the brain such as the cerebellum and amygdale. Information from all these regions is used at SC to perform a voluntary saccade. However, involuntary saccades corresponding to audio and visual stimuli are mainly based on SC localization.

Usually the auditory cortex region encodes auditory cues such as the time difference and level difference. These operations are performed in the Medial Superior Olive (MSO) region. However, higher order regions such as the SC, Inferior Colliculus (IC), and Planum Temporale (PT) are also capable of encoding such cues. The SC is the primary region of the human brain that responds to auditory and visual stimuli by generating a motor response to perform saccadic movement or subsequent head movement. On average, when it comes to efficiency of auditory localization, mammals can achieve an accuracy of $\pm 1^0$ in the horizontal axis and $\pm 4\text{-}5^0$ in the vertical axis (Hawkins, 1996).

2.3. Multimodal Behaviour of the Superior Colliculus

It is evident that the SC has the capability to receive audio, visual and somatosensory stimuli from various regions of the human brain. Neural activation experiments conducted by Stein and Meredith confirmed that the SC can generate responses for both audio and visual stimuli (King, 2004). The responses for such stimuli can be observed in terms of eye or head movements due to their connectivity with the spinal cord. Multimodal behaviour allows both animals and humans to perform effectively under noisy or multiple stimuli conditions.

This behaviour need not always be associated with multi-modal stimuli. Sometimes stimuli arriving from different sources can also be handled by the SC. The visual stimuli transmitted through magnocellular and parvocellular retinal ganglion cells unite at various levels of the SC. These signals have the feature of multiple and parallel streams of information preservation. With such a capability, these signals are analyzed for various aspects of the visual environment individually (Waxman, 2009). Similarly the optic tract axons terminate in a highly synaptic space that can help in generating a map-like environment. The axons of ganglion cells along with optic tract extend to the SC, forming a retinotopic map. Due to an extension of the SC through the spinal cord via tectospinal tracts, the retinotopic map is used for stimuli localization with the help of eye, neck and head movements. These movements represent both involuntary and voluntary movements generated by the SC.

Rapid movements of the eyes on a horizontal axis are often termed ‘saccadic movements’. Though their purpose is to rapidly fix the vision on a target, the type of fixation can be of various types. Saccadic movements can be commanded (general), fixation (on a target) and reflexive (involuntary). Reflexive movements are usually observed following the appearance of an object in the visual field of the eye, or any disturbance in the audio field of the ear. However, rather than the SC acting alone, the cerebellum also plays a vital role in the generation of fixation saccades. In either of these cases stimuli are localized using the above criteria by moving the eyes or head towards the direction of the source. Since saccades are

pursuit in their behaviour, they can stabilize the foveae of the eye continuously and clearly even on a moving object.

From the above observations, it is evident that the SC performs sensory stimuli integration for generating saccadic movements. Stimuli can refer to a single stimulus of audio or visual, multiple visual stimuli, multiple audio stimuli and audio and visual stimuli together. The need for integration occurs when there is a simultaneous arrival of more than one audio and visual stimulus at the SC. Unimodal stimuli integration then takes place in the SC to identify an effective response. However when it comes to the simultaneous arrival of audio stimuli, due to interference effects, stimuli with similar audio properties will be interpreted as noise unless at least one of the stimuli has a unique property such as frequency or amplitude.

Many techniques are designed to handle the so-called ‘cocktail party effect’. However when it comes to a classroom situation, for example, where students use low voice levels when generating audio stimuli, integration is a difficult task due to the recognition problem. This is not only with audio but also visual stimuli. Hence the strength of stimuli is one such property that can affect the SC response.

There is an argument that the SC considers the priority of visual stimuli due to its direct contact with the eyes through the optic tract, but this is only when stimuli of different strengths arrive at different time intervals. If a human subject is seated on a swivel chair and rotated for some time, when the chair comes to a halt a visual stimulus received is overridden by any audio stimulus that arrives at the ear. In this particular case, initially the visual stimulus was overridden by the audio one. A later audio stimulus is also not effective when it comes to the integration process, due to the unstable state of receiving stations (eyes and ears). This signifies that for SC both the stimuli are equally prioritized when it comes to integration.

In the following figure 2.4, integration process can be classified based on the input

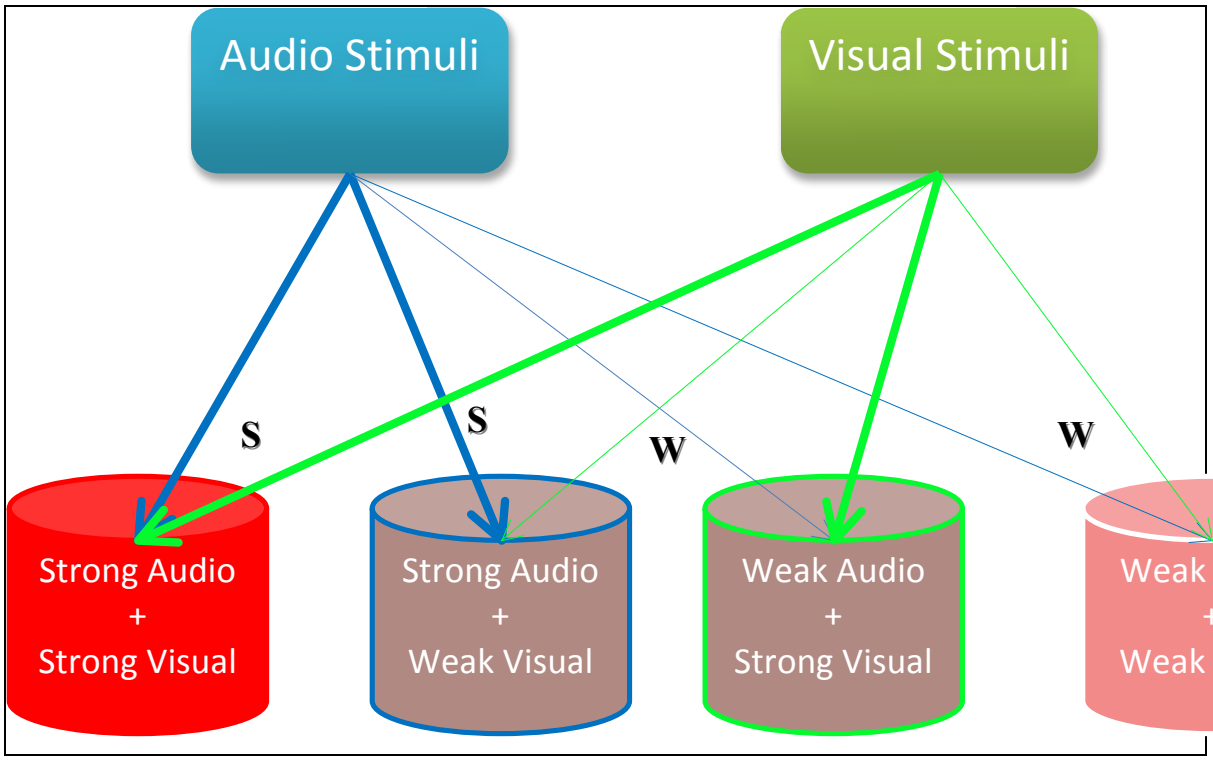

Figure 2.4 ***Stimuli combinations for integration:*** *Diagrammatic representation of various combinations formed with the weak and strong stimulus of audio and visual stimuli that are possible when integrating them.*

stimuli strength. The time of stimuli arrival, along with the strength of the stimuli, are the two major factors that influence the integration process. In figure 2.4, 'W' represents the weak stimuli and 'S' represents the strong stimuli of corresponding visual and audio stimuli. The representation shown illustrates the possible stimulus combinations that can emerge during the process of integration.

When it comes to the outcome of these combinations, a weak combination need not always have to produce a weak response; similarly with a strong combination. Following the neural response experiments conducted on the SC of cats by Stein and Meredith (Meredith, 1986a), two different phenomena are proposed in understanding the integration process with stimuli strength:

- Enhancement
- Depression

These two phenomena can be observed in most of the combinations of the weak and strong stimuli. However, from the stimuli classification obtained from figure 2.4,

the occurrence of these phenomena can be understood. The phenomena of depression and enhancement are mainly based on the distance between stimuli along with their strength, irrespective of the type of stimulus. In the case of a weak and strong combination, a winner-takes-all criterion usually applies. This can be categorised under enhancement. During the combination of two strong and relatively close stimuli, there will be an enhancement of the integrated output rather than either of the individual ones. Similarly during the combination of two weak stimuli relatively closer in terms of stimuli intensity, there will be an enhancement in the integrated output rather than either or both of them.

On the other hand, depression is the phenomenon where the system is left in a state of confusion in determining the angle for localization. During the combination of two strong stimuli, which are far away from one another, the integrated output generated will be more depressed, than either stimulus. Hence the outcome will be in the same state as before, which is empty. Similarly during the combination of two weak stimuli relatively far from one another, although the inputs are detected, the integrated output will be strongly depressed. This results in no output being generated.

2.4. Literature on Multisensory Integration

This section reviews neuroscience research based on a similar criterion of exploring the multisensory behaviour of the SC. It is carried out in the context of this thesis and how useful it is to support the research hypothesis, and hence the design and development of the computational model.

Stanford evaluates the neuroscience view of the computations carried out by neurons of the SC for multimodal integration of sensor stimuli (Stanford, 2005). Neuron responses are not considered as “high” or “low”, but are ‘super additive’, ‘additive’ and ‘sub additive’. These responses can be used to explain the maximum responses that the SC can produce in modality-specific cases. Modality-specific study provides an opportunity to observe the computations that take place in cases of low response and high response. This research provides a platform for

explaining the enhancement of integrated output for audio and visual integration in the SC.

According to Beauchamp, biological evidence exists for multimodal integration that takes place for audio and visual information in the deep layers of the human brain system (Beauchamp, 2004). The author describes the integration with a focus on behavioural tasks and their influence in different aspects that are encountered during the process. However, it is not clearly stated that how the decision is made in determining the final outcome of the integration in terms of audio and visual input information.

Gilbert demonstrates how spatial information about the source of a stimulus is available at the receptor surface for visual and audio sensory systems (Gilbert, 2008). To support this, a pit viper example is considered where integration takes place between visual information and mechanoreceptor information. Mechanoreceptors (available both on skin and hair) are the sensory detectors that can determine the change in air pressure or vibration. They are also sensitive towards odours. For instance, pit vipers use infrared information from pit organs along with visual information, which then travel together for summation of inputs in two modalities. Since the odour detected by the mechanoreceptors is not sufficient to determine the direction of the source, visual cues are used in the integration process to localize pray. Variation in the integration also occurs when the angular velocity of the prey is recognised along with the change in the intensity of smell in the air of the source. At this point, when the source is recognised, a high body saccade is noticed. The visual field of the animal, with the source viewed in same field, has a strong influence in the body saccades.

2.5. Literature Review on Integration of Audio and Visual Data

This section reviews literature describing various modelling techniques for performing audio and visual integration. In the following all such literature is provided with a classification based on the implementation technique used. Different researchers implement the concept of multimodal integration on various

platforms based on their requirements. Through this literature review these techniques are analysed so that the observations can be used during the design and development of the integration network.

2.5.1. Probabilistic Approach

Anastasio proposed an integration model based on the assumption that “SC neurons that show inverse effectiveness, compute the probability of the target present for moving the saccades” (Anastasio, 2000). The principle of inverse effectiveness is stated as an increase in the strength of multisensory integration in response to the decrease of individual sensory stimuli (Holmes, 2009). The proposed model for multisensory integration provides an explanation for the inverse effectiveness phenomenon. When it comes to spontaneous bimodal probabilities, the model has produced non-conclusive evidence for inverse effectiveness. The authors try to show that SC neurons use probabilities for the localization of stimuli sources. Figure 2.5 is a diagrammatic representation of the integration model discussed. In the figure, probability ‘p’ is the chances of occurring audio and visual given both the stimuli arrive at the Superior Colliculus. When designing a multimodal integration model of the SC, Bayes’ probability concepts may be useful when working on the enhancement of output stimuli, but the authors have not given a reason for the behaviour, or why only inverse effectiveness is considered when determining the enhancement, which may be due to the contradictory effect shown in a small number of neurons.

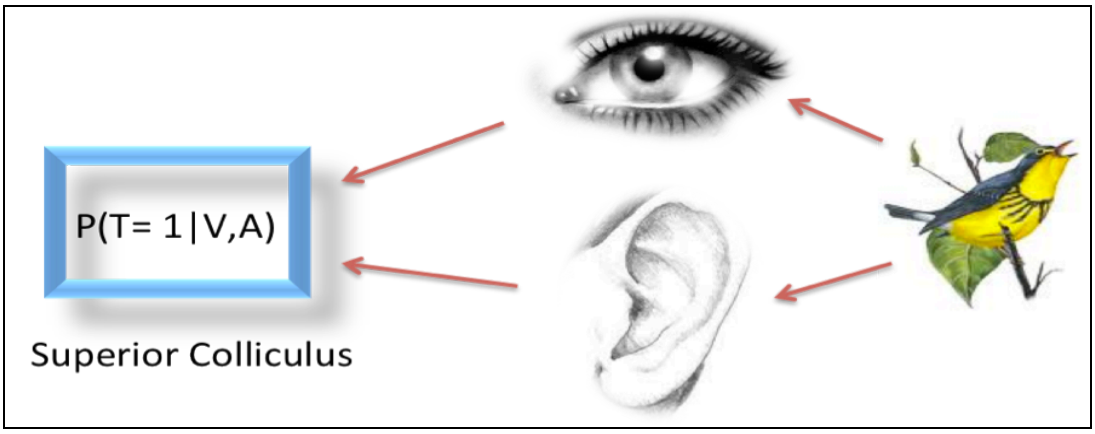

Figure 2.5 ***Anastasio's model of the SC for multimodal integration of audio and visual stimuli*****:** *Pictorial Representation of Anastasio's Model of superior colliculus for multimodal integration of audio and visual stimuli. This image depicts the transmission of both audio and visual stimuli through their sensory aid to the SC. Here Anastasio's probabilistic model will perform integration.*

The tracking model developed by Wilhelm et al., uses vision and sonar-based components on account of their low cost for mass production (Wilhelm, 2004). A Gaussian distribution is used to model the skin colour for making it easy to identify the face in the visual sequence. For the detection of colour, automated colour calibration and a white balancing algorithm are used. Sonar sensors that cover 360 degrees in dual levels with a pre-processed mechanism are used for eliminating noise. Thus obtained sonar data is used in locating the face in the visual data.

Hence, the sensor fusion described in this report of Wilhelm uses a stochastic motion model with a Gaussian distribution. This system is able to track the localized face (image) even if there are people moving in the environment. Though the system is able to track the image, it is only based on its location. If the object is moving during localization then the proposed tracking is not suitable, as it keeps changing from frame to frame. However, it is well suited for a fixed source.

Xiaotao Zou and Bir Bhanu have described two different approaches for multimodal integration using audio and visual data. First, a Time Delay Neural Network (TDNN) extracts audio and video data at feature level separately and then fuses both data forms. Second, a Bayesian Network (BN) jointly models audio and video signals and tracks humans by Bayes inference. According to Stork, detection

of motion that handles sequential data during multimodal function is possible with the fusion of audio and visual data at feature level (Stork, 1992). Normalized cross-correlation for feature selection in the TDNN architecture is considered as being efficient for identifying the difference between successive images. A sound spectrogram is used to break down the sound into steps for audio inputs to the network (Zou, 2005).

Bayesian networks may be useful when processing graphical representations with probability models. This model can be enhanced to handle time series data using a Dynamic Bayesian Network. A statistical model, a Transformed Mixture of Gaussians, is used to model the frames. Assuming all the probabilities are Gaussian, audio data is generated using the time of arrival to the microphones. A static Bayesian Network (BN) is used to link the sequential audio and visual data involving the covariance matrix and parameter estimation with an expectation maximization algorithm based on the standard Bayes' rule. High accuracy and less training time are achieved in detecting the object in the BN (Zou, 2005).

Using a probabilistic approach Bennewitz has determined on which person attention is focused by the agent in multiple people conversations (Bennewitz, 2005). For that decision, this approach uses visual and speech input. In getting the information of a person in the visual path, the technique (feature extraction using the dark parts of the eyes and cheeks etc) is effective for images of considerable brightness. As the number of persons in the conversation increases, it becomes more difficult to detect the correct person. The speech information is processed with automata and state machines using lexical analysis, limited to only a few words or phrases. As the number of words or phrases increases, the slower the automaton machine becomes. This is due to the g*aze direction* technique, which helps to find the traces from the remaining input in the case of multiple stimuli. Hence this approach is potentially a good technique for multimodal scenarios. This paper is a good demonstration of human-robot interaction, especially in scenarios involving conversations, meetings and discussions in small groups.

For the development of a multimodal robot interaction system, a model for speech communication in human-robot interaction has been developed with the use of simple linguistics, irrespective of grammar, along with gestures and contextual scene knowledge (Huwel et al., 2006). A Hidden Markov Model is used for parsing the speech and a semantic parsing algorithm used for determining its meaning. The model focuses more on speech analysis and generating the action, depending on the semantic parsing. A system called “Control” is designed in such a way that the multimodal processing is done at this stage for all types of communications. The BIRON robotic system is used to verify the above-mentioned concepts in an experimental environment. It is not clearly explained how the multimodal understanding of speech and the contextual scene are combined. Also, this model shows that human robot understanding can be improved when speech is combined with contextual space and gestures.

2.5.2. Neural Network Approach

The model proposed by Trappenberg (1998) is mainly focused on a competitive neural network with spiking neurons of short range (excitatory) and long range (inhibitory) firing rates. Due to the lack of consideration of 4 types of neurons responsible for saccade generation in SC, the acquired results from the simulation are not close enough compared to the results that are observed from animal testing. This is due to consideration of only fixation and burst neurons. An average firing neuron network is more sensitive to further updates and modifications compared to a spiking neural network. If the same spiking network is trained using winner-takes-all (competitive) learning, its performance is improved, which further generates outputs that will have more chance of producing similar results to animal experiments done by Stein and Meredith (1993). A spiking neural network with all four neurons (fixation, burst, build up and excitatory) can form a more apt and realistic full functional model (Trappenberg, 1998) and (Kyriakos and Jurgen, 2007).

Quaia et al., (1999) provides a model for a saccadic system where the functionality of the SC is minimal compared to cerebellum circuitry (Quaia, 1999). According to

the authors, the role of the SC is only to provide the directional drive towards the target for the eyes. However it is up to the cerebellum to determine the appropriateness and accuracy of the directional drive. The burst, build up and fixation neurons available in the deep layers of the SC are used to determine the direction. The processing from the cerebellum is used to improve the directional drive, track the target, and end the saccade.

Two contrasting models for multimodality, with and without integration of human information processing, are evaluated in experiments conducted by Dominic W Massaro (2004). The paper shows that the Fuzzy Logic Model of Perception (FLMP) predictions are quite supportive for many experimental cases on BALDI, an embodied conversational agent. The Single Channel Model (SCM), which is a non-integration model, processes the stimuli in single channels only. A particular time scale is considered and information is processed through either visual or audio processing channels, but not both. The fusion of visual and audio information in FLMP does not follow any sort of pattern, which means it can be synchronous or asynchronous with the time frame. The fusion may be early or late. In either case integration will have an influential effect on the outcome. Another model is fusion at the feature-level or decision-level. The influence of these fusion models can have improvement on Embodied Conversational Agents (ECAs) than human machine interactions.

According to Wolf and Bugmann, Natural Language Processing is a slow process compared with Image Processing when considering long sentences, rather than just action words (Wolf and Bugmann, 2006). Hence the use of time scale for semantics determination is a suggestive idea when developing a multimodal system that can process the above inputs. The proposed constraint algorithm for multimodal input processing is effective for applications where the knowledge set is constrained, but the platform for implementation is not. When including time semantics, a network that can be sensitive towards minor changes in the input, along with quick processing and response generation, is required. Hence a platform like a neural network is effective as far as semantic mapping and timing is concerned. In the proposed future algorithm, the scope of the network can also be

extended to unconstrained environments, as linguistic processing is time consuming with the growth in sentences. This will contradict the time and mapping semantics of the algorithm.

Jolly et.al., propose a Compounded Artificial Neural Network (CANN) for making quick and more effective decisions in a dynamic environment like robot soccer (Jolly et al., 2006). The learning of the Artificial Neural Network (ANN) is carried out with an Evolutionary Algorithm (EA) with crossover and mutation, as well as back propagation techniques. However as the population grows, the performance of the EA decreases due to the increase in the decision space. ANN logical decisions are made according to the rule base. As the network grows, accuracy in prediction decreases. To eliminate it, the primary level (before the input layer) is added to generate the inputs from trained ANNs of ${}^{n}C_{2}$ combinations, where n is the number of robots in the team. This determines that for the successful generation of output at least 2 inputs are necessary. With this CANN model, however, the problem of space verses accuracy is not resolved, but comparatively high accuracy in decision-making with increase in population size is achieved. As the number of robots increases in a team, for example 10-11 players for soccer, the primary level is so huge that the inputs have to reach the main network with some delay, in which the final decision, though accurate, may not be appropriate due to the delay in processing. So in this case, expanding the team is limited.

Cuppini has provided a mathematics-based neural network model of multimodal integration in the SC along with an insight into possible mechanisms that underpin it, as shown in the figure 2.6. This model details the enhancement and depression phenomena, along with cross modality, similar modality and inverse effectiveness. Unimodal neuron activity characterized by non-linear phenomena is easy to study by considering quantitative mathematical tools such as probability. Gaussian functions are used for the spatial representation of neuronal and synapse activity. Using a Mexican hat function the strength of the activity is assigned to the corresponding activity function so that the activity of the final multimodal output can be determined. The disposition of the hat from unimodal to multimodal explains the enhancement and depression phenomena either in between the modalities or

within a modality. It is considered that the stimuli are always sigmoidal and non-linear (Cuppini et.al., 2007).

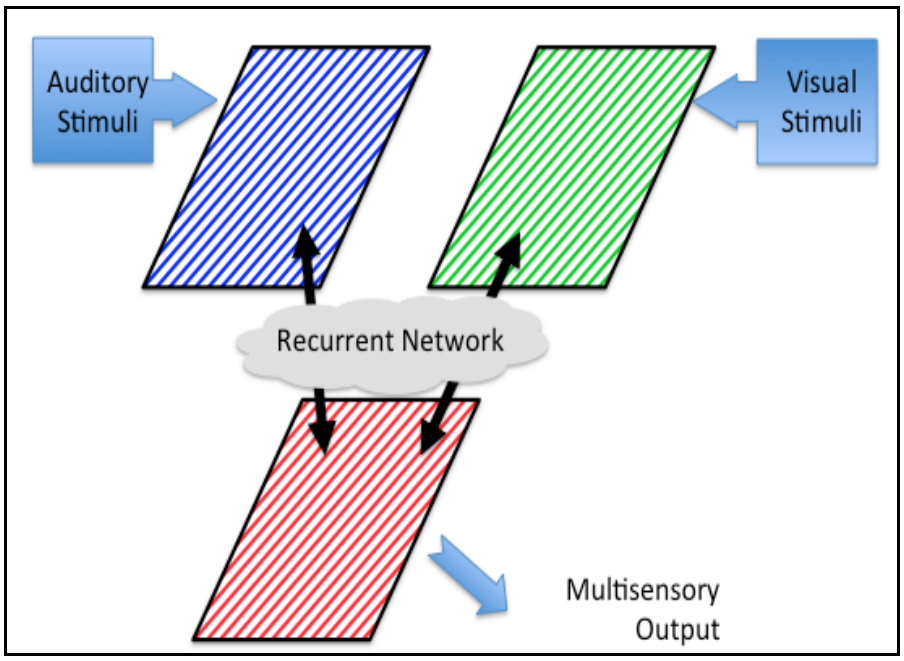

Figure 2.6 ***Crisiano Cuppini's neural network based integration model*****:** *Recurrent neural network with feed forward mechanism from unimodal to integrated output and vice versa*

The model of Cutsuridis mainly identifies issues of how the saccades are generated once the motor command is activated, especially for targeted and voluntary saccades. Irrespective of its complexity, Cutsuridis has used the concept of an anti-saccade task in developing a decision-making model of the SC (Cutsuridis et.al., 2007). Anti-saccade is the time taken for the eye to actually deviate in the opposite direction from the source. This model identifies that there are other cells that take part in saccade generation just before their actual firing. These cells can be studied with this anti-saccade task. By using this information, decision-making in the SC is explained.

This concept is quite convincing at a theoretical level, but may not be effective in implementation since all the inputs are considered to be linear. No biological evidence is available for supporting this inference. The model is expected to perform well only when the synaptic currents (neuron activity) is high. It is a new concept, but for a decision making task in the SC a huge complex network model is

suggested. Furthermore, the anti-saccade concept might be used to support some intermediate layers of the SC in decision-making, as those are the places where the integration (final decision) is expected to emerge.

In another article the author demonstrates the functionality of the SC, focusing mainly on real-time audio source localization (Trifa et.al., 2007). Audio localization is calculated using Interaural Time Difference (ITD) and Interaural Level Difference (ILD), with a cross-correlation function on a spiking neural network for biological resemblance in functionality. This model pre-processes signals before they arrive at the actual network for noise reduction purposes and then localizes using Generalized Cross Correlation (GCC) with phase transformation. Finally, an integrated distributed control framework is developed. The network can use the visual data for carrying other modalities, such as recognition, identification and tracking. The paper describes a sensitive model for audio localization in noisy environments. However the concept of multimodality is not utilized as far as source localization is concerned. The focus is mainly on noisy audio inputs and their localization. The result is also compared with ITD, ILD and GCC models, but not with the integrated models. As in the former case, accuracy and precision is high.

According to Armingol use of AI techniques such as Genetic Algorithms and Search Algorithms in a driving application for visual processing with colour enhancements is effective (Armingol et.al., 2007). It covers many possible situations such as pedestrians crossing, speeding and traffic signalling that helps a driver to make decisions. However, the camera covers only the straight road ahead of the vehicle - it does not cover the back or side views. In the case of the mirror image, either a back camera with audio support, or an existing camera, should be adjusted to an angle so that a mirror image comes into view which can be used to identify the vehicles at the back. However the extraction may not be efficient as the back mirrored image appears very small and is not enough to run the extraction algorithm for identifying fast moving vehicles. Hence audio is used along with a rear camera to integrate with visual processing, which will be useful in heavy traffic situations, changing lanes and overtaking, contributing to a Driver Assistance System.

In a paper by Casey and Pavlou, a neural network model is designed to simulate the behaviour of the SC (Casey and Pavlou, 2008) as shown in the figure 2.7. It involves processing audio and visual stimuli that are non real-world discrete inputs, since the authors are testing the integrated results as spatial representations and comparing them with biological data. Rate-coded algorithms are used for representing sensory topographical Self Organising Maps (SOMs). According to

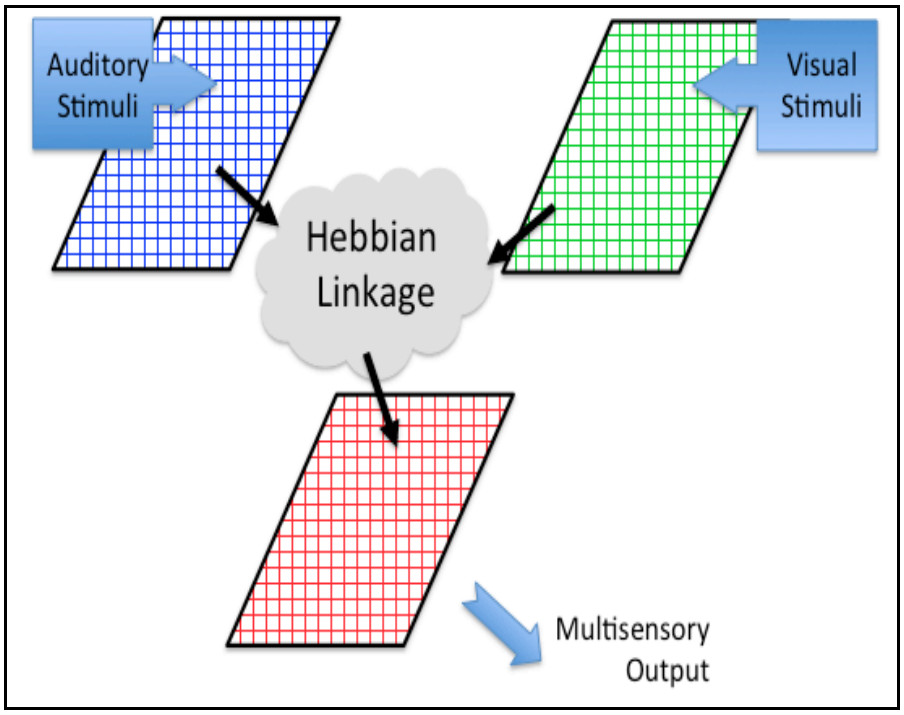

Figure 2.7 ***Casey and Pavlou's self organizing maps based integration model:*** *SOM neural networks for topographical representation of multimodal stimuli where the input layers are connected with hebbian linkage that helps to learn the audio and visual stimuli.*

the authors, alignment of sensory maps can be successful even with multimodal representations due to the mapping feature of SOM network.

Concatenating the individual modalities provides the comparison of multiple modalities. Though SOMs can provide a first approximation to the neuroscience view (Kohonen, 1982), a rate-coded algorithm has its limitations and hence the model is more static in its range of processing the inputs. The range of inputs covered is 35% - 46% towards the integration from the whole input data collected (Casey, 2009). If the model is trained on real-world inputs then this can be further

decreased due to additive integration technique. If the inputs taken are very few then limited accuracy can be achieved. This model can support suppression and enhancement of integrated output, as a first high-level approach towards multimodal integration (Stein, 1993). The applicability of the model is limited at this stage due to the narrow input stimuli range.

2.5.3. Application-driven Approach

In a paper by Stiefelhagen, the audio and video features are integrated separately such that the individual contributions of microphones and cameras will not affect the final decision of the tracking system (Stiefelhagen, 2002). Particle filters for audio and visual data are used for localizing the speaker. This paper is focused on audio and visual perception in a smart lecture room. In a specific example like this, where performance of the integration model is a critical issue, individual tracking of audio and visual data provides a more specific localization. Consider the case where a lecturer is in focus and a student stands and speaks simultaneously. In this case the multimodal system will help to track the person. This is a good example of where the applicability of a multimodal system can provide accurate and efficient results in making the decision with limited complexity (Stiefelhagen et. al, 2006). In another case, such as a group discussion, a multimodal system can direct the cameras to decide which person to focus on.

In their research on wearable devices Hanheide provide a novel idea for human computer interaction by integrating visual and inertial data processing (Hanheide et.al., 2005). Integration with head gestures can provide rich vocabularies necessary for communication. In a way the multimodal integration of visual and head gestures with inertial data can provide better communication between human and robot with the help of wearable sensory and computing devices. This system uses the head (holding a camera) for movements to generate commands by interacting with the environment. In case the user wants to change the selection of his choice, the way for navigating to the choice is not available. In this proposed paradigm items visible in the environment have to be assigned semantics so that

they can trigger the commands. However, as the environment grows, the semantics set increases. In the case of the appearance of a new item that is not known, it is not clear what the action is.

The work of Cucchiara proposes a different type of Multimedia Surveillance System using biometric technology for visual feature extraction for person identification in a closed circuit television application (Cucchiara, 2005). Contradicting issues like safety, privacy and ethics are well grounded with various practical examples that are currently in operation across the world. The multimodality (multi input dimensions) is used in a way to extract the best features from the various cameras including thermal, fixed, distributed and omni-directional. The omni-directional camera can be integrated with audio such that it can project the trajectory. The multimodality concept can be used for identification and tracking the person as an integrated mechanism in the surveillance system.

Designing a multi agent system for an intelligent multisensor surveillance system is in principle not a difficult task. However, according to Pavon, when it comes to the efficiency achieved by agents in co-operating and co-ordinating all the sensors, integrating the information is slow (Pavon et.al., 2007). In the case of centralizing all the systems, the limitations of the centralization architecture come to focus. The author has proposed a combination of centralized and distributed systems. However in this case, as the system grows, the more complex the design becomes. This reduces the performance of the system with time. Since it is a surveillance system, reaction times should be high.

In such cases, grouping similar sensors and considering them as an agent with a distributed network and then centralizing all the agents will improve speed and productivity. When it comes to the size of the group, scalability is an issue that needs to be dealt with for a distributed network at the sensor level. When it comes to designing such a system, there is a requirement for a high level language that can establish co-operation and co-ordination among the agents without compromising performance, scalability and efficiency. For the structure proposed

by the author for managing the agents, a huge network is required for processing and maintaining control.

When designing an integration model for security purposes, it is important to have certain features that can determine authentication of the input. Palavinel and Yagnanarayana have provided an approach using different inputs such as speech, images of the face, and both for authentication of an individual (Palanivel, 2008). The model discussed in this paper is an Auto Associative Neural Network (AANN) that receives inputs such as visual, acoustic and visual-speech (both audio and visual stimuli from the same source simultaneously). The focus is on authentication of the target for maximum security. For visual data images, feature extraction and detection is carried out on various facial features such as the eyes, the centre of the mouth and skin colour. Normalized vector data is used for both acoustic and visual-speech extraction with segmental levels. The AANN uses both the visual-speech and visual data for the total authentication. The results are more accurate for multimodal authentication than with a single input. However, more run time memory is required and the time of execution is greater. This is because it is necessary to carry out feature extraction from different features of the face individually and then provide them to the network for the integration.

Feature extraction is carried out directly on the input images, which are distorted after the process. Since the input is not replicated, every extraction needs a re-consideration of the input. When demanding high sophisticated security, memory is not an issue. However with speed comes efficiency, which cannot be effectively achieved due to the time-consuming extraction process. Hence it contradicts the model.

2.5.4. Conceptual Approach

The Integration methodology proposed by Coen proposes that perceptual stimuli processing is more viable than unimodal processing during multimodal integration (Coen, 2001). This may be right when the modalities are limited and there is some correspondence in their processing levels, including time. But when it comes to a

live environment, as the modalities increase, the complexity increases in finding the similarities between the processing levels, and sometimes there may not be similar levels. In such instances similarities are determined using *Individual Processing Channels***.** In the proposed multimodal system shown in figure 2.8, it was said that the input might appear at any level. This signifies that the received input is considered as its own irrespective of the source of input. By doing so the criteria of differentiating between signal and noise of each and every modality for which the model was developed is not met.

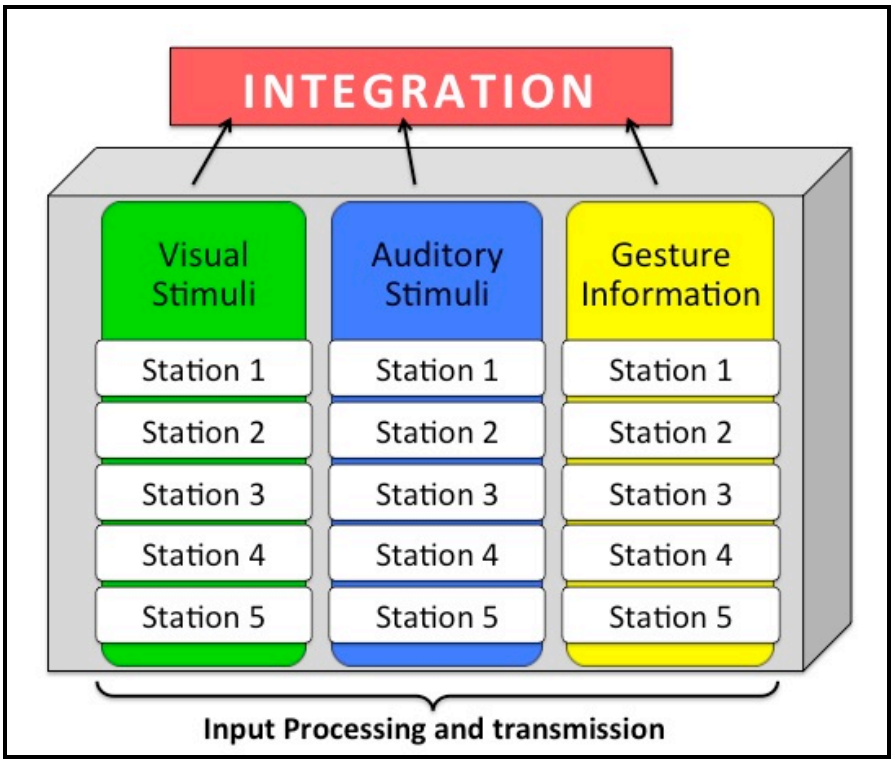

Figure 2.8 ***Individual processing channels based multimodal integration*****:** *Post-perceptual Integration system. Input information received from various stations across the network is individually processed at the specific station that transmitted for the integration of stimuli.*

Building such a vast, complex system for limited modalities and a limited environment is possible, but it is doubtful when the modalities increase or the environment grows. The "assumptions described by Piaget (1954) about multimodality in the real human world", are the only supportive evidence for the main concept in the paper. Apart from the Piaget assumptions, no other support is provided for explaining how "*the stimulus is processed as perceptual processing*

levels, not as individual processing levels in the human or animal brain system" (Coen, 2001).

A paper by Schauer is based on early fusion of audio and visual information for providing an integrated output (Schauer, 2004). The authors are inspired by the audio information pathway of the Inferior Colliculus along with the visual and multimodal pathways that are processed at the SC of the mid brain. Evidence shows that the sound stimulus is processed in the Inferior Colliculus. However the visual processing is carried out in superficial layers along with deep layers of the SC, and intermediate layers are responsible for multimodality. This shows that stimuli are processed to some extent in the corresponding units, and after integration (King, 2004) and (Stein and Meredith, 1993). For this early integration a novel network is proposed that can generate individual spatial maps of visual fields and audio stimuli. These maps are further integrated and a final multimodal map is generated. This multimodal map generation is based on a parameter optimization technique, which is an effective computational methodology to achieve the behaviour.

Yavuz provides solutions to various design issues and proves that optimizing the multimodal components at a computational level for integration in intelligent agents is effective (Yavuz, 2007). The focus is on efficient decision making at various levels to increase the efficiency at all possible levels including data acquisition, sensor information, further processing, dealing with various algorithms, and finally performance. The design proposed is huge as all possible performance levels and possible constraints are included.

Hardware considerations represent one main issue when optimizing the design. This paper considers mobility, navigation and autonomy of hardware. Along with hardware, various possible and alternative software that are compatible and optimal without compromising on performance are also adapted. Various systems are integrated to a single intelligent autonomous robot. They include electronic and mechanical interconnections of the various equipment. This conceptual system is complex when it comes to building it. The author recommends fuzzy logic based

behaviour integration where efficiency is expected to be more than any other system.

In a paper by Paleari, the author demonstrates human-computer interaction compared to human-human communication, including all the features and gestures usually followed (Paleari, 2006). A framework is described for multimodal emotion recognition. Fusion can be performed at feature level and at decision level. The extracted features are extrapolated with audio and visual data. However in the case of emotion, a gesture is added as in Scherer's theory to the extraction. This whole fusion can be provided from a multimodal fusion of the above-required modalities.

2.6. Summary and Discussion

This chapter provides an introduction at a conceptual level to the Superior Colliculus, stimuli localization, and the integration process carried out in the SC. A literature review has been undertaken on work carried out in understanding the SC integration, along with various attempts to perform a process for audio and visual data integration. Through this review three different implementation techniques are studied. Pros and cons of these techniques are examined and are used in subsequent further chapters of stimuli integration system development.

The biological importance of the SC is also described due to its presence in the mammalian brain system. This introduction describes the flow of stimuli information from the environment to the SC through sensory stimuli receivers such as the eyes and ears. It also reveals how the stimuli are transmitted into the SC along with the various changes the stimuli undergo during the generation of motor responses transmitted from the SC towards generating saccades and head movements. During this literature review interesting facts have been identified. These include biological evidence that suggest multimodal integration of sensory stimuli in the SC.

The chapter also provides a brief description of the motor response generated by the SC, its importance, and its role in the development of the multimodal integration system. In the next chapter a brief literature analysis of this area is provided so that a methodology can be derived, which is useful in identifying the effectiveness of the model.

The literature review is classified into four different types based on the type of methodology followed in implementing the multimodal concept. From each author's work, conclusions are drawn, which are later used in design and development of the integration model in this project. From the literature research, the probabilistic approach is considered unsuitable for this project due to the aspects of uncertainty intrinsic within it. This is because of a lack of biological influence or motivation on the model in both processing and development. Hence, considering into account the biological similarities extracted from the functionality of the Superior Colliculus detailed in chapter-2, a biological influenced model is proposed. The architecture of the model is derived from the Superior Colliculus neural findings described in chapter-3 section 3.2. This literature has laid the neural network platform for the architecture. The design and development aspects defined in chapter-4 justify the usage of neural network methods in particular RBF network. Similar is the state with experimentation and evaluation methodology. Observation and inferences that are made in this chapter are significantly used during the course of project.

Chapter 3

Methodology and Design Architecture of the Integration Model

3.1 Introduction

This chapter describes the transformation of the biological functionality of the Superior Colliculus (SC) into a computational model. The approach aims mainly at generating an integrated response for audio and visual stimuli. In this context, artificial neural networks (ANNs) are particularly attractive for this modelling because of their biological nature, learning and simultaneous processing. The focus lies in the design of the architecture of the integration model. This methodology considers the core problem and supports the solution with a feasible design of the architecture. Through this architecture the goal of the project can be achieved and validated.

The process of sensory information integration is an important task due to the complexity involved in transforming the biological model into a computational model. In this case, with audio and visual sensory information, the methodology plays a critical role in understanding how the research question is being analysed and evaluated. In this process both qualitative and quantitative approaches are followed, which helps in the transformation and design of the model.

3.2 Literature on Design and Architecture

The literature classifies different types of methodologies and approaches used for integrating audio and visual data as follows:

- Conceptual.
- Artificial Neural network.

- Probabilistic.

These approaches are unique in their own circumstances and are capable of providing feasible output. However, for this research a combination of these approaches is used at various levels, in order to satisfy the research question. According to the conceptual approach, it is important that the design and architecture is based on the central motivation of the research, which in this case is concerned with the SC. Hence, the methodology follows the audio and visual stimuli flow pattern of the SC, from the point of stimuli arrival, to the generation of motor control. Due to the relative similarity of neuron processing in the human brain, neural networks are considered to be a suitable architecture. This is because they enable parallel processing of audio and visual stimuli, together with control signal generation following integration of those stimuli.

In contrast, the above implementation could also be carried out based on a simple computational approach. Here a computational model could be constructed that can process the stimuli and generate a control command, which can integrate the audio and visual stimuli in both static and dynamic conditions. However, a computational approach can provide a solution to the problem only in static conditions.

In contrast, a neural network approach provides an ongoing solution where the problem changes dynamically with the environment (Stergiou, 2007). A neural network approach will have the advantage of an adapting learning mechanism, so that as the network is trained the output generated is also improved due to the error control criteria in the network processing. This is because the network is suitable for dynamic environments where learning can be adapted at any point during the training.

Hence, a neural network is considered as a base architecture for processing and integrating audio and visual stimuli, in order to generate motor control. In principle the architecture should contain three individual processing platforms, where audio, visual and integration mechanisms are carried out. Audio and visual units are connected to the integration layer, so that the stimuli flow towards audio and visual layers can be transmitted to the integration layer.

Hearing is a widely used means of localizing targets within the environment in the animal world (Chan, 2009). Due to the location of an ear on either side of the head, each with a capability to receive audio stimuli generated within a 180^0 range, the resulting 360^0 range gives the modality an advantage in terms of scope. This helps in detecting the target over a large field. The approach proposed is different from existing acoustic-based robotic applications. Many existing applications use computational Digital Signal Processing (DSP) techniques with the help of a large number of microphones in analyzing and capturing the sound stimuli. In contrast, the mechanism proposed here is based on a biological motivation using the mammalian acoustic system, which utilizes the audio data from the regions such as the IC, along with audio cortex principles, in receiving and analysing stimuli from the environment.

3.2.1 Audio Angle Determination

When it comes to localization of sound stimuli, azimuth is the primary factor that needs to be determined. In this context, azimuth is the angle at which the target stimuli are generated relative to a fixed frame of reference such as the centre of the eyes. This centre is always considered as 0^0, dividing the left ear side and right ear side as negative and positive directions of azimuth, as shown in Figure 3.1. In the figure Θ is the angle of incidence of audio stimuli at the centre of agent.

The direction of the audio source, either to the left or right side of the frame of reference, can be calculated using the *Time Difference Of Arrival* (TDOA) of the sound waves at the left and right ends of the receiving terminal. However, this computational *TDOA* is equivalent to the biological ITD of audio localization in the cortex of the brain system (McAlpine, 2003). When it comes to calculating *TDOA* it is important to identify two identical points in the left and right audio waveform in order to ensure accuracy. This similarity identification process is initially carried on the first sound waveform that is received at the same side of the stimuli source

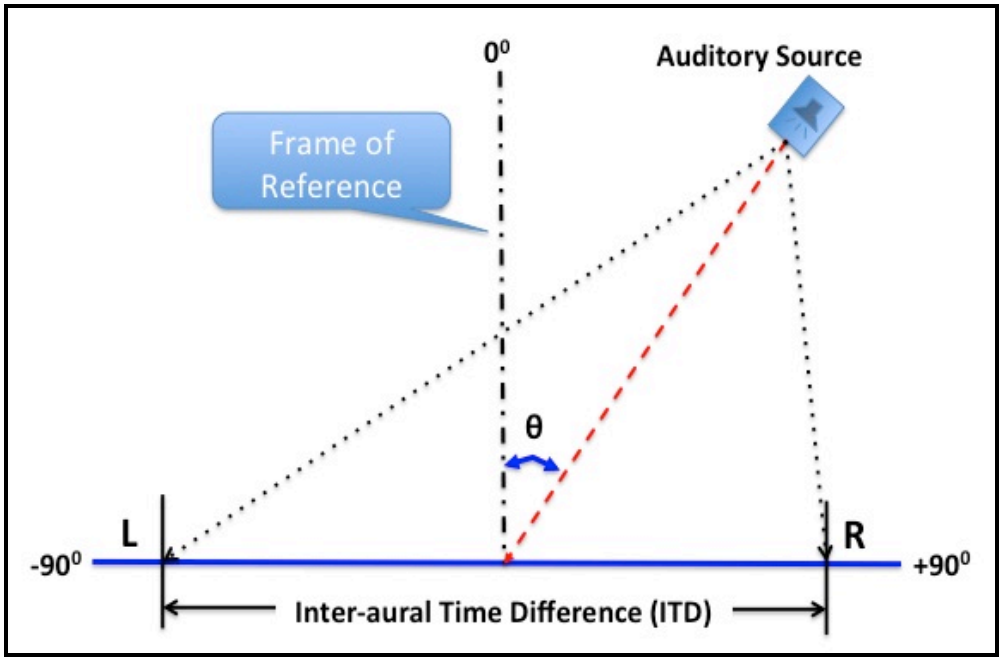

Figure 3.1 ***Audio localization visualization of stimuli transmission for left and right ear:*** *The angle (Θ) of received sound stimulus is determined from a fixed frame of reference located at the centre of both ears perpendicular to the base. A generated sound stimulus is received at the left (L) and right (R) side of the frame of reference. ITD is calculated based on the time gap available between the L and R locations for a particular stimulus at an instant of time.*

(ipsilateral) and later to the waveform of the opposite side of the source (contra-lateral) through the process of cross-correlation.

3.2.2 Cross-correlation

Cross-correlation is the process of identifying the location/region at which the signals exhibit similarity. However, in order to localize audio stimuli, the signals received at the left and right ear should be computed for the point of maximum similarity, or maximum correlation, when the stimuli are super-imposed. Hence, using the technique of cross-correlation, the point of maximum similarity of the left and right sound signals is calculated. Using this correlation value, the length of the vector stimuli is determined for both left and right ears.

On obtaining the vector length of the left and right stimuli the distance of the sound source from the centre of the ears is determined. *TDOA* is calculated using the variation of a signal from the point of maximum similarity. By doing so, the time

lapsed for the signal to reach the receiver beyond the point of similarity is determined. Having thus obtained *TDOA*, since the speed of sound is known, the distance between the audio source and the centre (i.e. the intersection point of the reference frame and the centre of the ears) is obtained.

Since the distance between the left and right ear of the agent is known, the angle at which the audio source is located from the centre is determined. A detailed explanation of how the angle is obtained based on geometrical triangulation is shown in section 3.4.

3.2.3 Visual Angle Determination

In common with the audio aspect, visual localization plays a crucial role. With the biological structure provided in chapter 2, when it comes to visual stimuli localization, or delivering attention, the scope is limited to the visual range of the human eye. Similarly, with a robotic agent, the scope is limited to the horizontal visual range of the camera in terms of saccade generation, along with agent head movements. Considering the fact that localization in the SC is instantaneous (for involuntary saccade generation), without intervention of the cortex directly, a most convenient method of visual angle determination is adapted. To emulate the quick and spontaneous response to stimuli in the SC, difference identification, using a frame delay technique called ‘difference image’, is used.

3.2.4 Difference Image

This process is based on the concept that changes in the visual environment are often identified from consecutive visual frames. Performing a brightness separation technique using difference images can always separate intensity or brightness variations. Using a criterion based on the factor of brightness, all possible variations in the visual field can be isolated as a difference image. This difference image, containing various intensities, can be transformed into Red-Green-Blue (RGB) components of brightness, through which the highest intensity at a particular instant of time can be identified and isolated.

Later this difference image is transformed into a weight vector and is interpolated to the visual frame such that the frame of reference can coincide with the centre of the visual vector. Figure 3.2 shows how these difference images are generated based on two successive frames, where the first frame is a null image with no activation, and the second frame has activation at two different locations. The third image is the difference image generated from the first two frames. Hence, with the help of geometrical correlation, the angle at which the highest visual variance is located can be calculated from the centre with respect to the frame of reference.

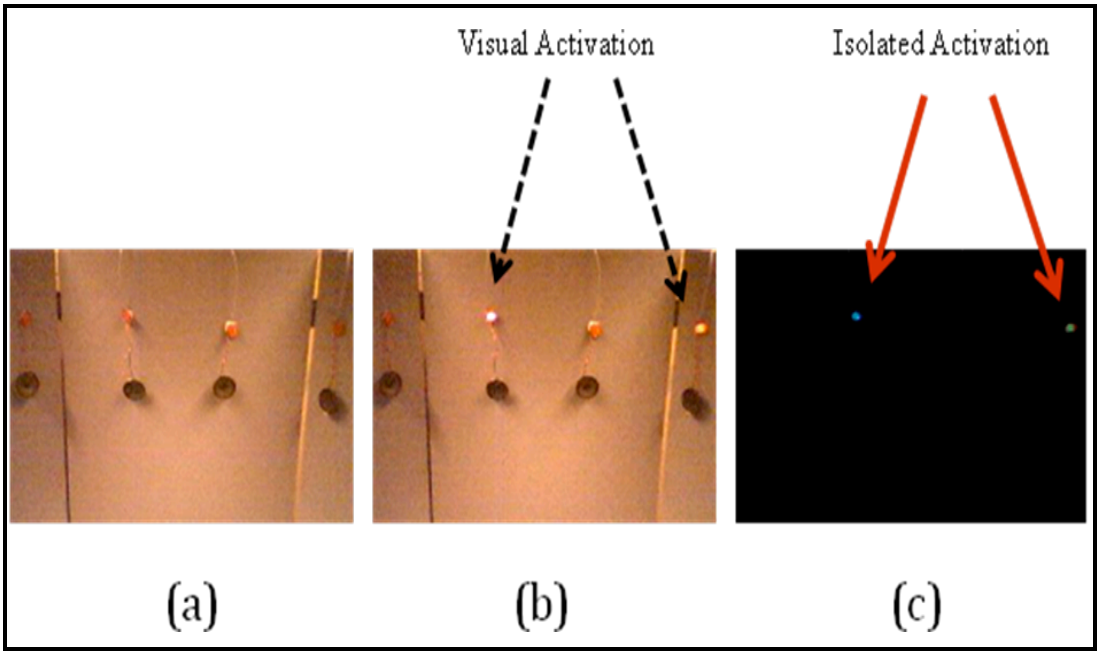

Figure 3.2 ***Visual stimuli isolation using difference image:*** *The image of visual environment containing a set of LEDs separated by 10^0 followed by speakers are provided in (a), (b) while (c) is a difference image. (a) The visual image obtained at t_0 from the camera of agent without visual stimuli (b) The visual image obtained at t_1 from the camera of agent with visual activation at LEDs located. (c) The difference image significantly providing the variation of stimuli at t_0 and t_1 at 0^0 and 20^0.*

The methodology described above concerns the processing details of audio and visual stimuli localization. Using this methodology an architecture is developed that can process stimuli and localize the source in terms of angle. The following section describes how the above methodology can be transformed into an architectural design based upon the SC.

Localization that is carried in the previous section, has considered speed of stimuli in air medium as constant. When it comes to real time application, situations arise causing a medium between source and destination. In such cases, speed factor is variable and depending on the type of stimuli it influences TDOA as well. This is another research prospect that can be considered for future work as, influence of variable mediums on multimodal behaviour of audio and visual data.

3.3 Architecture

The SC of the human brain provides the motivation for the multimodal computational architecture developed during this work. The form of the instantaneous output delivered by the SC for the primary stimuli in the multimodal environment laid the foundations for the computational model. This approach transforms the biological model into a computational model. This model is different from earlier integration models in terms of processing levels, architecture and minimal error for maximum network performance. Hence, a dual layered architecture was considered, where one layer receives input from different audio and visual stimuli available in the environment, while the other performs the integration of these stimuli based upon a synchronized time (with an estimated delay of 3.2 seconds to align the agent to the frame of reference) cycle for generating motor responses, as shown in figure 3.3.

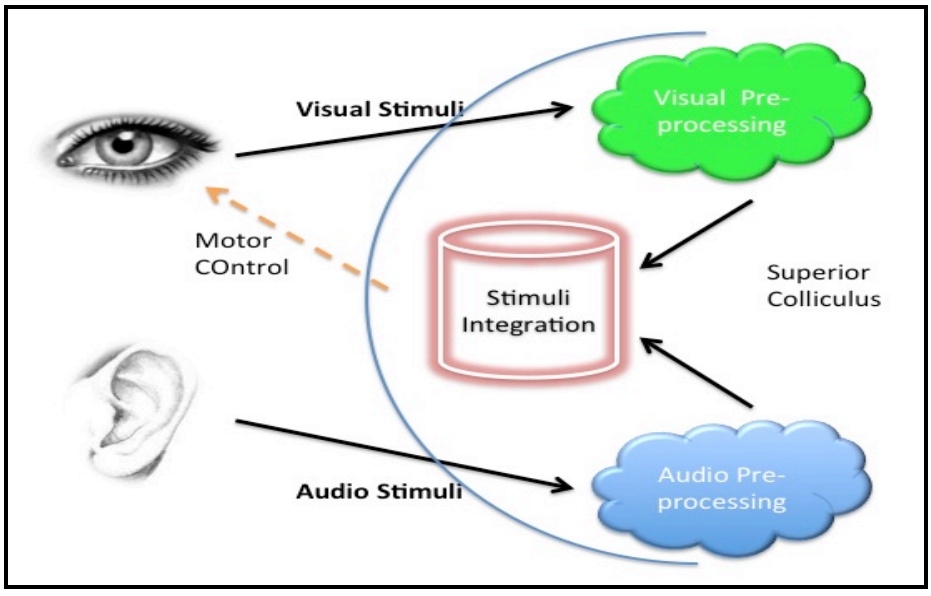

Figure 3.3 ***Stimuli processing based layer architecture of the SC:*** *A layered network structure capable of processing inputs from both audio and visual input layers which are later transmitted to the integration layer, using vector transformation, where integration is carried out.*

The Concept behind the architecture can be summarised as follows:
For audio input processing, the TDOA is calculated and projected onto the audio layer. The audio input is provided to the model in the form of audible sound signals within the range of the microphones. Similarly for visual input processing, a Difference Image (DImg) is calculated from the current and previous visual frames and is projected onto the visual layer. The network receives both visual and audio input as real-time input stimuli. These inputs are used to determine the source of the visual or audio stimuli. The audio and visual layers are then associated for the generation of the integrated output. Even in case of the absence of one of the two inputs, the final outcome on the angle of displacement for the generation of eye or head movement is made based upon the available input stimuli. An asynchronous timer at the integration layer verifies this phenomenon of multiple stimuli arrival. In the case of simultaneous arrival of different sensory inputs, the model integrates both inputs and generates a common enhanced or depressed output, depending on the signal strength of the inputs. The particular focus here is on studying the appropriate depression and enhancement of the integrated output.

3.3.1 Experimental Platform

In order to investigate this methodology, a series of datasets had to be collected for both unimodal and multimodal stimuli. In order to support the rationale behind the approach from a biological viewpoint, the experimental framework of Stein and Meredith was considered (Stein, 1993), as shown in figure 3.4. Stein used this platform to observe and study the behaviour of a trained cat during multimodal circumstances. In this platform, when audio and visual stimuli are activated with the help of speaker and light, the cat's behaviour is monitored.

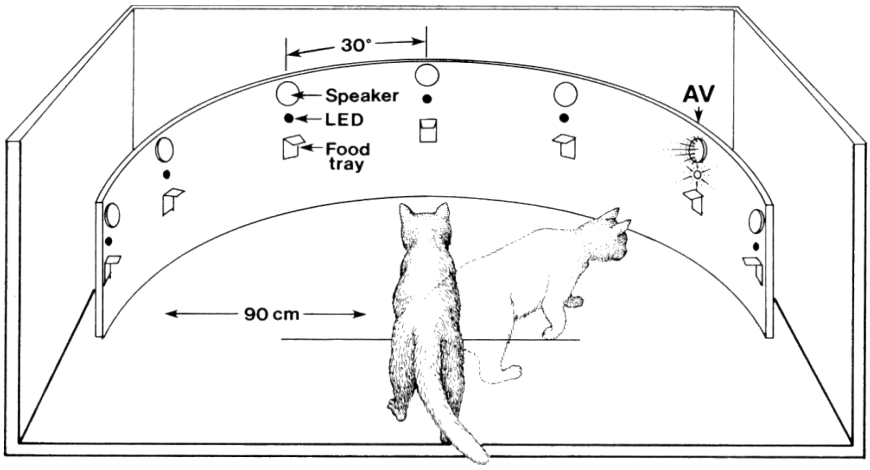

Figure 3.4 ***Stein's behavioural experimental platform:*** *Behavioural experimental-platform setup, for testing a cat's multimodal behaviour during audio and visual input stimuli along with response monitoring using food trays. Image courtesy: "The Merging of The Senses" by Stein and Meredith of 1993.*

Based on the single neuron behaviour paradigms for examining unimodal and multimodal sensory stimuli orientation (Stein et. al., 1988, 1989) on cats' behaviour for motor responses generation, a semi circular environment was designed. This could generate the stimuli for audio and visual signals that a trained animal (a cat in Stein's experiments) could respond to. The set-up involved the animal at the centre of a circle, where a series of speakers and Light Emitting Diodes (LEDs) were located in pairs, along with food trays spaced at 30^0 intervals in a semi-circular manner. Although the intention of the experiment was to demonstrate multimodal behaviour, it is useful to examine the responses observed by Stein in understanding the SC behaviour. Given audio stimuli through the speaker, along with visual stimuli from the LED, the animal was expected to reach the food tray below the speaker or LED depending on the multimodal output.

The behavioural platform was used to perform a series of trials with different mammals based on spatial coincidence, disparity and resolution trials. This study demonstrated the behaviour of the SC in various cases, along with the types of stimuli. Data collected from electrophysiological and behavioural experiments was compared and many similarities were observed. Hence, based on the size of the population, it was observed that spacial trials could be classified under coincidence as enhancement, and disparity as depression.

Their behavioural experimental platform provides a good starting point for carrying out a series of experiments for this research as projected in figure 3.5.

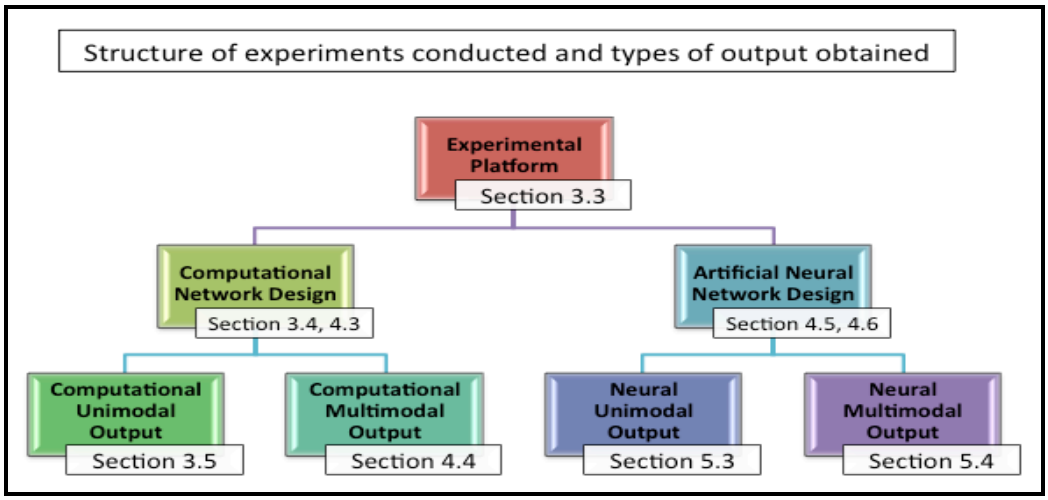

Figure 3.5 ***Experimental structure:*** *Using the experimental platform defined in figure 3.4, describes the types of networks that are tested on the platform and also the output generated from the corresponding network. The 'section' part notified in each block is the part of thesis that corresponds to the work.*

The environment created for this work includes a series of audio sources (speakers) and visual sources (LEDs) arranged in a semi-circular environment, so that each source is the same distance from the centre, within audio and visual range of the agent. Replacing the cat with a robot head, as shown in Figure 3.6, modified Stein's behavioural set up. The robot was equipped with a set of cameras that served as eyes and a set of microphones that served as ears, located in a similar position to the eyes and ears of a human. The robot has the agility to move the head in both left and right directions.

Using cameras and microphones as sensory information receiving devices, stimuli from the environment could be collected and fed to the integration network. As a result of visual or audio input, the aim is to orient robot's head towards the direction of the source as feedback to the stimuli. This platform could be used for both unimodal and multimodal input stimuli generation and receiving. One important aspect of using this behavioural platform is that environmental noise could be taken into account while detecting and tracking stimuli for the enhancement and depression phenomena. However these phenomena are always sensitive to noisy stimuli, which was critical for this research. This platform

is best suited to studies related to saccadic movements (horizontal) of both the eyes and the head.

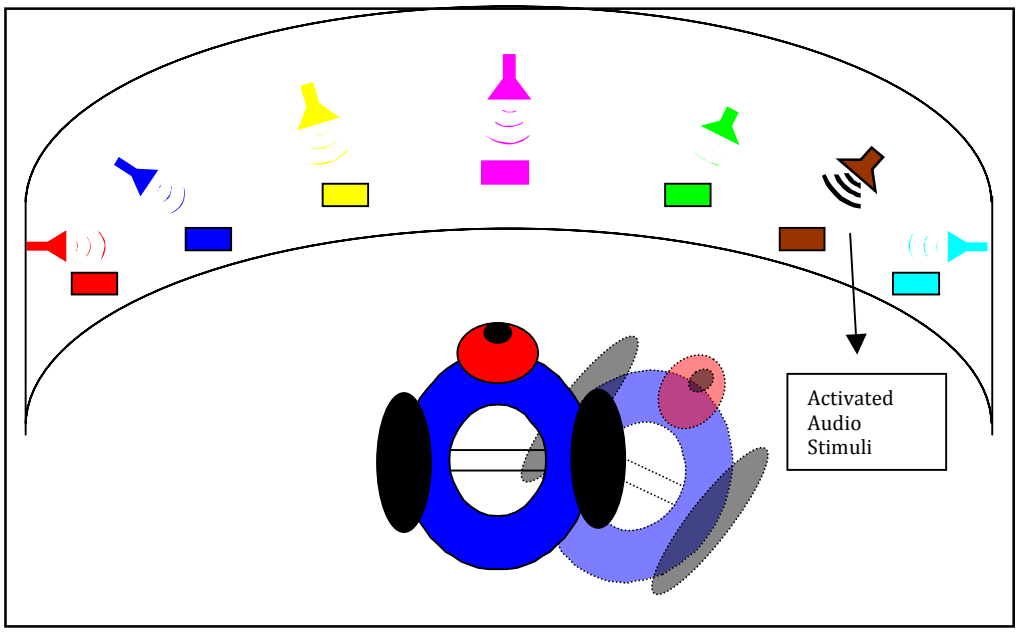

Figure 3.6 ***Agent based experimental platform:*** *Experimental setup and robot platform for testing the multimodal integration model for an agent based on visual and audio stimuli. An agent is dispensed at the centre of a series of speakers and LEDs' within the audio and visual range. Upon activation of audio stimuli from the indicated speaker, the agent aligns at an angle signifying the direction of stimuli source.*

In the above scenario, agent is surrounded by a series of mics' and LEDs at -30^0, -20^0, -10^0, 0^0, $+10^0$, $+20^0$, $+30^0$ respectively from left to right, while the mics are also located upto -90^0 and $+90^0$. The given graphical representation in figure 3.6 is the experimental demonstration of agent-based localization for multimodal behaviour of steins behavioural platform. The experimental results obtained form this environment is projected in the later sections of this chapter.

3.4 Computational Design (Stage-I)

In this section, the methodology described above for unimodal stimuli processing is transformed into a computational (non-neural network) design. A feasible strategy is adapted such that the computational design for the agent is efficient and is also capable of generating input data sets.

3.4.1 Audio Processing

The first set of experiments is based on collecting the audio data from a tracking system within the experimental platform setup. Audio sound source localisation is determined by using the inter-aural time difference for two microphones (Murray et. al., 2005) and the *TDOA*, which is used for calculating the distance from the sound source to the agent. The signal overlap of the left and right stimuli enables the time difference to be determined using equation 3.1.

$$TDOA = \left\{ \frac{length\left(xcorr\left(L,R\right)\right)+1}{2} - \max\left(xcorr\left(L,R\right)\right) \right\} \times S_r \quad \text{..... (3.1)}$$

In equation (3.1) 'xcorr ()' is the function that determines the cross-correlation of the left 'L' and right 'R' channels of a sound signal. Use of the 'max(xcorr)' function determines the highest correlation region in the signal. S_r is the sample time of the sound card used by the agent. Once the TDOA is determined, the distance of the sound source from the agent is calculated using equation (3.2).

$$\text{Distance} = TDOA \times SoundFrequency \text{ ..... (3.2)}$$

The result is a distance vector of a sensory map for further processing to generate the multimodal integrated output. This is shown in the Figure 3.7.

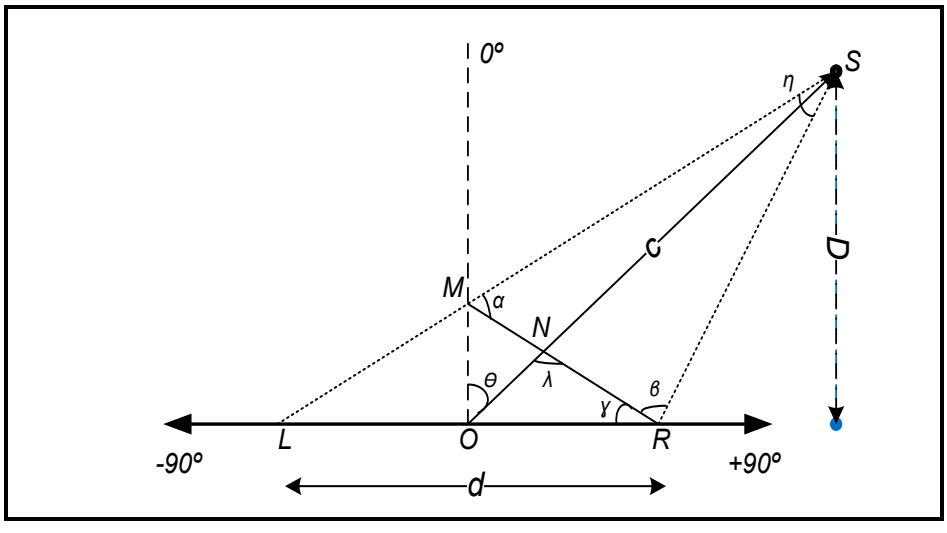

Figure 3.7 ***Audio source localization determination based on time difference on arrival:*** *Determination of sound source directions using TDOA where c is the distance of the source and θ is the angle to be determined based on TDOA and the speed of sound. The distance d between two microphones (ears), L and R, is known.*

However, for unimodal input data sets, we can determine the direction of the sound source in an isolated state using geometry along with the data available, including speed of sound, distance between the 'ears' of the agent, and the distance of the sound source from the centre of agent (the centre of the ears).

Assume the sound source is far away from the agent, i.e. *c*>>*d*, then $\alpha=\beta=\lambda\approx 90^0$ and the sound source direction can be calculated using triangulation as follows:

$$\theta = \gamma = \sin^{-1}\left(\frac{ML}{d}\right) = \sin^{-1}\left(\frac{TDOA \times Vs}{d}\right) \quad \text{..... (3.3)}$$

Where *Vs* is the sound speed in air

By using the distance of the sound source *(D)* and the distance between the ears *(d)*, the direction *(θ)* of the sound source is determined as follows:

$$Angle(\theta) = Sin^{-1}\left(\frac{D}{d}\right) \quad \text{..... (3.4)}$$

From the above methodology the unimodal data for the audio input is collected and the audio stimuli can be made available for the integration model.

3.4.2 Visual Processing

We now consider visual data processing, where a set of small active LEDs serve as the location of the visual stimuli in the environment. A change in the environment is determined based on the difference between subsequent images. By using a difference function, the difference between two successive frames is calculated.

$$\mathrm{DImg} = \left\| image_i - image_{i-1} \right\| \quad \text{..... (3.5)}$$

Where *DImg* is the difference image and *image (i)* where *i*=1 to *n* and so on are consecutive images received at the eye (camera).

A continuous traversing of the environment eventually identifies the activation. Based on the brightness intensity in the difference image, the activation is considered. Once the difference images are obtained containing only the variations of the light intensity, they are transformed into a vector. Once the vectors are extracted they can be used as direct inputs to the integrated neural model. However, in the case of unimodal data, difference images are processed directly to identify the area of interest as shown in figure 3.8.

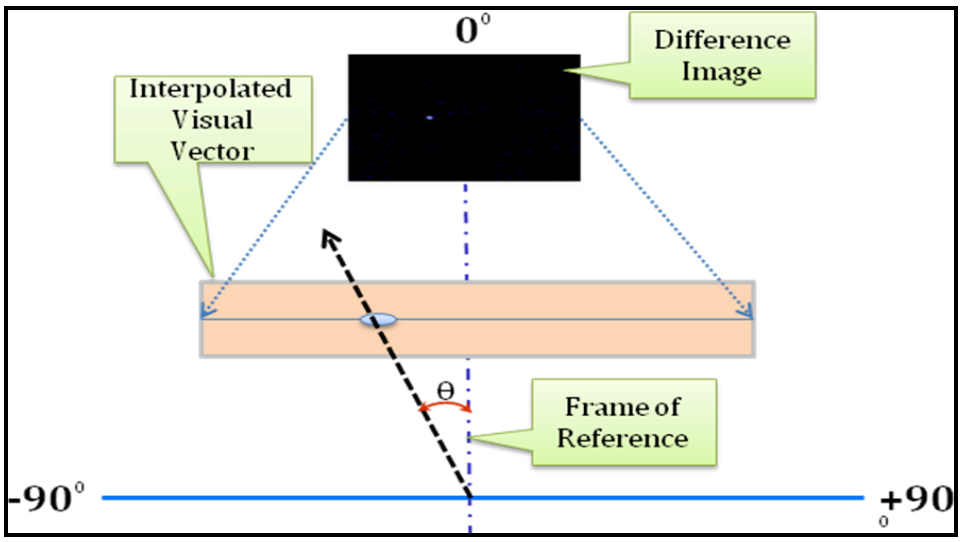

Figure: 3.8 ***Visual source localization calculation based on difference image:*** *Difference Image (DImg) used for scaling and to determine the location of the highlighted area of the image in which the dash line represents the length of the visual range and distance between the two cameras eye1 and eye2.*

The intensity of the light is also considered to identity activation with higher brightness. Breaking down the activation into RGB components enables this process to be carried out. Using this method a series of images is collected. From this vector the maximum colour intensity location (maxindex) is identified and extracted. With the help of this information and the distance between the centres of the eyes to the visual source, it is easy to determine the direction of the visual intensity changes in the environment using the formula given in equation 3.6.

$$\theta = \tan^{-1}\left\{\frac{(\text{maxindex} - \text{half\_visual\_width}) \times \text{visual\_range}}{\text{visual\_width x distance\_of\_sensor\_to\_source}}\right\} \quad \text{..... Eq. (3.6)}$$

This computational design provides a means to carry out unimodal stimuli experiments based on the methodology discussed earlier.

3.5 Unimodal Stimuli Experiments

Initially, the computational model was experimentally verified using the behavioural platform for unimodal input data collection of audio and visual stimuli. The agent in this case was a PeopleBot robot with a set of two microphones for audio input and a camera for visual input (MobileRobots Inc, 2006) as shown in figure 3.9.

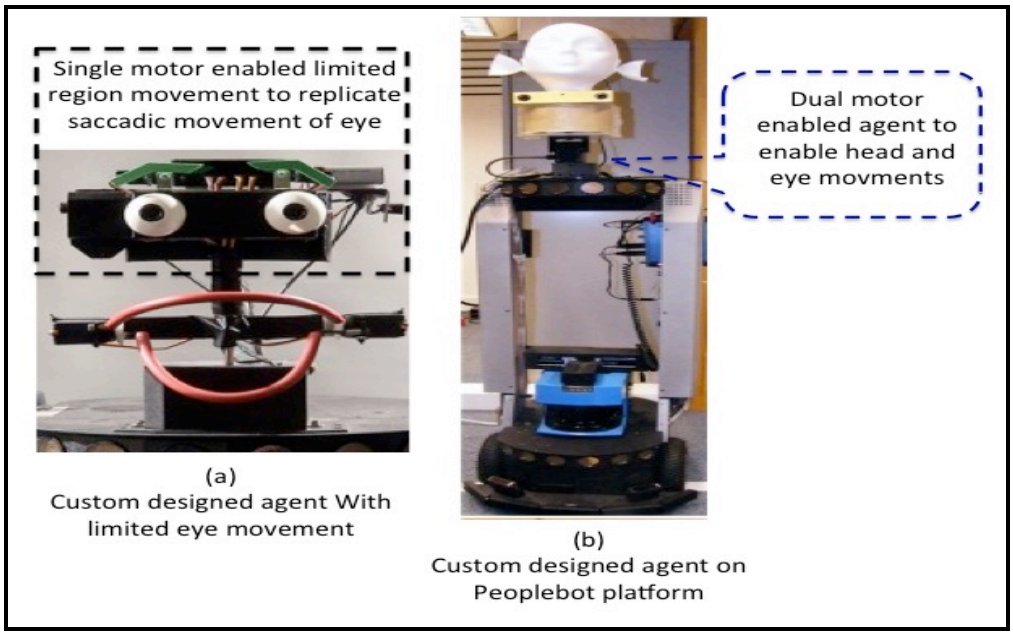

Figure 3.9 ***Agents used during the process of data collection and testing*****:** *Robotic platform (a) is used for audio and visual stimuli collection for unimodal data collection and processing. Agent (b) is used for multimodal data acquisition and has capability to deliver output in terms of head movement (similar movement of saccades).*

3.5.1 Audio Input

The agent used for audio data collection has two microphones attached on either side of the head resembling the position of the ears. The speakers are stimulated using an external amplifier to generate sound signals of strength within human audible limits, closer to the lower limit. For these experiments signals with smaller frequencies and variable amplitude were considered, since with these lower frequencies the multimodal behaviour can be identified and also the behaviour of stimuli can be studied with greater efficiency. Hence frequencies with a range of 100 Hz – 2kHz are used.

Sound stimuli were generated randomly from any of the different speakers on the behavioural platform, and by implementing the TDOA method, the direction of the stimulus was determined. On the arrival of audio stimuli at the deep processing levels of the SC, stimuli received from left and right channels are analysed using cross-correlation and the location of the source was determined.

This localization was based on the frame of reference described in the design section. The graphical representation in figure 3.10 shows sample results using a single audio stimulus with amplitude 8dB, at frequencies of 100Hz (minimum) and 600Hz (maximum) used during the experimentation. It was observed that audio localization seems effective at these frequencies and amplitudes. The stimuli were projected using an audio analyzer, which details the stimuli arrival on time (x-axis) to amplitude (y-axis) axis. Similarly, the localization was projected on -90^0 to $+90^0$ single axis plot, signifying the horizontal (saccadic path) space. Regarding the graphs shown in figure 3.10:

The sound stimuli presented in left and right channels were represented on a graph with the time on the x-axis and amplitude on the y-axis, for the stimuli initial and end points of both 100Hz and 600Hz. The left and right channels are provided on the time axis signifying the time of stimuli arrival which in this case is a

Similarly, the sound localization graph is location identification with respect to the directional stimuli and angle stretching across -90^0 to 90^0 horizontal.

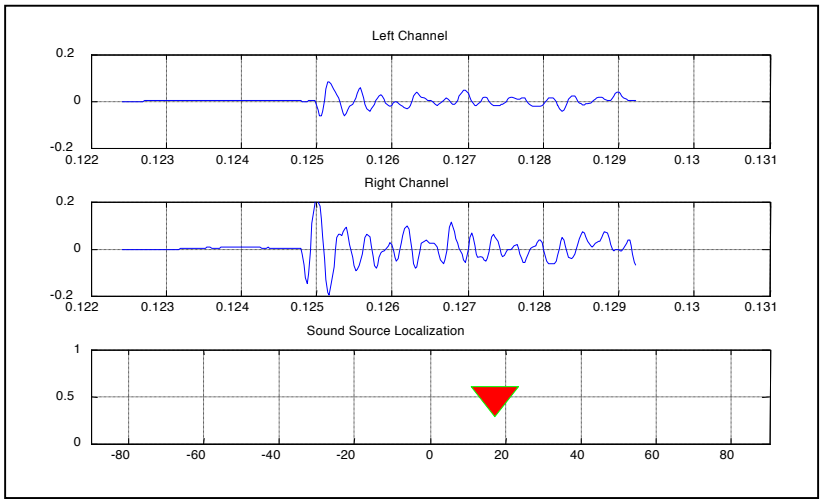

(a) Localization with Amplitude 8 & Frequency 100Hz across the horizontal saccadic frame (-90^0 to 90^0)

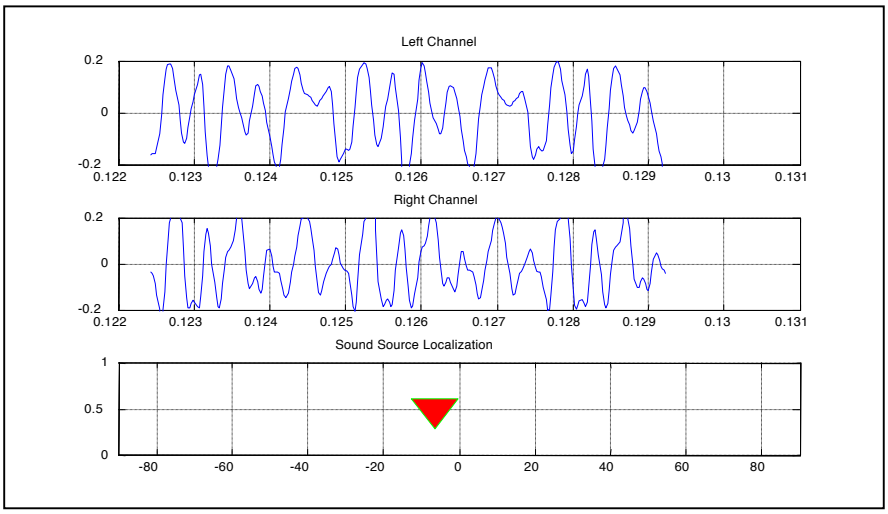

(b) Localization with Amplitude 8 & Frequency 600Hz across the horizontal saccadic frame (-90^0 to 90^0)

Figure 3.10 ***Localization of binaural audio stimuli with amplitude 8dB for frequency 100Hz and 600Hz:*** *Graphical representation of audio localization. When there is an audio stimulus available from the environment, it is interpreted according to the received times at the two ears of the agent. The signals received at the left and right ear are plotted on a graph of time on the x-axis and amplitude on the y-axis. Once the TDOA is calculated and the direction of the audio source is located it can be shown in the range from -90^0 to 90^0, which in this case is identified as (a) 18^0 and (b) -10^0.*

By running the above experiment for lower frequency ranges of 100 to 600 Hz with the amplitude level at 8dB, initial experiments were carried out and the results are presented below. For each frequency, the sound stimuli are activated at angles varying from -90^0 to 90^0. Table 3.1 presents the angles given by the tracking system for initial amplitude of 8dB, which are discussed in the above section. These angles are obtained by the audio processing unit for the principal frequencies indicated in rows to the designated direction in the columns.

Audio Localization Output Table													
Frequency (Hz) Vs Angle (degree)	-90^0	-60^0	-45	-30	-20	-10	0	10	20	30	45	60	90
100 Hz	-81.07	-61.39	-6.29	-31.44	-21.41	-8.4	0	10.52	21.41	33.97	41.07	63.39	50.04
200 Hz	-71.07	-63.39	-42.11	-33.97	-25.97	-14.8	0	10.52	21.41	35.59	42.11	63.69	80.2
300 Hz	-76.88	-63.39	-41.07	-29.97	-25.97	-14.8	-2.09	12.4	21.41	31.44	38.95	63.39	80.00
400 Hz	-73.19	-63.39	-41.07	-75.6	-33.41	-10.52	-2.09	10.42	16.98	36.59	41.07	63.39	73.41
500 Hz	-43.9	-63.4	-17	-22.14	-17	-10.5	0	10.52	21.41	29.29	48.4	63.39	53.41
600 Hz	-76.9	-61.38	-42.09	-31.40	-21.41	-10.2	0	10.52	21.41	31.44	41.01	62.01	80.02

Table 3.1 ***Audio localization output table:*** *Accuracy of the projected angles in degrees to various frequencies from 100Hz to 600Hz at amplitude 8db.*

Table 3.1 shows a sample set of audio data for which the experimentally obtained localization was relatively close to the target values. The errors obtained were presented in the following Table 3.2.

Audio Localization Error Chart							
Amplitude : 8 dB			***Noise Levels*** *: 0.4 – 4dB*				
Frequency Vs Angle	**100Hz**	**200Hz**	**300Hz**	**400Hz**	**500Hz**	**600Hz**	**Mean Error**
-90^0	8.93	18.93	13.12	16.81	46.01	-13.1	**15.12**
-60^0	1.39	3.39	3.39	3.39	3.04	-1.38	**2.20**
-45^0	1.05	2.89	3.93	3.93	2.91	-2.91	**1.97**
-30^0	1.44	3.97	0.03	2.80	0	-1.40	**1.14**
-20^0	1.41	5.97	5.97	3.21	3.0	-1.41	**3.03**
-10^0	1.60	4.80	4.80	0.52	0.50	0.52	**2.12**
0^0	0	0	2.09	2.09	0	0	**0.70**
10^0	0.52	0.52	2.40	0.42	0.52	1.41	**0.97**
20^0	1.41	1.41	1.41	3.02	1.41	1.01	**1.61**
30^0	3.97	5.59	1.41	6.59	0.71	1.44	**3.29**
45^0	3.93	2.89	6.05	3.93	3.40	1.01	**3.54**
60^0	3.39	3.69	3.39	3.39	3.39	2.01	**3.21**
90^0	39.04	9.98	10.0	16.59	36.59	9.98	**20.36**
Mean Error	**5.24**	**4.93**	**4.46**	**5.13**	**7.81**	**2.89**	**5.08**

Table 3.2 ***Audio localization error chart:*** *The error obtained in localizing the audio stimuli for each of stimuli generated from table 3.1.*

A graphical representation of the localization error is shown in Figure 3.11

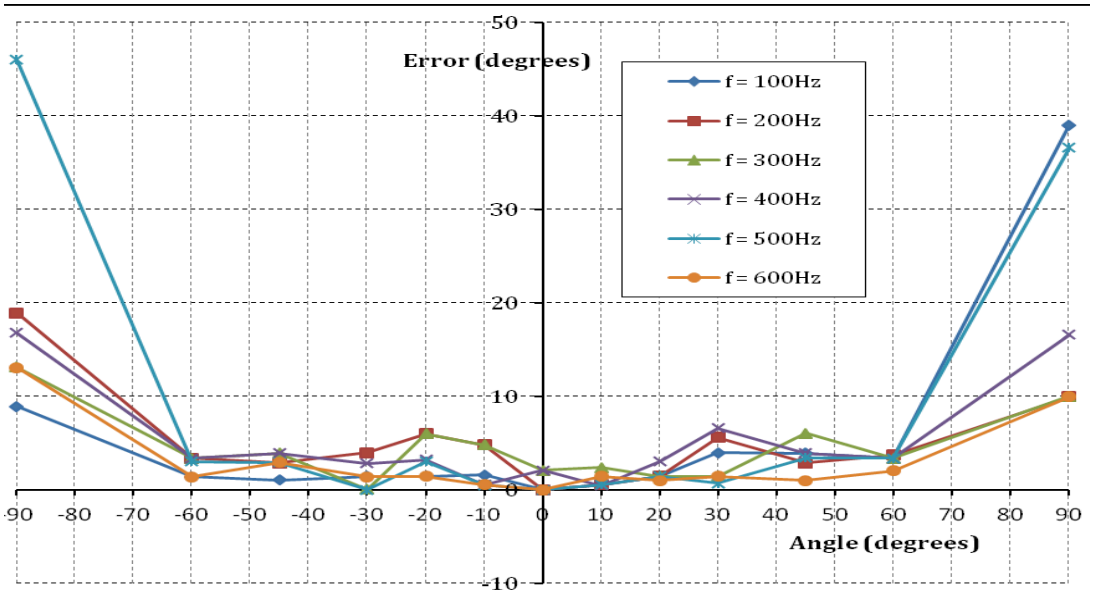

Figure 3.11 ***Audio localization error graph:*** *Graphical representation of audio localization error, featuring relative similarity of each frequency to the target localization.*

This shows the model works effectively for localization of lower frequencies, where the absolute mean error level is less than 10^0. The experimental outcome signifies the effectiveness of the approach along with the appropriateness of stimuli selection. However, in order to verify the success of the methodology a set of data samples were collected by varying the amplitude from 8db to 22db in intervals of 2 decibels. Similar experiments were carried out on the same frequency range with a change in amplitude in both laboratory and open (noisy) conditions. This resulted in an audio input dataset of 168 samples. These are presented in the next chapter.

3.5.2. Visual Input

The camera was able to cover 60^0, from -30^0 to 30^0. The series of frames collected as input from the camera are processed and the output should determine which of the LEDs is active. The frames are used to generate difference images, which contain only the changes that have occurred in the visual environment of the agent. They are calculated by measuring the RGB intensity variations from pixel to pixel in the two successive images. This series of difference images is used to identify any kind of change in the environment. The difference images are plotted on a plane covering -90^0 to 90^0 on the horizontal axis and signal strength (intensity) on the vertical axis. Figure 3.12 represents one such plot of the difference image signal intensity.

It is clear that visual coverage is 60^0 (-30^0 to $+30^0$) and auditory coverage is 360^0. When it comes to generalizing the axis, a scale of -90 to +90 is used for localization so that both audio and visual stimuli can be represented. However, the demonstration of the stimuli is carried out on much larger scale only for visualization of the stimuli. This criterion is adapted for all the stimuli representation in the thesis for both unimodal and multimodal presented in chapter-3 and chapter-4.

Using the plot shown in figure 3.12, the direction of the source from the centre of the agent is determined. The difference images are mapped onto a standard

Horizontal Scale Frame (HSFr), to determine the location of the activation as a data format to input the system. The HSFr is a scale that divides the 180^0 frame into 5^0 increments. Thus the generated final HSFr image varies according to the intensity projections of difference images.

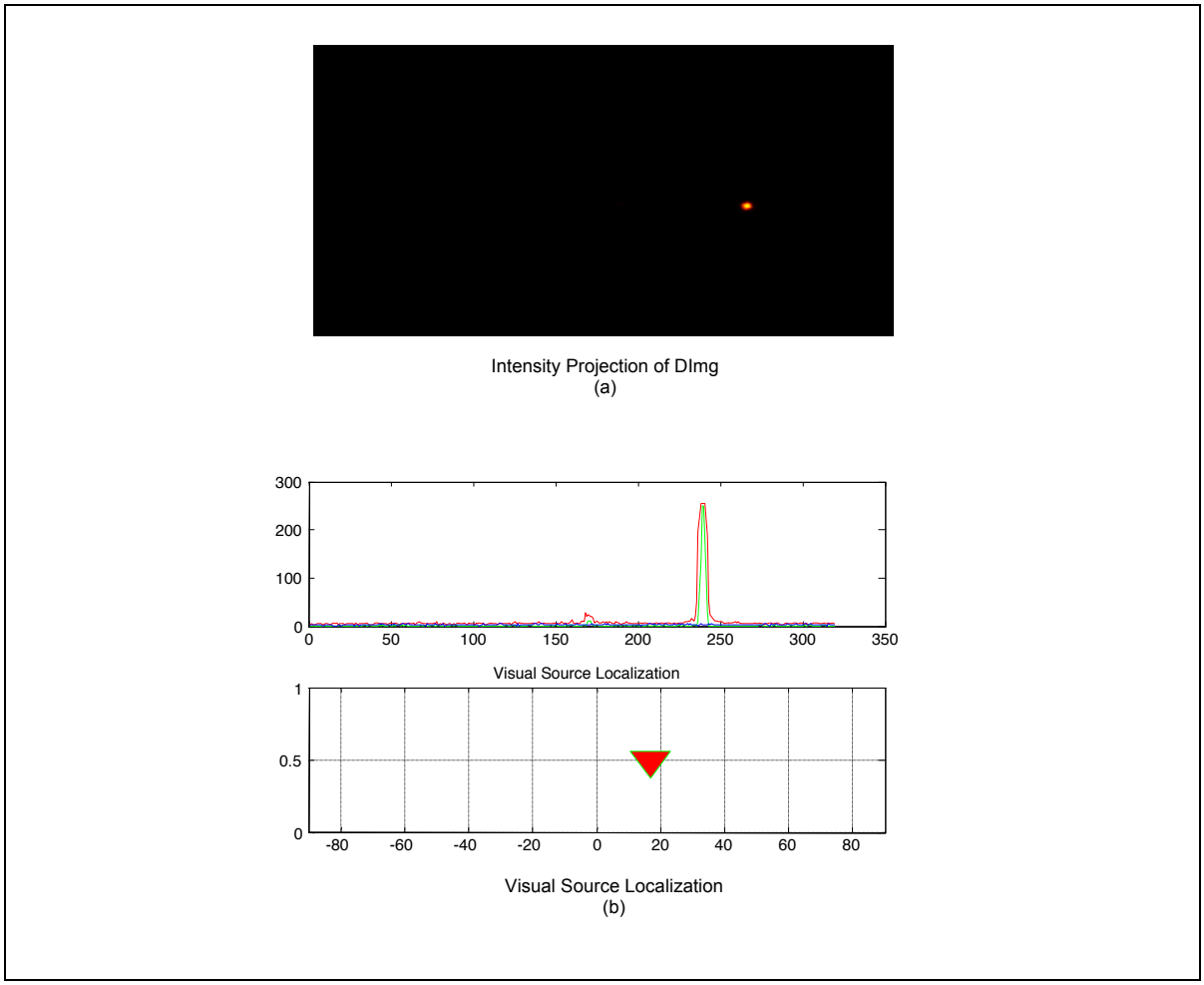

Figure 3.12 ***Visual localization using difference image:*** *(a) The difference image (DImg) is shown scaled to a unique size for all the images, to standardize it as a vector for the map alignment in the multimodal phase. (b) Horizontal Scale Frame image (HSFr) is a frame, which is scaled to* -90^0 *to* 90^0.

In this HSFr the horizontal axis was divided into 10^0 intervals. Hence, all the visual information that arrived at the camera was transformed into difference image intensity plot and finally plotted on an HSFr to locate the source in the visual environment. Within this data collection process, different inputs were gathered and later used as a test set for the integration model that could generate a multimodal integrated output.

By running the above experiment on the behavioural platform with given conditions, the results obtained are recorded as shown in the Table 3.3.

Visual Localization Output Table							
Noise level: Lights On (Day)				*Intensity: 0 – 0.5*			
Visual Intensity Vs Angle (degree)	**-30^0**	**-20^0**	**-10^0**	**0^0**	**10^0**	**20^0**	**30^0**
Set 1	-30.15	-18.98	-10.89	1.01	9.46	19.45	30.01
Set 2	-29.12	-17.63	-10.08	0.46	10.03	18.98	29.98
Set 3	-30.01	-19.01	-10.00	0.98	10.98	18.01	30.45
Set 4	-29.98	-19.89	-9.98	-0.11	10.00	19.08	29.46
Set 5	-30.72	-18.53	-10.76	1.46	10.01	20.75	30.54
Set 6	-29.12	-20.14	-9.98	0.15	10.05	19.96	30.01

Table 3.3 ***Visual localization output table:*** *Accuracy of the projected angles in degrees to various visual stimuli from different set of .*

For each of the stimuli transmitted, a visual aid (LED) is activated (turned on) at angles varying between -30^0 to 30^0. This range complies with visual range of the agent. Based on the unimodal output obtained, the following Table 3.4 shows the error obtained during the localization.

Visual Localization Error Chart							
Noise level: Lights Off (Day)				*Intensity: 0 – 0.5*			
Light Intensity* Vs Angle (degree)	**Set 1**	**Set 2**	**Set 3**	**Set 4**	**Set 5**	**Set 6**	**Mean Error**
-30^0	0.15	-0.88	0.01	-0.02	0.72	-0.88	**0.44**
-20^0	-1.02	-2.37	-0.99	-0.11	-1.47	0.14	**1.02**
-10^0	0.89	0.08	0.0	-0.02	0.76	-0.02	**0.30**
0^0	1.01	0.46	0.98	-0.11	1.46	0.15	**0.70**
10^0	-0.54	0.03	0.98	0.0	0.01	0.05	**0.27**
20^0	-0.55	-1.02	-1.99	-0.92	0.75	-0.04	**0.88**
30^0	0.01	-0.02	0.45	-0.54	0.54	0.01	**0.26**
Mean Error	**0.60**	**0.69**	**0.77**	**0.25**	**0.82**	**0.18**	**0.55**

Table 3.4 ***Visual localization error chart:*** *The error obtained in localizing the visual stimuli for each of stimuli provided.*

After running this experiment based on a six different sets, a number of difference images were collected. By transforming the image onto a horizontal map at 10^0

intervals, the angle of the source was identified. The error obtained during the localization from Table 3.4 is transformed onto a graph as shown in figure 3.13.

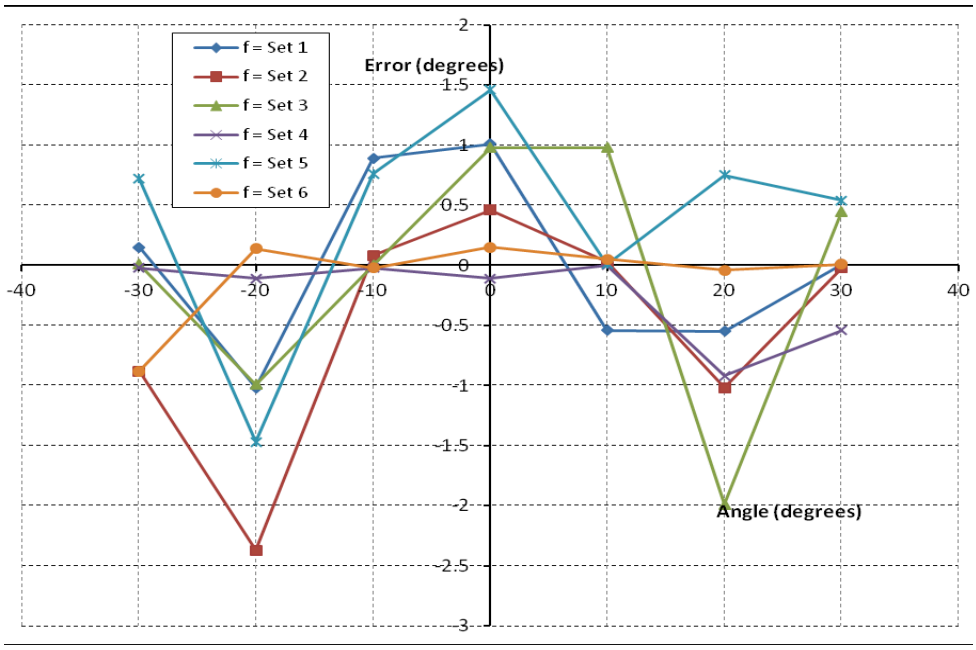

Figure 3.13 ***Visual localization error graph:*** *Graphical representation of visual localization error, featuring relative similarity of each stimuli to the target localization.*

From the above graph drawn between visual localization error and localization, the errors lie in the range of (-2.5^0, 1.5^0). On the other hand, the mean error is less than one degree. Though the error appears to be out of range (-2^0, 2^0), it was significant when it comes to demonstrating the effective output. From a series of visual experiments conducted with variable light and laboratory conditions, an input data set of 162 samples was generated.

Finally from the above unimodal data collection and analysis, it is observed that a satisfactory similarity was obtained from both audio and visual experiments compared to the target. With the audio experimental data, considering the level of accuracy within $\pm5^0$, 80% of observations were similar to the expected targets. Similarly with the visual input data, considering the level of accuracy within $\pm2^0$, 90% of observations generated were similar to target results.

3.6 Computational Design (Stage-II)

In this phase, a methodology for audio and visual stimuli integration is proposed in order to investigate the integration criteria along with enhancement and depression phenomena associated with it. As discussed in Chapter 2, multimodal integration is a widely researched concept whose efficiency is determined based on the requirements and targets.

3.6.1 Integration Phenomena

During integration, the signal strength was also included in the network for generating the output. Stein and Meredith have previously identified two phenomena, depression and enhancement, as crucial for multimodal integration. In the approach here, the visual constraints from consecutive frames for confirming whether or not a signal of low strength was noise, have also been considered. By reducing the frequency to 100Hz for a weak audio signal and by also varying the LED intensity in the behavioural environment, it was possible to generate a weak stimulus to study the integration phenomena response.

A synchronous timer was used to verify and confirm whether the visual and audio stimuli are synchronized in terms of Time Of Arrival (TOA). If the arrival of the stimuli is asynchronous then an integration of the inputs is not necessary, as the location of the source can be determined depending on the unimodal processing. In cases of multiple signals with a synchronous TOA, the *signal strength* is considered for both signals. Once the strongest signal is identified then preference is given first to this signal and only later an additional preference may be associated with the other signal. This case occurs mainly with unimodal data, such as a visual environment with two different visual stimuli, or an audio field with two different audio stimuli.

3.6.2 Design Criteria

Initially computational approach was adapted to verify the mechanism of integrating audio and visual stimuli based on stimuli strength and time of arrival. Although the outcome is multimodal, when it comes to applying the model to applications where the agent has to receive live feeds of input data, the required level of accuracy is not achieved. This is because of noise levels that are included in the input data, along with the level of prediction states. Hence, to increase accuracy, the introduction of a filter would have been appropriate.

One possible solution might have been a Kalman filter, due to its inclusive 'predictor-corrector' nature. The Kalman filter is an efficient and widely used mechanism in stimuli processing applications to reduce noise levels. However, the computational model is a static mechanism towards generation of multimodal output (Funk, N, 2003). A static modelling integration model cannot produce an efficient output, since the error from input to input remains unchanged. Hence to ensure error reduction, a learning mechanism is introduced using a neural network concept. In the next chapter, integration is studied in detail along with the feasibility study and applicability.

3.7 Summary and Discussion

This chapter provides an introduction to the methodology adopted to fulfil the research question. The methodology provides a sensitive and systematic combination of qualitative and quantitative aspects such that it can be executed at all possible states of its development. This methodology describes the process of research implementation at conceptual, design and computational levels to project a clear view of design and development.

Initial sections of this chapter describe inputs that are needed and outputs that can be obtained by using multimodal integration. Due to the non-availability of input data sets, the methodology proposes input data-set generation and collection. Hence an experimental platform is considered that is helpful for both input data set generation, experimentation of multimodal integration and testing.

This chapter also describes the cross-correlation and difference image mechanisms that are adapted for audio localization and visual attention. Computational design aspects of how stimuli localization is carried out in both audio and visual stimuli cases, based on mathematical formulations, are also discussed. These formulations suit the requirements by considering possible factors that affect localization and multimodal integration.

Finally, the design is carried out in two different stages, where Stage-I deals with unimodal stimuli processing and generation along with multimodal stimuli generation. Stage-II deals with multimodal stimuli processing along with integration model generation and development. In the next chapter, a detailed study is carried out on integration mechanisms in terms of methodology, design, computational design and experimentation. Architectural aspects of the integration model are also described.

Chapter 4

Neural Network Modelling of Multimodal Stimuli Integration

4.1. Introduction

As a continuation of the methodology, in this chapter the design and development of the integration model is discussed in detail. The methodology includes audio and visual stimuli determination, integration design formulation, and model development. During the development process, a computational approach towards integration was first attempted, where it is evaluated to determine its effectiveness. This helps in identifying problems that must be overcome when developing the new architecture.

The proposed neural network approach is adopted to overcome the difficulties of the computational approach with the help of the learning concept and training of the network for an effective multimodal outcome. The chapter details the design and development of the neural network, along with implementation and testing. The network was later subjected to learning and during the process, the role of dimensionality reduction towards training and testing was also discussed. The multimodal outcome for the neural network approach is verified against the projected outcome and the success of the model including accuracy was determined.

4.2. Multimodal Stimuli Determination

In this section, the integration of audio and visual information based on the SC is described. The received audio and visual inputs are preprocessed considering the

functionality of the optic chiasm (indicated in figure 2.2) and the information flow in the optic tract, along with information from the audio processing region of brain, IC. This preprocessing generates the *DImg* from the captured visual input along with the TDOA for the audio stimulus, as shown in Chapter 3. The preprocessed information enters the SC network, which performs multimodal integration of the available stimulus, and the corresponding motor output is generated. The flow of information is shown in figure 4.1.

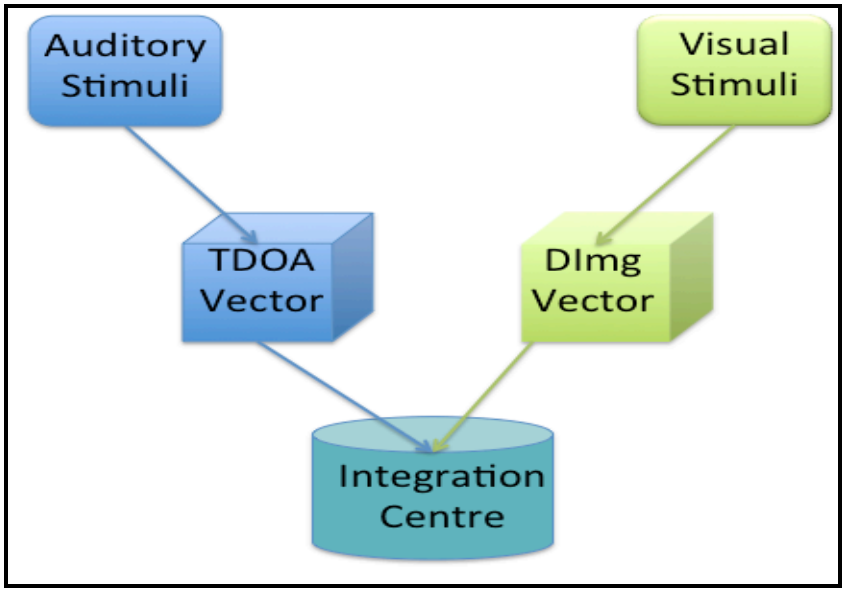

Figure 4.1 ***Stimuli flow mechanism from environment to the SC:*** *Schematic representation of stimuli flow from the external environment to the superior colliculus model*

The network model is mainly focused on stimuli processing in the form of spacial maps to resemble the actual integration in the deep layers of the SC. Hence, the model is considered to have two types of inputs towards integration:

- the *TDOA* audio map
- the *DImg* visual stimulus map

The input audio stimuli arriving at the integration network will be in the form of a vector, which is the transformed version of the input *TDOA*-based stimuli. Similarly the visual input to the network is the vector-transformed version *DImg* of the original stimuli. These resemble the various transformations that audio and visual

stimuli undergo during their transmission from the eyes and ears to the SC. In order to consider the effectiveness, especially for multimodal stimuli cases, the vectors are also equipped with stimuli intensities, as established in Chapter 3. The vector outcomes of audio and visual stimuli are not of the same magnitude due to stimuli intensity variations.

Since the integration model is focusing on horizontal saccades, only the variations on a horizontal scale are considered at this point, although this can be extended to vertical saccades by using a two-dimensional feature map representation. To identify the maximum intensity cases of multiple stimuli, a Bayesian probability-based approach is used to determine the signal that is input to the network. A synchronous timer is used for counting the time lapse between the arrivals of the various stimuli of the corresponding senses. Hence, the occurrence of multiple unimodal stimuli is detailed.

In order to integrate the stimuli it is necessary that the vectors should be equi-dimensional so that a common platform can be used for integration. Hence, the unimodal vectors can be interpolated on to a single reference frame (containing localization and intensity data only) in the form of vectors such that stimuli data can be optimized without loss of information. Alternatively, the dimensionality of the vectors can be altered. The visual stimulus obtained from the input in the range (-30^0, 30^0) is processed to generate *DImg*. Since the visual stimuli obtained from this experiment have lower range of coverage, scaling of the vector is adapted. The vector transformation of *DImg* is scaled to 180^0 HSFr. The final obtained visual vector will be on 180^0 reference. However, if the received stimuli had greater range of coverage similar to auditory, then scaling factor can be avoided. Similarly, the audio stimulus was initially collected over a range of 180^0 (based on the location of the stimuli source). Later the generated *TDOA* is used for localization and is projected onto 180^0 scale. This also corresponds to the localization of the unimodal instance. When it comes to determining localization for multimodal instances, due to the presence of various stimuli vector reference, the stimuli vector data is interpolated to a common reference such as HSFr.

When both the vectors are available within the required dimensional space, the process of integration is carried out. As established in section 2.3 of chapter 2, stimuli integration takes place only on the simultaneous arrival of audio and visual inputs. It is clear that integration arises only when the stimuli arrival is synchronous. In such a case, a stimuli intensity factor is considered to identify the next gaze point for the agent. Hence, for each and every stimuli vector generated, the weight is also calculated.

In the case of audio data, a weight vector represents the strength of the sound stimulus, and the intensity of the stimulus peak generated. However in the case of a visual stimulus, the weight vector is an encoded Red-Green-Blue (RGB) representation that determines its intensity.

4.3. Integration Model Design and Processing

Based upon the audio and visual vectors described above, an integration model is designed in order to perform audio and visual integration. From the literature review (Chapter 2), based upon the two stimuli arriving simultaneously, a dual layered integration model is proposed. This model depicts the processing of the SC in stimuli arrival and transmission across the network. Figure 4.2 shows the basic functionality of how the processing is to be carried out.

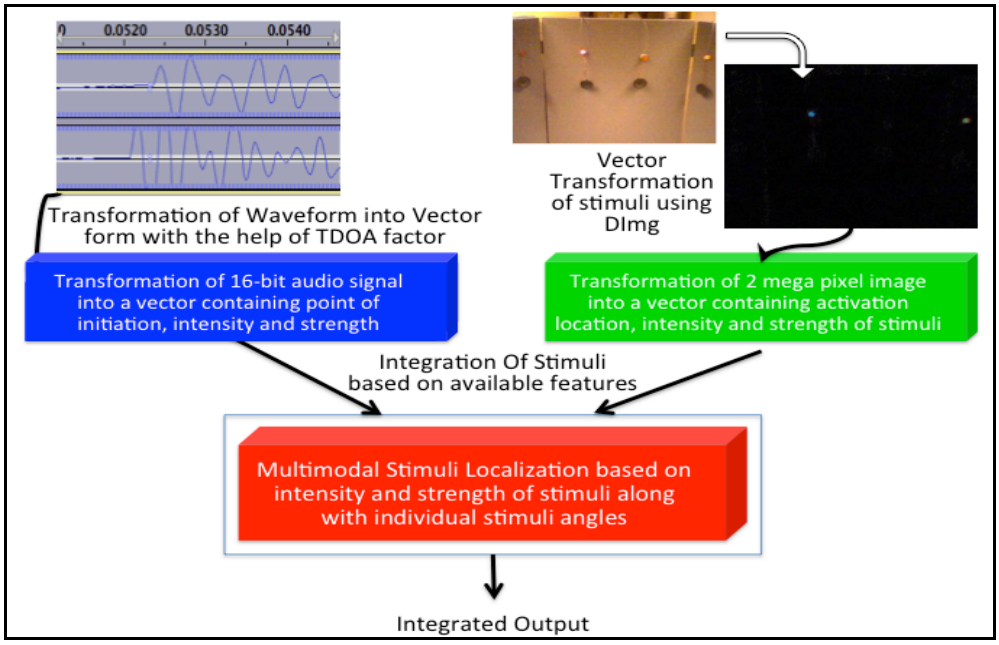

Figure 4.2 ***Detailed transformation mechanism from unimodal stimuli to multimodal output*****:** *Integration Model depicting the transformation of stimuli into vector form, outlining the step-by-step changes towards integrated output generation*

In figure 4.2 the process of stimuli transmission from unimodal to multimodal states with the help of integration is described. However, when it comes to the computations that are used to process the integration, they vary depending upon the approach. Based on the literature review it is observed that various computational approaches can be used to perform the integration. In this thesis the integration model development is initiated with a computational approach. The approach is modified accordingly based on the requirements and performance.

4.4. Computational-based Integration Model

This approach is also called a computational approach, which uses conventional computational methods to perform the integration of audio and visual stimuli. The outcome of the integration model is an average that is located within or around the audio and visual stimuli vectors.

For example traditional averaging of stimuli will provide a region of concentration that is in between them. Since the integrated output can be localized to either of the input stimuli, a weight factor is considered that defines the strength of the

stimulus. Using this factor the output is a region of concentration that is higher in weight for one of the stimuli, depending on their relative strength.

4.4.1 Integration Criteria

The processing of the integrated output is as follows:

$$\text{Integrated Output} = \frac{\{(W_v \times V_1) + (W_A \times A_1)\}}{(W_v + W_A)} \quad \text{..... Eq. (4.1)}$$

Where, each factor of the equation depends on the input stimuli obtained.

W_v = Visual Vector Weight is the absolute value of the vector transformed visual stimuli containing the weights of the activation in the given range of stimuli.

W_A = Audio Vector Weight is the absolute value of the vector transformed audio stimuli containing the weights of the audio spikes in the given range of the stimuli.

V_1 = normalized Visual Intensity is the summation of red, green and blue values of the intensities obtained in the difference image to the column ratio of the pixels from the camera used.

A_1 = normalized *Audio Intensity is the highest peak recorded in the audio stimuli analysis, which is used during cross-correlation for stimuli localization.*

This equation 4.1 determines the weighted vector outcome in terms of the directional vector of the integrated source location. This signifies that the outcome concentration is biased to the area of higher strength. Finally, since that integration output concentration cannot always correspond to the source of origin, the stimulus closer to localization is considered as source of stimulus origin. This signifies the integrated mean always lies between the two variables, and the chances of integrated output exceeding either of the localization are less.

4.4.2 Integrated Outcome

The integrated output generated from a range of inputs using the computational approach is shown in table 4.1. The table contains the individual localization obtained at the end of the pre-processing state along with stimuli intensity. The integrated output is determined based on eq. 4.1, and source directional information is expressed as an angle (degrees) from the center of agent, while the corresponding intensities are normalized and expressed within the range (0, 1).

The difference between the experimental integrated output and the expected output is determined as an error and is provided in Table 4.1.

Input	Visual_Source Angle	Vis_Intensity	Audio_Source Angle	Aud_intensity	Expected_Output Angle (E)	Integrated_Output Angle (I)	Error_Obtained (I-E)
1	-16.5	0.41	-17.34	0.08	-16.5	-16.632	0.132
2	17.35	0.62	-8.57	0.32	17.35	8.468	8.882
3	17.35	0.62	10.73	0.30	17.35	15.205	2.145
4	-30.7	1.00	21.87	0.06	-30.7	-27.912	-2.788
5	-16.53	0.35	33.97	0.09	-16.53	-5.992	-10.538
6	17.35	0.47	-17.34	0.08	17.35	12.219	5.131
7	17.35	0.42	31.97	0.45	31.97	24.841	7.129
8	-30.86	1.00	6.42	0.36	-30.86	-20.931	-9.929
9	17.35	0.51	17.34	0.11	17.34	17.348	0.002
10	17.35	0.51	31.44	0.18	17.35	20.930	-3.580
11	17.35	0.53	-17.34	0.15	17.35	9.727	7.623
12	17.35	0.53	-6.42	0.95	-6.42	2.063	-8.483
13	17.35	0.52	10.73	0.92	10.73	13.127	-2.397
14	-30.86	1.00	21.87	0.13	30.86	-24.835	-6.025
15	17.35	0.42	-4.27	0.28	17.35	8.753	8.597
16	17.35	0.42	-19.59	0.68	-19.59	-5.511	-14.079
17	17.35	0.43	-8.57	1.00	-8.57	-0.758	-7.812
18	17.35	0.44	6.41	1.00	6.41	9.728	-3.318
19	17.35	0.43	24.19	0.78	24.19	21.750	2.440
20	-30.7	1.00	-15.12	0.38	-30.7	-26.410	-4.290
21	17.35	0.47	-15.12	0.81	-15.12	-3.232	-11.888
22	17.35	0.47	-8.57	1.00	-8.57	-0.229	-8.341
23	-16.5	0.31	8.57	1.00	8.57	2.640	5.930
24	-30.87	1.00	31.44	0.54	-30.87	-9.126	-21.744
25	-30.37	1.00	17.34	1.00	17.34	-6.468	23.808
26	-30.37	1.00	-26.55	1.00	----	-28.460	---

27	-16.5	0.25	-8.57	1.00	-8.57	-10.181	1.611
28	17.35	0.44	-8.57	1.00	-8.57	-0.709	-7.861
29	17.35	0.20	19.59	0.27	17.35	18.428	-1.078
30	-30.87	1.00	26.55	0.70	-30.87	-7.286	-23.584

Table 4.1 ***Computational multimodal integration output table*****:** *Table containing the output generated from the computational model, from the input stimuli localization data and their intensities normalized between 0-1.*

In the Table the highlighted row-30 signifies the following:

Column 1 is the visual source angle (-30.87^0) reached from the multimodal stimuli with stimuli intensity (1.00) in column 2. Column 3 is the audio source angle (26.55^0) reached from the multimodal stimuli with intensity (0.70) given in column 4. Column 5 determines the output generated by the integration model which in this case is -7.286^0. However the labeled data signifies the target output as -30.87^0 based on the intensity of stimuli. The final column of the table presents the angle error that the model has generated during the process.

4.4.3 Error Determination

From the results obtained using the experimental platform, a sample set is provided to determine the typical deviation or error obtained through the computational approach to multimodal integration. Figure 4.3 shows the error between the expected and obtained integrated output.

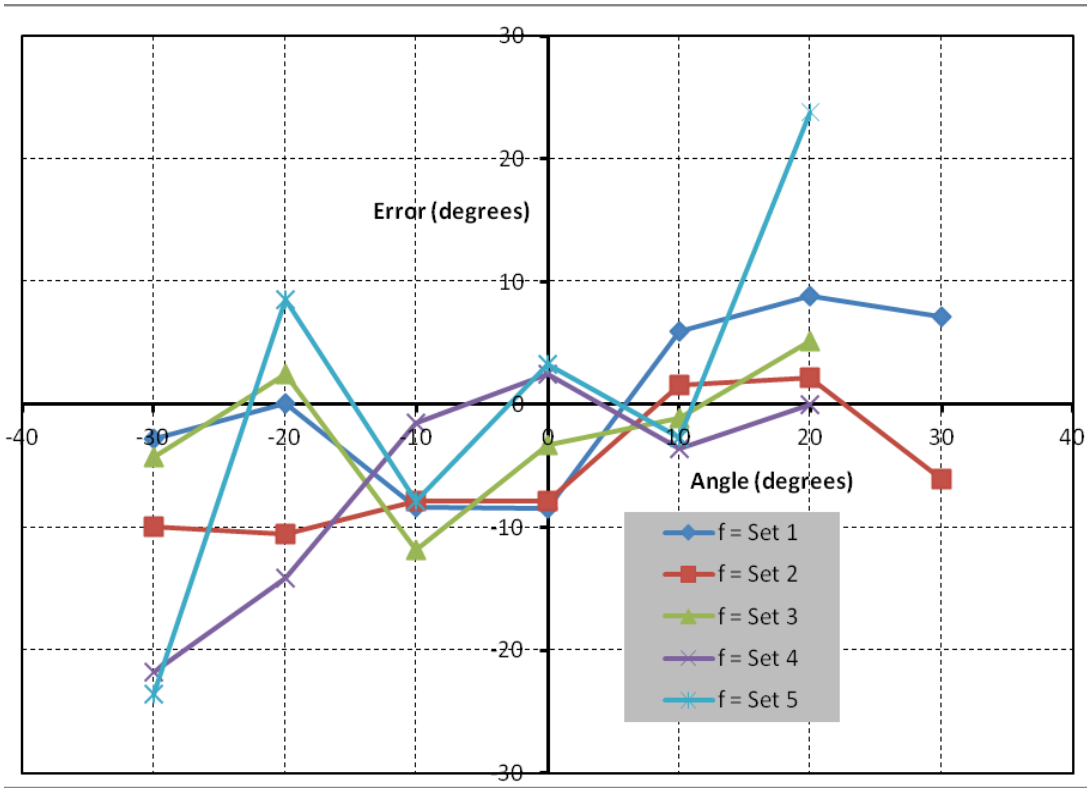

Figure 4.3 ***Error representation of computational model output*****:** *Error analysis graph from the above random selection of multimodal outputs. This plot is the representation of error in the available input space signifying the maximum error obtained.*

Figure 4.3 indicates the distribution of error, from the available inputs. The obtained error lies in the range (-25^0, 25^0), which is over the estimated $\pm 5^0$ of variance. Hence, an alternative approach to multimodal integration is justified on performance.

It is observed that the error is significant. However, using non-linear interpolation (Park, 1997) based on von Mises angular distribution, parameters governing the integration function can be used instead of a least mean square function to reduce the error obtained (Harremoes, 2010). This leads to a minimal error along with a smooth localized output for the integrated data.

An alternative computational approach could involve the use of a filter such as the non-linear Kalman filter (Landis, 2005). However, since the principal aim of this project was to develop a biologically inspired architecture, the approach was not

pursued further, and an alternative approach using artificial neural networks is considered.

4.5. Neural Network-based Integration Model

In this section, the methodology concludes with a neural network based integration model. This is developed using the computational approach in conjuction with a neural network platform in order to overcome computational difficulties, such as error determination and reduction, without affecting the computational speed. It also reduces difficulties associated with on-going data processing and transmission, such as vector transmission and dynamic data processing.

4.5.1. Why neural networks

Neural networks represent a widely used data processing method whose computational patterns are close to biological behaviour patterns. Neural networks are known for their computational efficiency through parallel processing, even in the presence of noisy data. Since the concept of neural networks is developed from the computational patterns between the neurons of brain system as shown in figure 4.4, they are classified as simple inter-connected message transfer multiprocessing states/stations that can perform computations at a higher level (Smith, 2003).

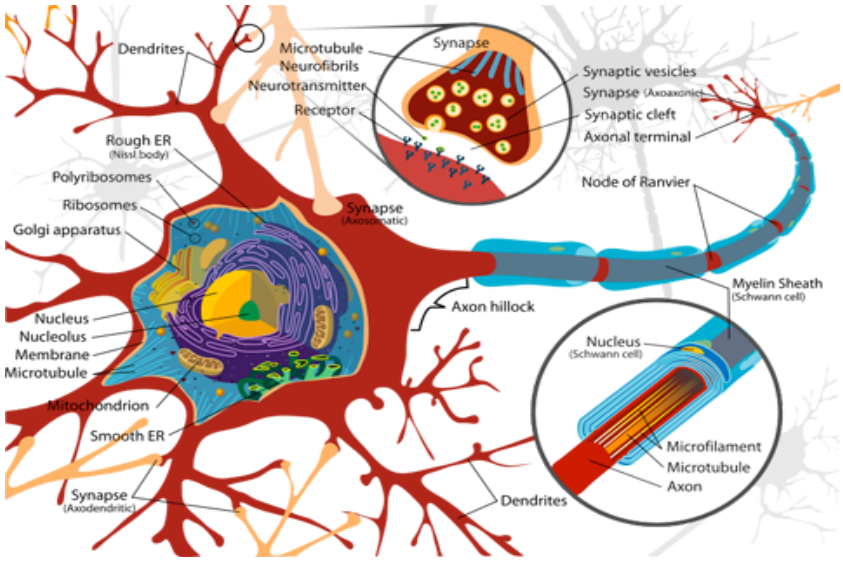

Figure 4.4 ***Biological neuron of human brain*****:** *Neural activity in human brain. The image signifies the inner structure of brain neurons and their neuron transmission across dendrites. Image courtesy by Software Creation Mystery*

Neural networks are used mainly in applications dealing with deriving patterns from imprecise data. When it comes to computations, a neural network adapts to the input data and uses a parallel computation methodology in deriving a solution. Unlike traditional computing methods, it is not always necessary to feed the network with conventional algorithmic methods. However, a feasible combination of neural networks and conventional algorithmic methods will often render an efficient outcome (Stergiou, 2007).

In this project a dynamic combination of audio and visual stimuli are fed to the network. Hence, the chances of noise in the form of distortion of the stimuli, or external noise, are significant. To improve the efficiency of the network it is very important that the model adapts to the input stimuli and generates an effective audio-visual integrated output. Alternatively, implementing learning criteria will help improve the performance of the network along with an adaptation towards new input data. Finally, the neuron computations performed in the SC of the brain can be modelled using a biologically inspired network to perform the audio-visual integration. This is the rationale behind the use of neural networks as a platform for the development of the audio-visual integration modal inspired by the Superior Colliculus.

4.5.2. RBF Motivation

Considering the aspects discussed in the literature review, it was considered important for the model to be biologically inspired to enable instantaneous transformation of multimodal stimuli into accurate motor commands. Due to the need to process both audio and visual layers, the model was required to perform multi-tasking. The input data that is delivered to the network model may not be linear data. Hence the model should perform effectively even with non-linear data. Based on the above processing requirements, a Self Organizing Map (SOM) network is a potentially effective choice due to the mapping feature that simulates the localization properties in the input space of the brain system. A SOM network is based on determining the density of input concentration over a deterministic dimensional space. Compared to other neural network techniques, the SOM is considered more effective for classification modelling than prediction (Khan, 2009).

The SOM network has previously been used for localization problems (Casey and Pavlou, 2008), however, any missing or incomplete data sets will result in a completely deviated or out-of-range output. This causes ineffective localization, resulting in poor performance, and due to the clustering nature of the network, the SOM even tries to cluster the noise present in the data, causing a deviation in the localization (Pang, 2003).

The Radial Basis Function (RBF) network has similar properties, such as biological plausibility, for implementing neural phenomena. RBF networks are effective in complex localization problems even with non-linear data (Bors, 2001) involving data features of multi-dimensional space (Powell, 1987). When it comes to data transformations and interpolation of input feature data, RBF networks can effectively perform the weight adjustments such that criteria for the integration can be satisfied (Broomhead, 1988). Similarly, the RBF can effectively optimize the model output with the available training set and improves efficiency as the training set increases (Moody, 1989). When it comes to training, on-line training features adapted by the RBF fit the changing data sets (Bors, 1996). A Matlab model of the

RBF network is shown in figure 4.5 detailing the functional working and data transmission.

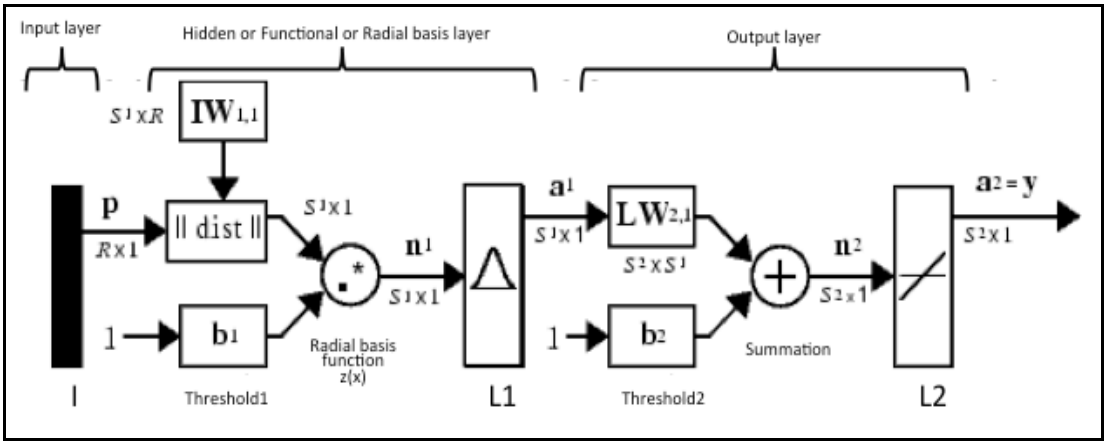

Figure 4.5 ***Radial Basis Function neural network model using Matlab*****:** *A typical RBF network containing input, hidden and output layer detailing the data processing and transmission.*

In the above network:

I – Input Layer
L1 – Hidden Layer operating on highest activation
L2 – Output Layer operates on linear function
b^1, b^2 – bias or threshold at layer 1 and 2
$IW_{1,1}$ – Represents the weight allocated with respect to input layer
$LW_{2,1}$ – Represents the weight obtained from L1 allocated to output layer
||dist|| – Distance function
s^1, s^2,R – Represents the matrix order so that the computations are applicable

The network is a typical radial basis neural network with input, hidden and output layer, as shown in figure 4.5. The input to the network was transmitted from the input layer to the hidden layer, where the radial basis function is applied. In the hidden layer, with the allocation of random weights to the hidden neurons, with highest activation were identified. Using input weights on the radial basis function against a given threshold, the output generated was transmitted to the output layer through L1. In the output layer, the received activation, the linear weights of the neurons and the thresholds were accumulated and the summation was transmitted as output to L2. At L2, a linear deterministic value is generated as output of the network.

An RBF network was chosen to design the integration model. During the design process, initially the radial basis function has to determine the weights of the network for generating the required output. However, a distance function is considered as an activation function as shown in eq. (4.2) along with larger scope for inputs (radius for the function in input space). To generate an activation function that can entertain a varied range of inputs along with deterministic output, a generalized function is required. A generalized activation function requires a greater number of neurons for its generation.

$$Z(x) = O_i(x - u) \qquad \text{..... Eq. (4.2)}$$

Where *x* and *u* are the initial and center of the input vectors that have initiated the RBF network in the integrated output function.

The activation function should be able to classify the patterns from the input entries. Due to the lack of generalization, a Gaussian distribution function is used instead of a discrete function. Gaussian functions are known for their consistency for the output irrespective of the number of hidden units.

The Gaussian activation function is defined by equation 4.3:

$$Z(x) = \beta \sum_{i=1}^{n} W_{(i)} e^{\|x - u_{(i)}\|^2} \qquad \text{..... Eq. (4.3)}$$

Where W_i, β are the current weight of neurons between the input and hidden layers, respectively. The weight parameters in the function have considerable influence on the entity that can change the final output of the network.

Training algorithm:

1. Initialize the system states
2. At hidden layer:
   - Using the distance function determine the weight of each input vector ($IW_{i,i}$)
   - Compute output at the hidden layer (L1) using RBF function Z(x)
   - Determine the highest activation using b1

- Transmit the output to hidden layer (L1)

3. At output layer:
   - The weights ($LW_{j,i}$) at the hidden layer are fixed based on the successful generation of output
   - Thus obtained weights are used to determine output using summation function along with bias (b2)
   - The gradients at this level for the obtained activations with respect to weights should be zero, signifying the target
   - Using linear separability, the final output of the network is obtained

---

To construct a RBF network it is important to determine the network features. Hence the following features are considered for the design of the radial basis function network. Figure 4.6 is the network design and implementation carried out using Matlab.

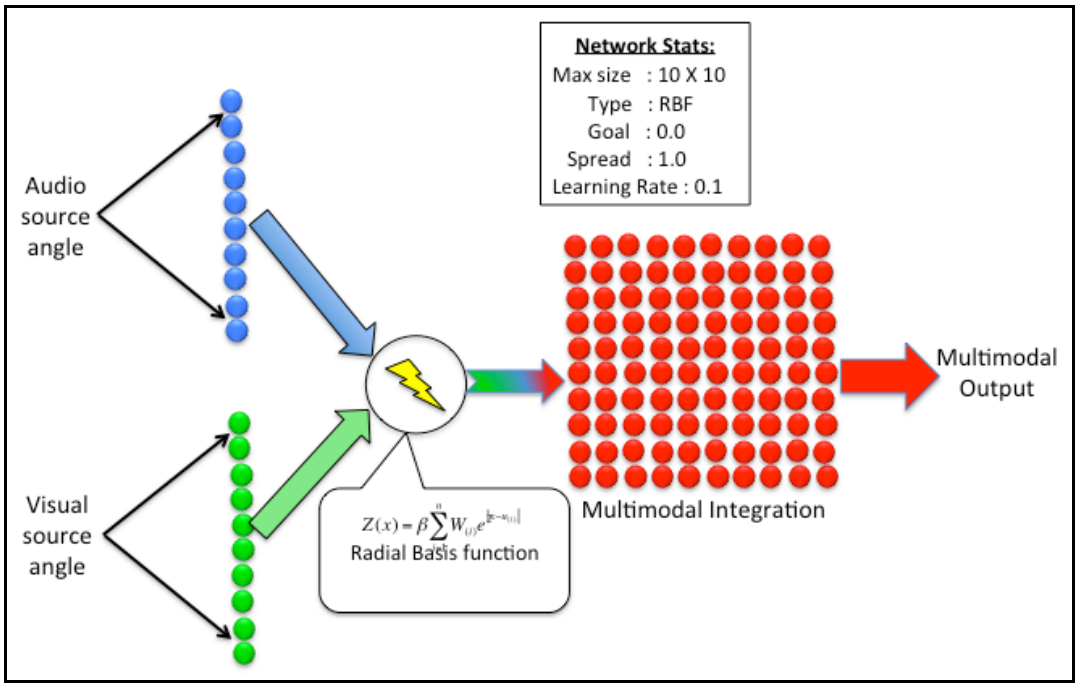

Figure 4.6 ***RBF based multisensory integration neural network model*****:** *Multisensory Integration model. Radial basis neural network model used for generating multimodal output for both unimodal and multimodal stimuli inputs.*

The network is a 3-layer structure with input, hidden and output layers. The hidden layer is supplied with neurons during the process of network development based

on the modification of the radial basis function towards the goal. The network is provided with variables such as input vectors, target vectors (expected output), error or goal along with a limit on the number of neurons. The radial basis function spread, which defines the radius of the activation function across the hyper dimensional space of the hidden layer, is initially large. A larger spread has to be used to make the approximation smoother, without increasing the number of neurons for generalization.

Considering the input layer, it is capable of receiving information from the environment in the form of visual or audio vectors. This vector information is thus passed on to the hidden layer that uses a Gaussian activation function to determine the absolute distance between the hidden dimensional space and the input vectors. Later, with dimensionality reduction of the data-sets and with the help of a summation function, the output is delivered to the output layer.

4.5.3. Dimensionality

In this section, the details of how dimensionality is varied during the course of integration and how the transformations are carried out are discussed. Dimensionality usually arises when there is feature selection involved in larger data sets. During classification, various parameters or dimensions are used to enable the isolation of required features from the input space. During the process, according to Bellman, as the input space grows larger, many parameters or dimensions are required to perform feature isolation (Bellman, 1957). This eventually gives rise to the dimensionality problem i.e., “input space and dimensionality are linear in nature”, generating sparse data sets for information classification and organization problems.

While feeding the input patterns to the neural network, in the case of huge datasets, if no pre-processing is carried out then the number of computations required to process the network increases. In the case of radial basis networks, an

increase in the number of computations for pre-processing requires more hidden units. An increase in hidden units will eventually affect the performance of the network by slowing it down. For practical applications, where speed and space are constraints, it is important that dimensionality reduction should be carried out for improving the network throughput.

Considering the primary motivation for the development of a multimodal integration model with biological inspiration, dimensionality reduction is initially carried out on the spatial features of the untagged input dataset obtained from the environment. According to Xiuju Fu, data dimensionality reduction can reduce the complexity of a network structure, along with increasing the efficiency of data processing (Xiuju Fu, 2003). Though different statistical approaches such as Bayesian with the use of Markov chain Monte Carlo methods are available, a nearest neighbour search is used due to the reliability of the distance function.

Hence, during the development of the RBF network, while receiving the input from the environment at the pre-processing state, the input stimuli are subjected to feature extraction. Since the output of the model is intended for generating saccades, only the input data (from the received stimuli) that is required is considered. By doing so, sensory stimuli with only required features, such as stimuli strength, intensity, time of arrival and depth of signal, are carried to the next state, without loss of data. During the process the visual data undergoes the transformation shown in figure 4.7.

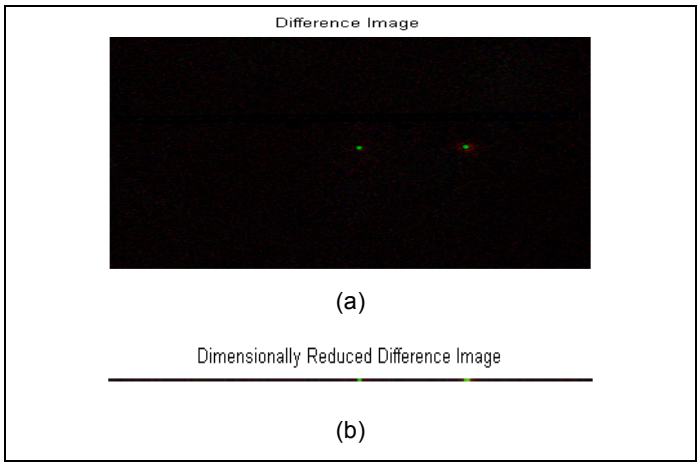

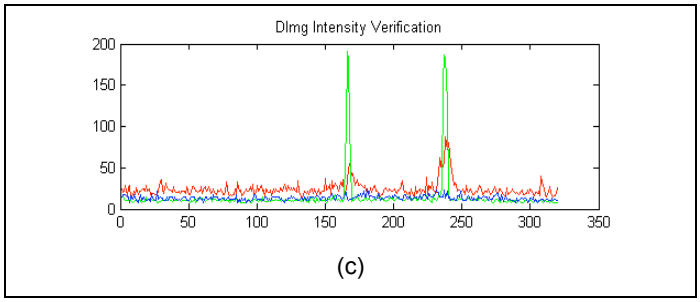

Figure 4.7 ***Dimensionality variation in visual stimuli***: *(a) is the difference image that is collected from the environment, while (b) is the feature extraction segment of figure (a). Figure (b) is considered as dimensionally reduced due to the elimination of the vertical axis. Hence variables such as horizontal axis, intensity and depth are transmitted to the network. (c) Represents the light intensity of the reduced difference image, signifying null loss of data.*

When it comes to data from the received audio signal, it is important to determine the maximum similarity point between the left and right ears for an accurate identification. Hence, from the received stimuli the integration model, extracts the similar features using the TDOA along with signal strength over a smaller range of signal that has maximum similarity, as shown in figure 4.8. By doing so, the amount of signal that is inspected for the current state is minimized prior to the multimodal integration.

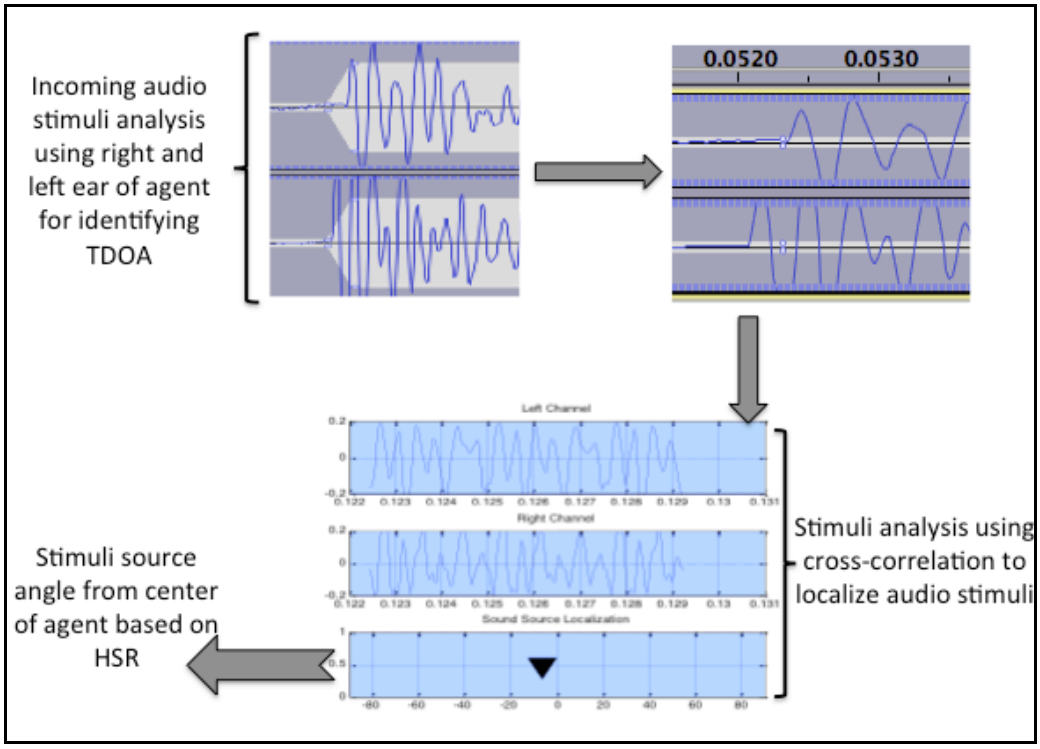

Figure 4.8 ***Audio Analysis using limited stimuli to identify localization:*** *Audio analysis description using the binaural separation and stimuli localization using cross-correlation based on stimuli arrival.*

Once the pre-processed data is available at the integration model, in order to increase the computational efficiency, only factors that influence the multimodal stimuli for localization are considered. Similar to the common platform that is used for referencing the unimodal localization of audio and visual stimuli, a common Spatial Reference (SRf) platform is used to analyze the stimuli. However, strength and intensity of the stimuli are two primary factors that are prioritized during the process.

With the above-mentioned series of modifications concerning computational time, network design and development, the integration network model was developed to perform the integration of audio-visual stimuli that arrive simultaneously at the agent.

4.5.4. Learning Criteria

Learning was an important aspect of neural network design that involves the process of training the network with the available data, so that after the process the network was able to provide the desired outcome (Cheshire Engineering Corporation, 2003). It was carried based on the weight adjustment of the neurons such that least possible error will be generated while delivering the output. The processes of learning in this multimodal integration RBF network was carried in three steps related to centre, weight and width of the network.

On obtaining the outcome from the integration network, in order to determine the output from the training pattern, the k-nearest search algorithm was used in which the distance between the individual outputs within ‘k’ distance ranges was

considered. Also the computational time that was required to perform the distance function was useful for quick response generation. The following algorithm was used to determine the nearest output from the training set.

K-nearest neighbour algorithm:

1. Compute Euclidean distance between the target and available training space
2. Determine the sample space that fall within the range of acceptable localization
3. Using root mean square error, determine the nearest neighbour optimally using training space
4. Determine the weighted average of the nearest source location as the output of the integration model and transmit the error back to the model.

Since the inverse of distance is proportional to the weighted average, the k-nearest neighbour should always be better than the predicted.

Initially, a function (radial basis function) is derived, such that the weights of the neurons can be generated. This function is the core (center) of the network. Later, the derived function should be approximated (generalized) to an extent to perform the required task for the network. This function is responsible for generating the neuron weights in the network. Finally, the width or network training rate, which performs the training, was based on the initial weight and time steps that are used during network initiation.

The radial basis neural network model is trained over associative learning such that the association of the stimuli strength can be calculated at the maximum location of integrated intensity. The network is trained over 900 epochs and the performance graphs are as shown in figure 4.9.

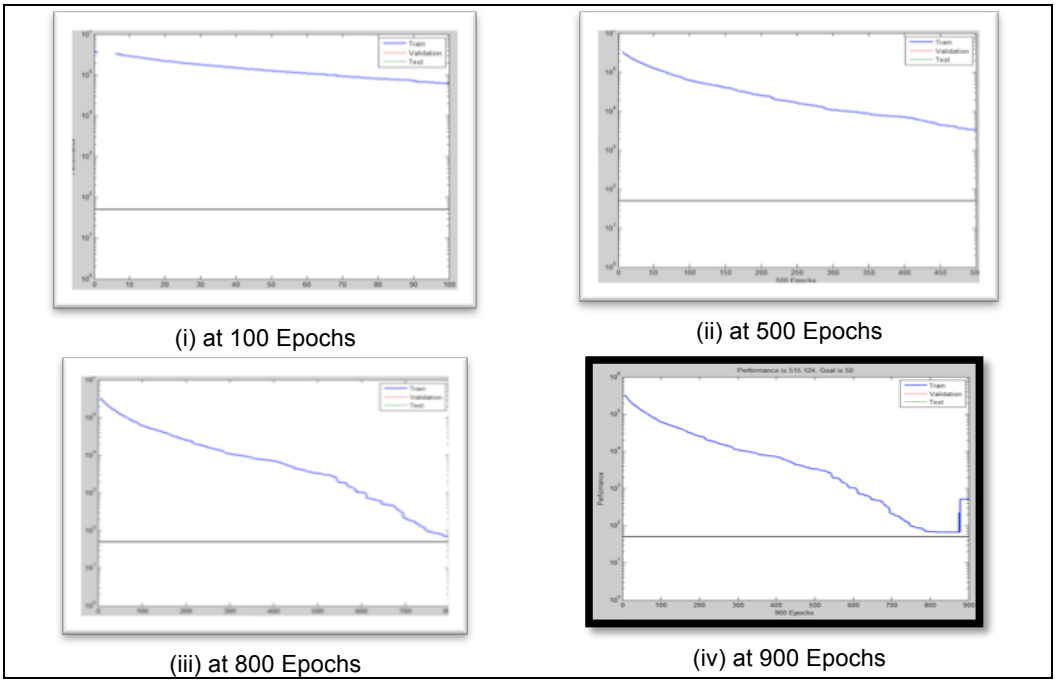

Figure 4.9 ***Learning performance states-1 during multimodal training*****:** *Learning performance states-1. Performance of learning for the integration model during the training process that is drawn between network performance and different number of epochs are provided.*

Learning is initiated with a random selection of goal. However, the target is to set goal=0. During the process of training, as the number of epochs is increased, a gradual reduction in the goal is identified signifying the decline in the graph from figure 4.9. From 800 epochs onwards, the performance graph is constant and parallel to the x-axis. This indicates the stable or threshold state of the training which can seen from figure 4.10

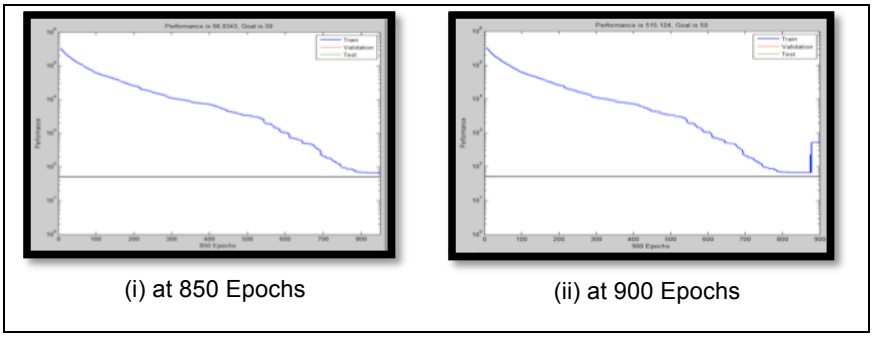

Figure 4.10 ***Learning performance states-2 reaching threshold*****:** *Performance of learning for the integration model during the training process that is drawn between network performance during the final epoch just before and after threshold is provided.*

At 850 epochs, the learning state of the model is considered as optimal due to the steady decrease in the network error. At this state, though the goal is constant, performance of the integration model decreases. Hence the obtained state of the neural network is used to perform audio-visual stimuli integration.

Considering learning of the model at various epochs states, the consistency of the model is also verified with the test samples. The graph thus represents the learning performance of the integration model. Though the learning process is smooth, the final given goal or target is not achieved. However, considering the extent of output at the minimal error state, the network output is effective. The accuracy achieved by the network was provided below.

4.5.5 Neural Network Training

During the process of neural network training, the error obtained after every 100 inputs states of the network was considered. At each input step, the mean error generated at all the source locations was considered. Figure 4.11 is a graph showing the training errors after every 100 inputs.

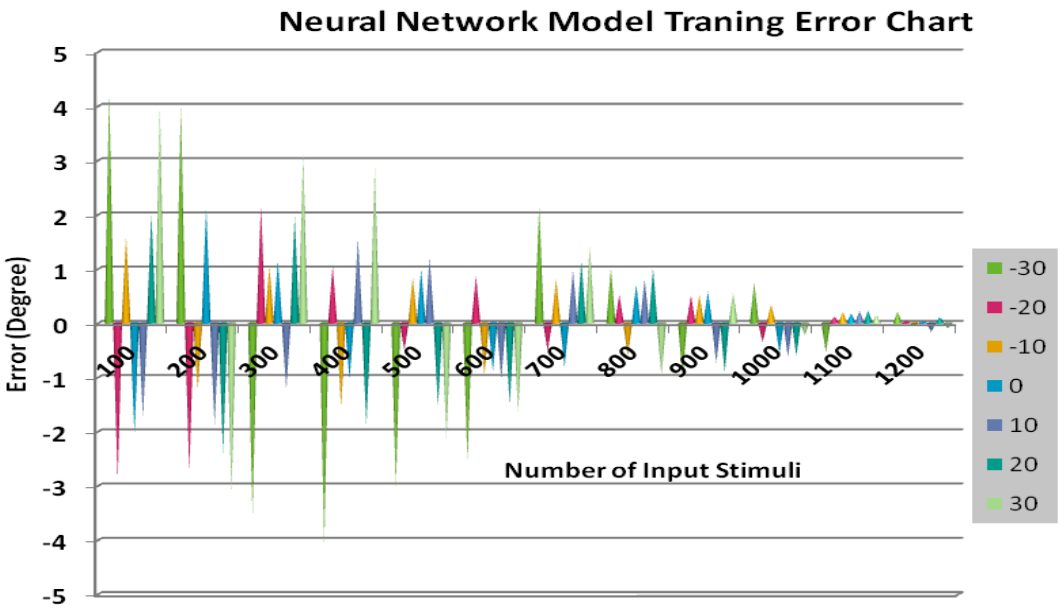

Figure 4.11 ***Error graph of neural network model training states*****:** *Error graph of neural network model featuring the range of error that was encountered during network training at given input source locations.*

Figure 4.11 shows the gradual decrease in the error, with the increased number of inputs. This indicates the effectiveness of the neural network model in obtaining a more efficient output. This also complies with the accuracy factor, demonstrating the neural network integration model was more accurate (less error) in generating integrated output. In this section, the performance of the integration model was visualized based on both learning and training criteria.

4.6. Integration Model

Considering the features described above, a neural network model was developed using radial basis network function. The network receives audio and visual stimuli information in the form of vector data containing localization and intensity information. This information is transmitted to the integration model to generate corresponding motor output for saccade generation. The developed network is mounted on a PeopleBot agent and is subjected to the behavioral experimental environment. This time the agent is exposed to the simultaneous transmission of audio and visual information. A synchronous counter identifies the delay present between the received multimodal stimuli and determines whether to consider the unimodal or integration model. During the experimental verification, multimodal stimuli that are synchronous are used.

Before discussing the experimental work, it is noted that multimodal instances can also appear with visual stimuli. However, when it comes to audio stimuli, which is supplied through IC to the SC, multimodal instances are bypassed and the final audio outcome is transferred to the SC. Hence the multimodal audio case does not belong to stimuli integration aspect of SC. In the case of visual stimuli, since the optic tract is directly connected to the SC the chances of receiving simultaneous stimuli were greater. This connection signifies the availability of stimuli at the SC,

which are presented in the next section using the HSFr and subjected to localization based on the stimuli intensity.

4.6.1. Experimental Outcome

The neural network model contained within the agent is tested using the behavioral platform with experiments involving the simultaneous bombardment of visual and audio stimuli. During the experimentation, the following integration output cases are identified.

Integration Case Studies:

(a) Multiple visual input stimuli: In the case of more than one visual input in the environment, the difference image vector is generated, identifying the areas of visual interference from the environment, as shown in figure 4.12(a). From the difference image vector the intensity of the signal is identified in terms of RGB values, as shown in figure 4.12(b). Examining the variations in the spikes generated, the intensities of both red and green are considered. The first and last peak show that the green spike is lower in intensity compared to the second peak. Considering the second, the green and red spikes are high in intensity when compared to the rest. However, the plot of the maximum values of the available RGB intensities determines the position of the source. By plotting the position onto a [-90, 90] scale the location of the source is determined, which in this case is -30^0.

(a)

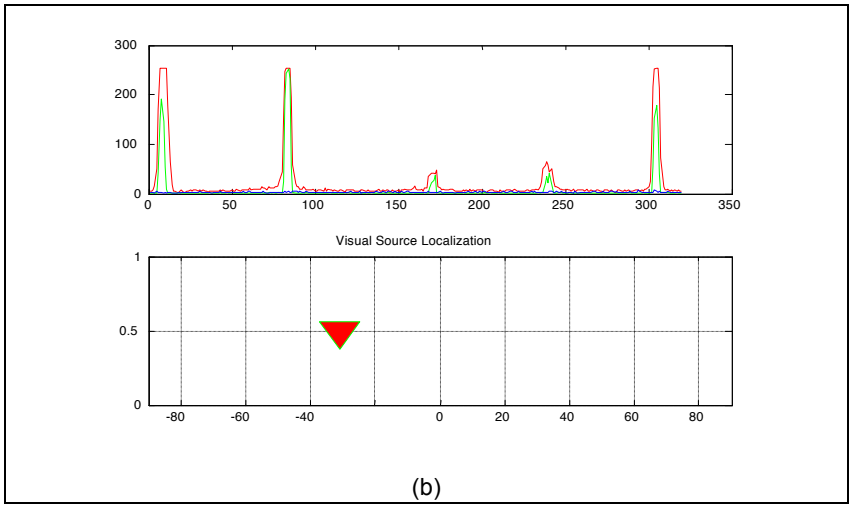

Figure 4.12 ***Response of multiple visual input stimuli localization 1*****:** *Example of multiple visual input stimuli received by the agent and how the visual localization is determined using the difference image and intensity information. The maximum intensity is identified in the second peak where all RGB values are highest when compared with the rest of the peaks.*

Even in circumstances of simultaneously available, multiple visual stimuli, the integration model perform a similar intensity determination methodology by projecting the one with the highest. An example is shown in figure 4.13(a), where there are five stimuli. Later the highest intensity stimulus is projected on to HSFr to perform the localization. During the highest peak determination, the use of RGB components determines the effectiveness of the Gaussian method for identifying the difference between the stimuli and eliminating them as shown in figure 4.13(b).

The criteria of multimodal integration appear when both the audio and visual stimuli are available at the integration model simultaneously. During the course of integration, depending on the stimuli intensity and their output behaviour, the following cases are classified. During the classification, the output state of the integrated signal is used to determine the enhancement and depression phenomena.

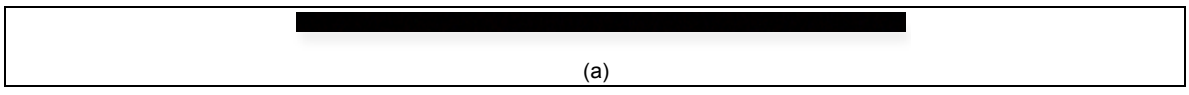

(a)

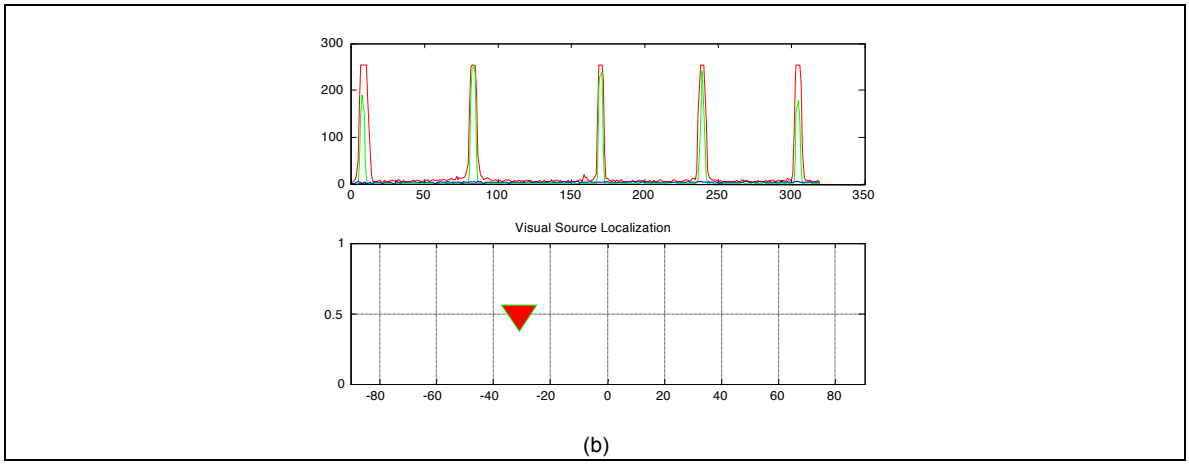

Figure 4.13 ***Response of multiple visual input stimuli localization 2*****:** *(a) depicts multiple visual stimuli and the response generated when multiple inputs arrived at the integration model. (b) Shows the maximum intensity peak location and how the destination stimulus localization is determined.*

(b) Weak audio and strong visual stimuli: If a low intensity audio signal and a visual signal with a strong intensity are received at the same time by the multimodal integration system, after verifying the time frame to confirm the arrival of the signals, both inputs are considered by the integration system. After preprocessing the signals, the localization maps are generated on the HSFr. In the graphs we can observe that the stimulus in the audio plot has a very low intensity and the source is determined accordingly, which is 15^0, as shown in figure 4.14(a). For the visual stimulus, the single spikes in red and green are considered for the maximum signal value, which is 5^0, as shown in figure 4.14(b). When plotted on the standard space scale, the sources are identified as being at two different locations, but the overall integrated location is identified as being close to the stronger visual stimulus. This is at 6^0 as shown in figure 4.14(c). In this case the integration mechanism considers the strength of the visual signal compared to the audio signal.

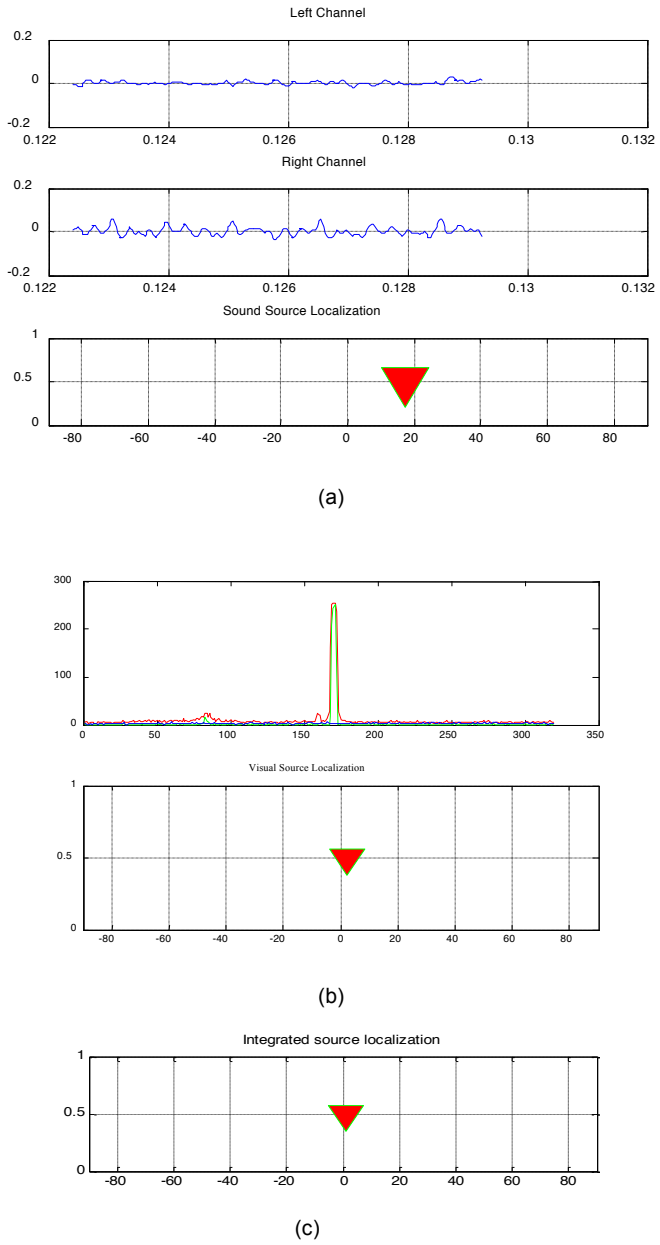

Figure 4.14 ***Response of low audio and strong visual stimuli localization*****:** *Audio and visual input with strong visual stimulus determining the main preference for the localization. The output signifies the orientation of output towards the strong stimuli.*

(c) Strong Audio and Weak Visual Stimuli: In this case the intensity of the audio stimulus is stronger than the intensity of the visual stimulus. TDOA has localized the audio stimulus around -9^0, as shown in figure 4.15(a). When it comes to the visual stimulus, the highest RGB component is green (representing a depletion in intensity), and there are two activation stimuli. Here there is a consistency in the

green spike, while the red spikes vary, as shown in figure 4.15(b). The location of the two inputs is on different sides of the centre. Hence, during the process of integration, the audio stimulus plays a vital role in generating the multimodal output. When the multimodal output is generated, the location of the integrated output is closer to the audio stimulus as shown in figure 4.15(c).

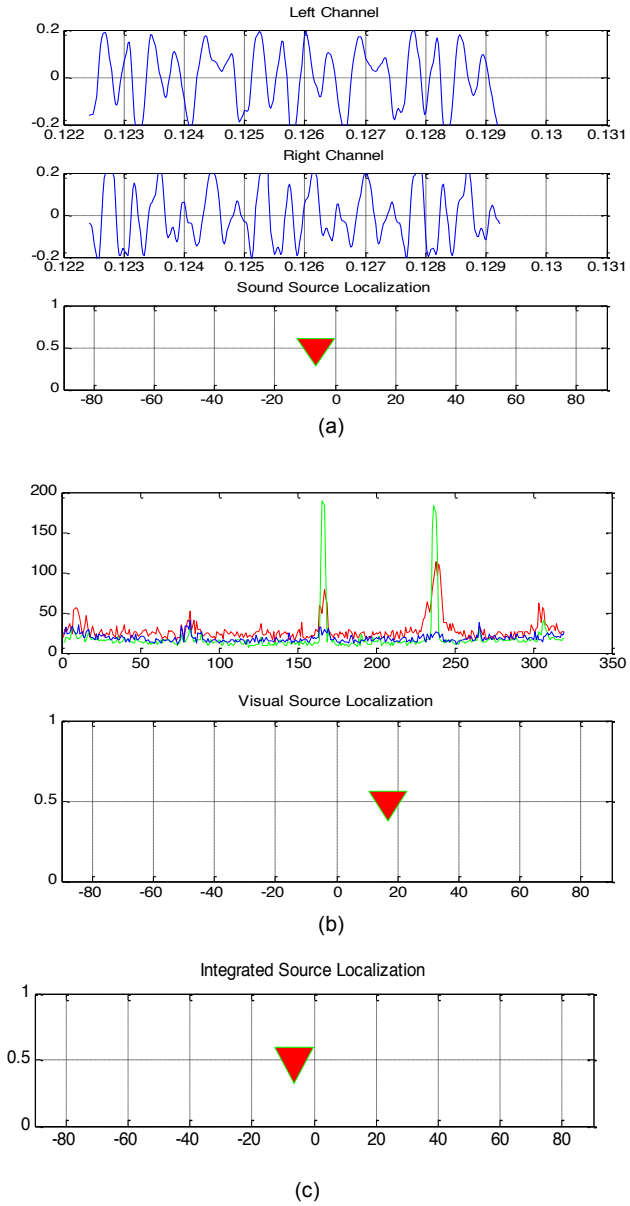

Figure 4.15 ***Response of strong audio and low visual stimuli localization*****:** *Multimodal input case with strong audio stimulus. The integrated output is biased by the intensity of the stronger stimulus, which in this case is audio.*

The above two representative cases are observed during multimodal integration, with one of the signals being relatively strong in its intensity. The integration model

focuses on the stimulus with the highest intensity, which therefore influences the integrated decision.

(d) Strong visual and strong audio stimuli: In this scenario, when the sensors receive the signals, their modalities are plotted on an intensity graph to determine the signal intensity. In the intensity graphs shown in figure 4.16, the sources are located on either side of the centre and the activations are of high intensity. When the output is computed, the source is located close to the visually detected peak.

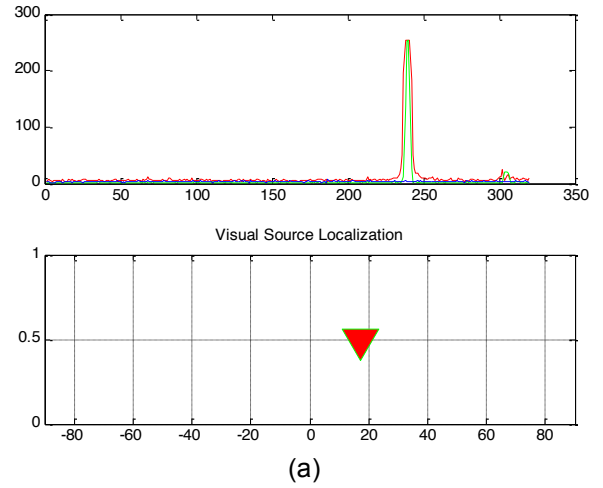

(a)

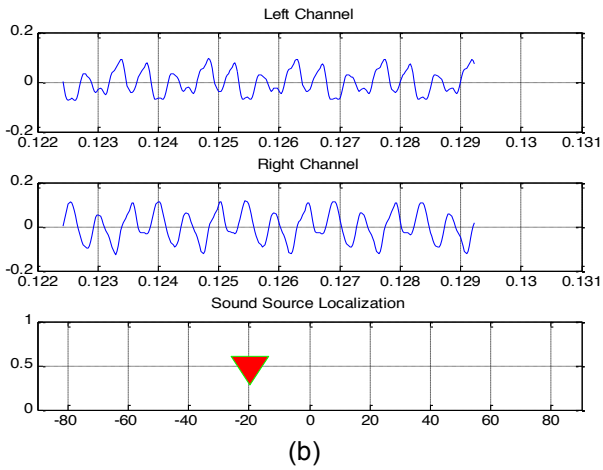

(b)

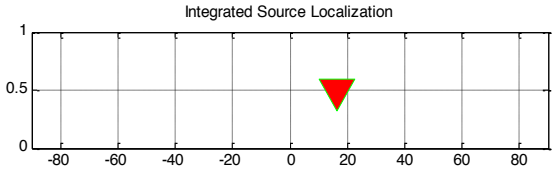

(c)

Figure 4.16 ***Response of strong visual and strong audio stimuli localization*****:** *Example of multimodal enhancement response. The integrated output is generated based on a distance function between the audio and visual intensity.*

In this case it is not clear whether the SC will prioritize in every case of integration. However in the case of multiple strong intensity stimuli the visual stimulus will have the higher priority, while the strong audio stimulus will have some influence on the multimodal integrated output. Hence the integrated output localization is closer to the strong stimulus, which is shown in figure 4.16(c). This signifies the partial prioritization towards visually strong stimuli.

(e) Weak visual and weak audio stimuli: In circumstances where both visual and audio signals are of low intensities, the behaviour of the SC is often difficult to predict. In this case, the SC can be thought of as a kind of search engine that keeps traversing the environment to locate any variations within it. When both audio and visual signals are of low intensity, the SC suppresses the audio signal. Though the visual signal is low in its intensity, as far as the SC is concerned, it is the only sensory data available. Therefore, the source is identified much closer to the visual stimulus, as shown in figure 4.17.

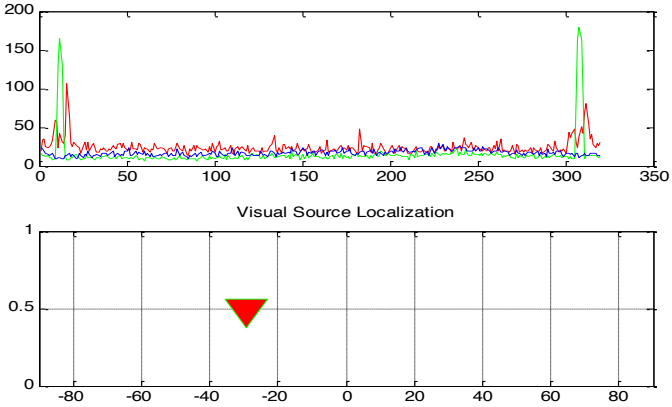

(a)

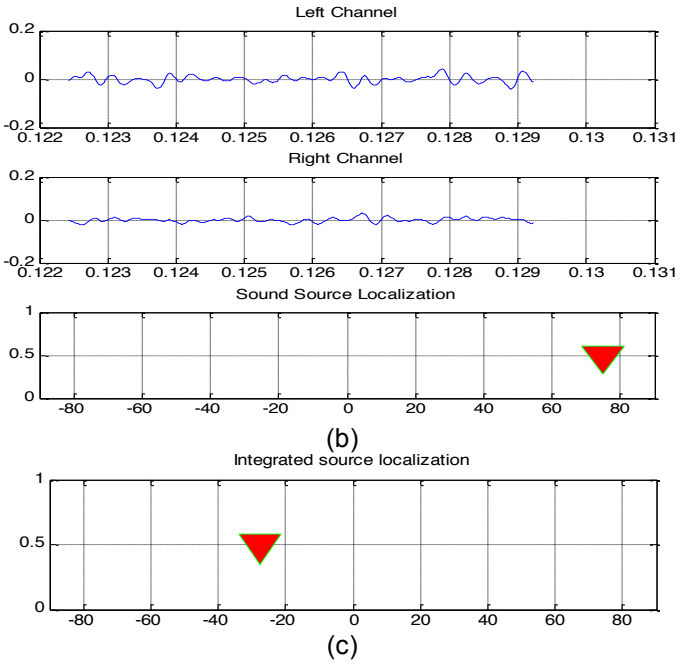

Figure 4.17 ***Response of low visual and low audio stimuli localization (Enhancement phenomena)*****:** *Example of multimodal enhancement response. The integrated output is generated based on a distance function between the audio and visual intensity where the audio signal is suppressed due to its low intensity and the visual stimulus is the only input available. Hence the distance function is biased towards the visual stimulus enhancing the final output.*

In some cases, depression may occur if the visual stimulus is out of range or the audio stimulus is becoming less intense. This can also happen if the audio stimulus is out of range and the visual stimulus is weak. This case signifies two factors. One is with the availability of stimuli, while the other is associated with strength or intensity. In the figure 4.18:

(a) represents the non availability of the stimuli causing no localization.

(b) represents the availability of audio stimuli with weak intensity. This shows the model exhibiting depression behaviour.

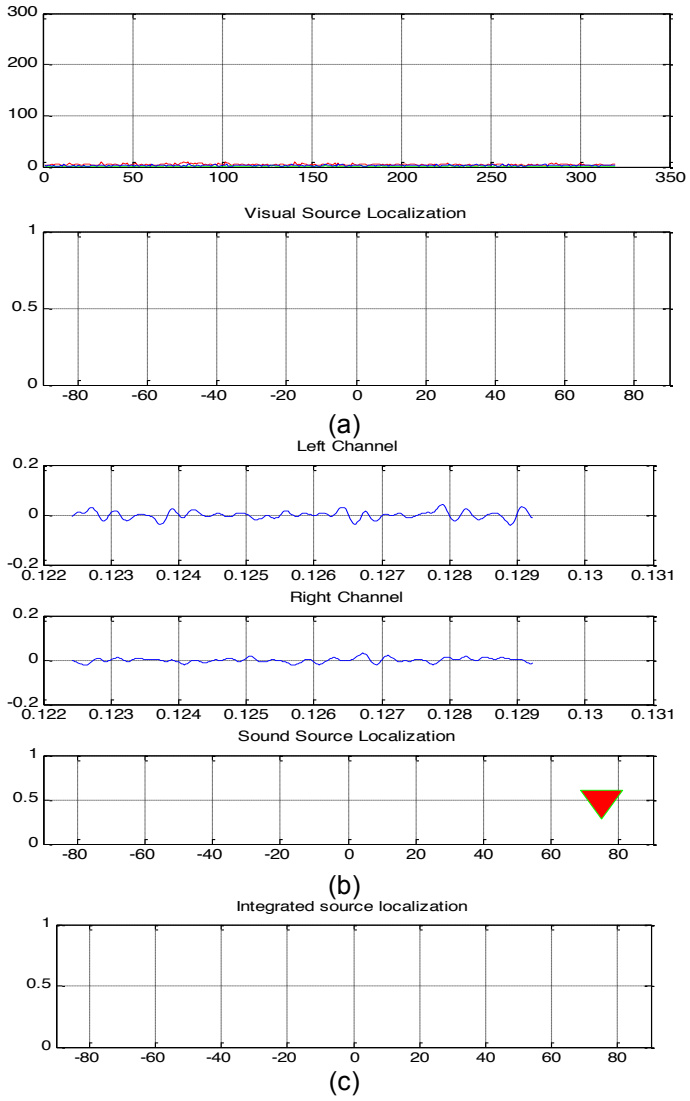

Figure 4.18 ***Response of low visual and low audio stimuli localization (Depression phenomena)*****:** *Multimodal depression responses: a weak or low intensity audio signal has suppressed the total multimodal response and generated a new signal that can achieve the response accurately, but with weak signal strength. This phenomenon is observed once in twenty responses, whilst in the remaining cases the model tries to classify the stimuli in one or other above-mentioned ways to generate the output.*

4.7. Integration Model Evaluation

In this section, the accuracy of the neural network model is compared against the computational model at all the source locations. Based on the output obtained

from a test set, error states that are generated at every source location are considered.

4.7.1. Computational Verses Neural Network Model

Using the computational integration model provided earlier in this chapter, the mean error obtained across the source locations from -30^0 to $+30^0$ is represented in figure 4.19.

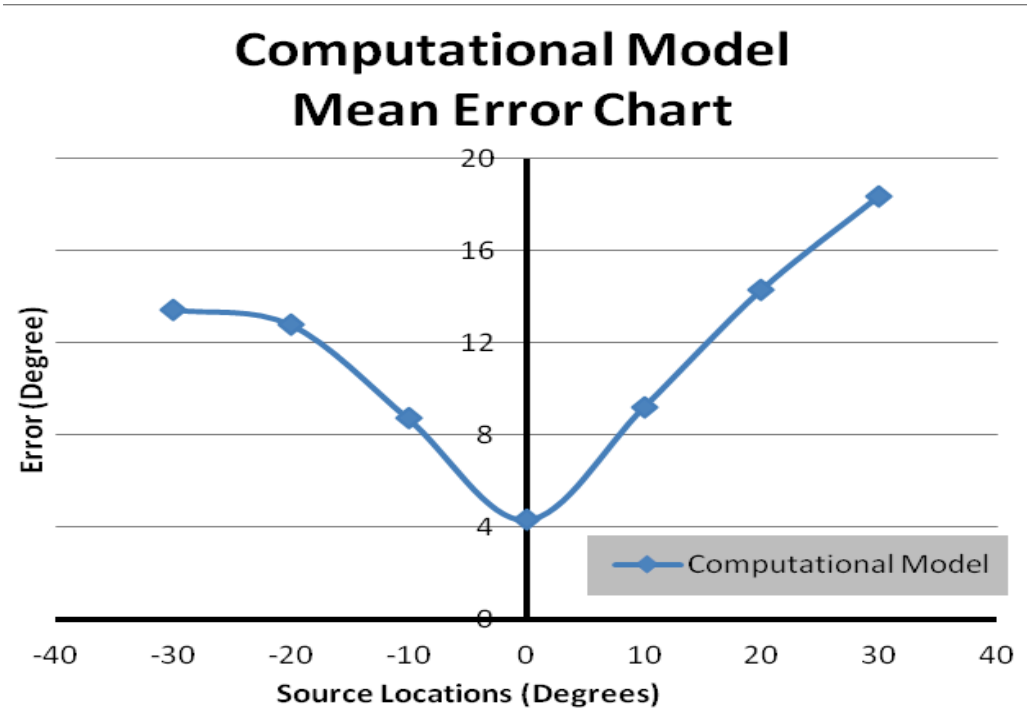

Figure 4.19 ***Computational Model Mean Error Chart:*** *Error graph of computational model featuring the range of error that is encountered during integration output generation for the test set.*

From the graph it is apparent that the mean error ranges from approximately 5^0 to 18^0. This graph demonstrates the error obtained at all stations that are used for localizing the stimuli source. Since the error rises above $\pm5^0$, the use of saccade degree of variance does not influence integration output.

Similarly, a neural network mean error chart is shown in figure 4.20 to identify the range of error generated.

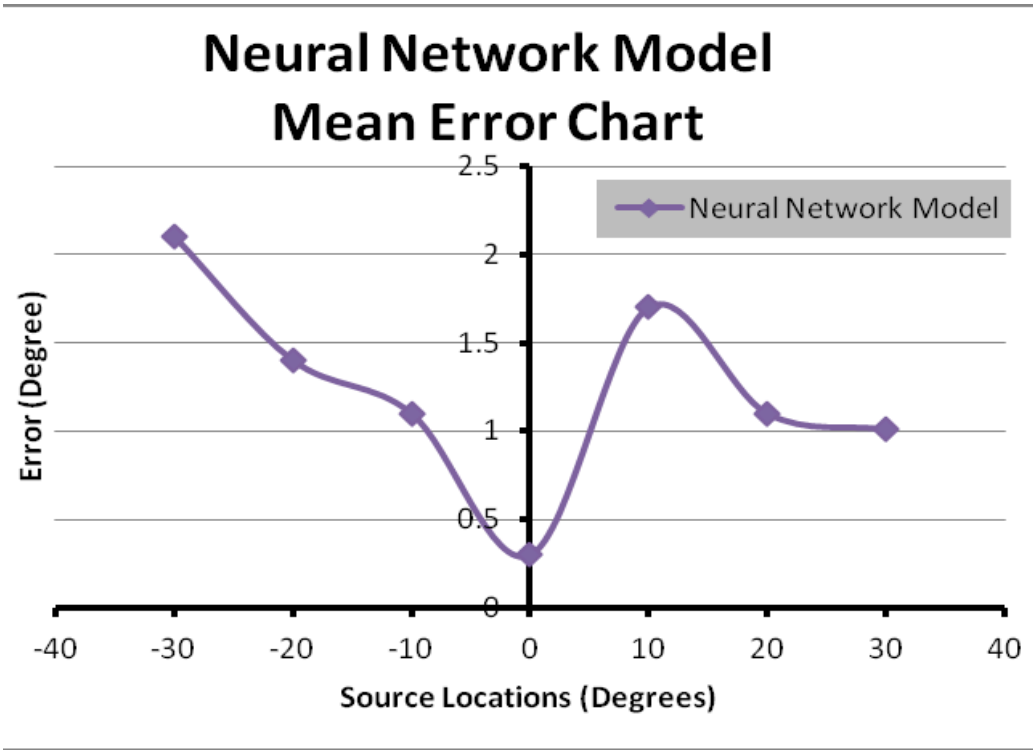

Figure 4.20 ***Neural network model mean error chart*****:** *Error graph at stimuli localization stations featuring the contribution of multimodal error that is encountered during integration output generation for test set.*

Figure 4.20 shows that the range of error lies between approximately 0.2^0 to 2^0. This error range excludes the saccade degree of variance. Based on the error generated, the neural network model output is approximately 20 times more accurate than the computational model output. Including the degree of freedom to $\pm 5^0$, for both computational and neural network error graphs, the neural network output is three times more effective than the computational output.

In figure 4.21 a comparison between the error states of the neural network model and the computational model is shown, to highlight the relative accuracy achieved by both approaches.

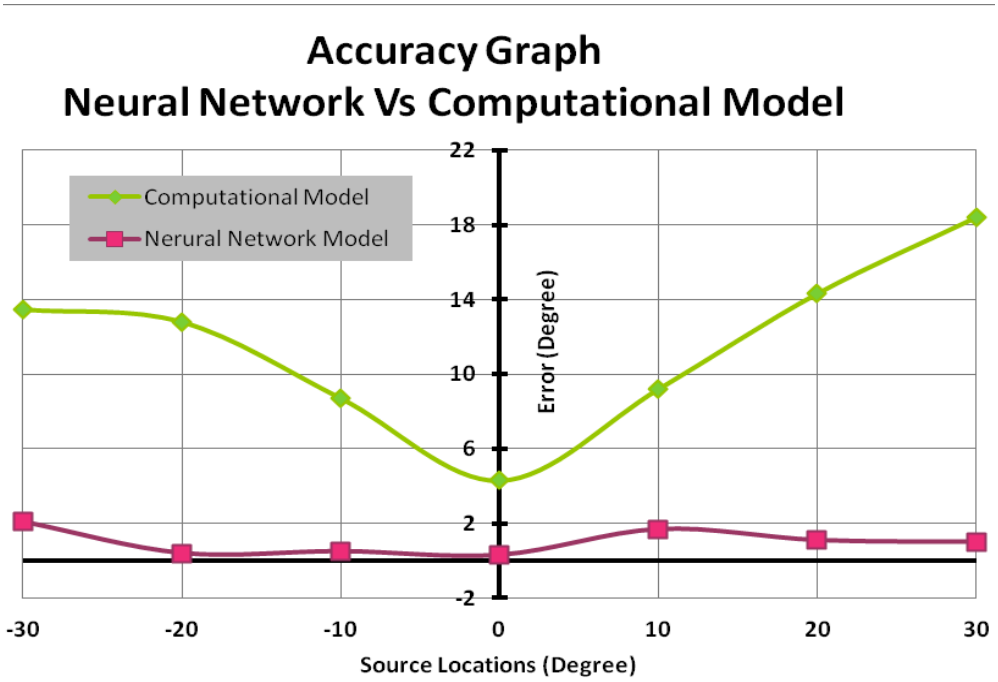

Figure 4.21 Accuracy graph between neural and computational integration model: *Accuracy graph featuring error states of neural network integration model and computational model for given stimuli locations .*

4.8. Summary

This chapter is a continuation of the methodology from Chapter-3 detailing the integration process and implementation details. Initially it describes the integration formulation containing audio and visual data processing. A schematic representation of the integration process is shows, how it is carried out, along with the requirements for avoiding difficulties involving computations.

Later, design aspects of the integration model are proposed irrespective of the development platform, using intermediate processing stages and critical features that are necessary for the model development. This design is based on the biological stimuli processing analysis generated from the SC mentioned in Chapter 2. During this stage, the possible developmental platforms are discussed.

Based on the literature review, computational-based integration model development is adapted to ensure the computational aspect of the model is

feasible. This section details the development and working aspects of the model, along with the results that are achieved during the process. However, the level of error achieved during the process is of greater concern. The error reduction discussion in the computational approach eventually supports a neural network platform, suggesting reduction in the computational time and a minimal error when the model is given stimuli from a live environment.

In the next section the feasibility of a radial basis function neural network approach is discussed along with the network development, including the network structure and working platform to implement integration criteria. During the process, the dimensionality aspect that involves the size of input data is also discussed, where stimuli pre-processing is adapted at the development stage to enhance the network efficiency. Dimensionality issues with the input feature set are discussed in the next chapter, which describes how effectively the data set is used in making the network effective.

Finally, the developed neural network is subjected to the behavioral experimental platform and the output is generated. Samples of outputs were projected where enhancement and depression phenomena are identified. An important research goal of the project is achieved as the integration model is capable of generating enhancement and depression phenomena in multimodal output generation. The model is successful in generating the multimodal output for the given inputs. As far as the initial tests are concerned, the output is adequate. However, when it comes to efficiency, the model has to be tested and evaluated for determining performance in terms of accuracy. In the next chapter a detailed experimental analysis and evaluation were described.

Chapter 5
Experimental Analysis

5.1. Introduction

In this chapter, the results of the experiments described in the previous chapter are analysed to verify the success of the model. During this process, unimodal experiments are initially considered and the performance is analyzed. Similarly, integration experiments are considered with both unimodal and multimodal data under varied circumstances for enhancement and depression. Later, the input space is classified for training and testing. Based on the learning criteria, the integration model is subjected to learning over the training data set and tested. The obtained test results are used to compare the computational integration model with the neural network integration model.

The next section, discusses how the stimuli space was used to perform the training and testing of the model, along with classification of the sub-space for the training set and test set.

5.2. Preparation of Training and Test Data

During the experimentation, data was collected in two different phases. Initially unimodal audio and visual data was obtained. Multimodal data was collected using the same experimental platform with the simultaneous arrival of audio and visual data.

From the obtained datasets, samples from each category were initially used to verify the success of the unimodal experimental phase. Both audio and visual

unimodal localization experiments were performed using the static data samples. These datasets were re-used to test the performance of the multimodal system with unimodal data. During this data collection phase, multimodal data samples were also collected from the experimental platform with labelled inputs under similar conditions.

In the multimodal experimental phase, the integration model was tested using audio and visual multimodal data. In the following sections, a series of tables are provided which show the error in the multimodal output. Although the output of the integration model was accurate to approximately $2 - 3^0$, a higher degree of accuracy was desirable. Hence the neural network was subjected to supervised learning, so that the error could be reduced and the output accuracy could be increased. In order to train the network effectively, it is important that the learning criteria and the dataset partition for training and test sets are also effective.

Initially the integration model was trained using only the multimodal data input. In the multimodal data, a random selection of each sample from each category is formed into test data. The remaining sub-space is used as training data for the neural network. Apart from the above dataset, the integration model is also tested on another dataset that is generated from the simultaneous transmission of both unimodal audio and unimodal visual data, effectively generating a multimodal input. Though the transmission conditions are similar to that of multimodal input, the outputs vary due to their different intensity levels. Hence, this variation leads to generation of different outputs. However, they serve as a test and validation set for determining the success and performance of the integration model.

5.3. Unimodal Experimental Analysis for Localization

The unimodal experimental setup with audio and visual stimuli is used to investigate accuracy of localization. Further investigations involved multimodal inputs in the sub-space. However in this section, the unimodal input stimuli that are collected are used to determine the success under variable conditions.

5.3.1 Unimodal Audio Localization Analysis

Different audio stimuli collected from the behavioural platform are used to test localization accuracy. Based on the results generated, the error is processed and analyzed to determine the performance of the unimodal audio localization. The collected audio input space is classified into eight different types based on the source amplitude levels. The following results are from the computational model.

Out of the available input space, samples are selected in the range 8 - 22dB as follows: 10, 12, 16, 20 and 22dB. The selection of stimuli frequency and amplitude was made based on the audible-limit of hardware equipment used by the agent. Localization attempts are carried out with 8dB signals, but these were found to be insufficient for stimuli localization. The background noise in the laboratory ranged from 0.4 to 4dB. During testing, unimodal inputs with frequencies ranging from 100Hz to 600Hz are localized. The results obtained are shown in Tables 5.1 to 5.5. From the output states, the localization error is used to determine the effectiveness of the model.

The localization error is determined by measuring the difference between the actual and predicted source location. All these output and error states are recorded in Tables 5.1 to 5.5. Each table also shows the mean and standard deviation of errors for each audio frequency and each source location.

Audio Sample 1:

Source amplitude = 10dB

The error obtained during the localization is tabulated as follows in Table 5.1

Audio Localization Error Chart for Sample 1								
Frequency Vs Angle	**100Hz**	**200Hz**	**300Hz**	**400Hz**	**500Hz**	**600Hz**	**Mean**	***St Dev***
-90^0	8.93	3.93	3.12	6.81	6.06	0.06	**4.82**	***3.12***
-60^0	1.39	3.39	3.39	3.39	3.04	-1.38	**2.66**	***1.92***
-45^0	1.29	2.89	1.07	1.07	0.17	2.09	**1.43**	***0.94***
-30^0	3.45	1.97	-0.03	2.6	1.86	0.40	**1.72**	***1.32***
-20^0	2.66	2.03	1.97	0.41	0.02	-1.41	**1.42**	***1.54***
-10^0	1.43	2.8	0.78	0.52	0.56	0.24	**1.06**	***0.94***
0^0	1	-0.5	2.09	2.09	0	0	**0.95**	***1.13***
10^0	0.73	0.32	2.4	0.42	0.52	0.52	**0.82**	***0.79***
20^0	1.87	1.01	1.41	0.02	1.41	1.41	**1.19**	***0.63***
30^0	3.97	2.59	1.44	2.59	-0.71	1.44	**2.12**	***1.58***
45^0	1.33	0.89	2.05	0.93	1.41	0.01	**1.10**	***0.68***
60^0	2.89	3.69	3.39	3.39	3.39	2.01	**3.13**	***0.60***
90^0	11.98	6.98	6.0	5.59	4.59	1.98	**6.19**	***3.31***
Mean	**3.30**	**2.54**	**2.24**	**2.29**	**1.83**	**1.00**	**2.20**	***0.76***
St Dev	***3.38***	***1.91***	***1.52***	***2.09***	***2.02***	***1.18***	**2.02**	***0.75***

Table 5.1 *The localization error in degrees for the input data sample 1 using amplitude of 10dB.*

The mean provided in column and row indicate the mean with corresponding source location and input frequency respectively. Similarly with standard deviation,

represents the extent of deviation that can cause at each mean from the respective row and column. The errors shown in Table 5.1 are represented graphically in figure 5.1

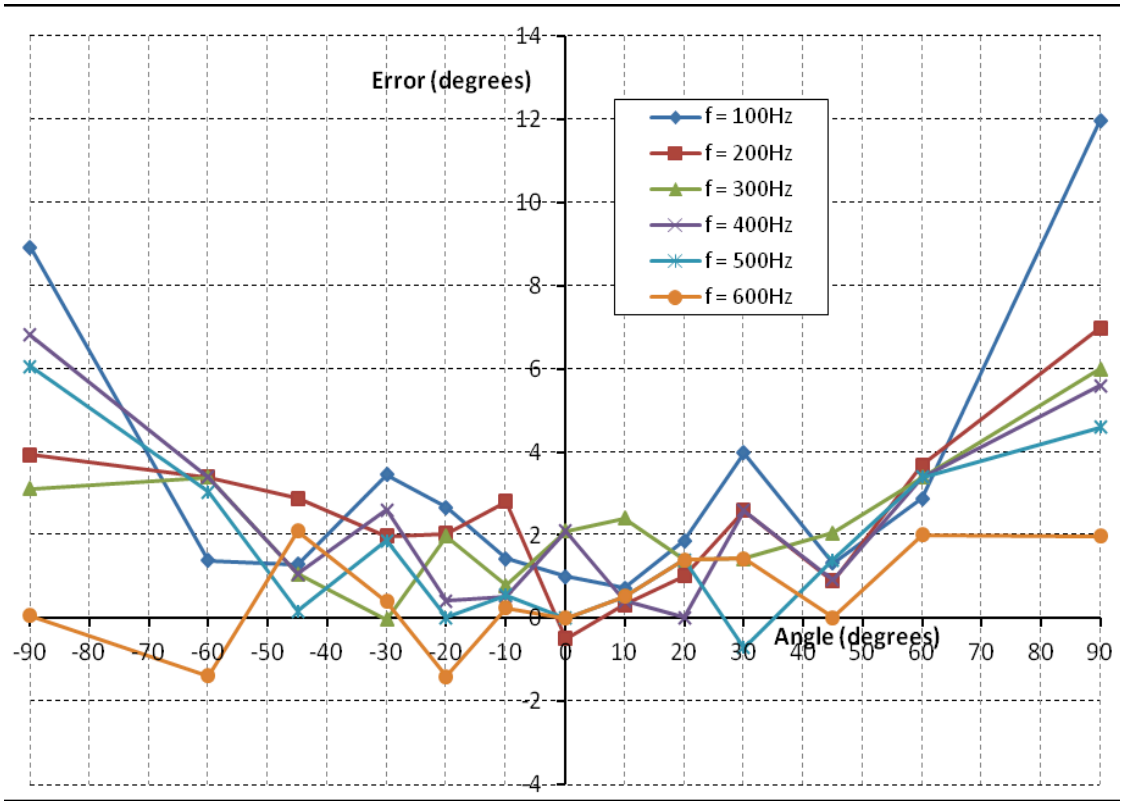

Figure 5.1 ***Response of unimodal audio localization error for sample 1:*** *Graphical representation of audio localization error shown in table 5.1. In this graph the range of error lies between (-2, 12) degrees*

Figure 5.1 shows the error variation across the audio range (-90^0, 90^0). It is observed that the error significantly increases for angles in the range ($\pm60^0$, $\pm90^0$). However in the range of (-60^0, $+60^0$), the error lies within (-2^0, $+4^0$). Also, as the frequency of the stimuli increases, the error significantly reduces. This signifies that the integration model is more effective for higher frequencies. The strength of the stimuli decreases gradually starting from the centre. This signifies that the model is influenced mainly by the strength of stimuli, rather than frequency.

Audio Sample 2:

Source amplitude = 12dB

The error obtained during the localization is tabulated in Table 5.2

Audio Localization Error Chart for Sample 2								
Frequency Vs Angle	**100Hz**	**200Hz**	**300Hz**	**400Hz**	**500Hz**	**600Hz**	**Mean**	***St Dev***
-90^0	6.73	2.83	3.02	4.61	2.09	0.96	**3.37**	***2.03***
-60^0	1.19	2.12	0.39	0.01	0.16	0.98	**0.81**	***0.79***
-45^0	0.02	0.91	1.03	2.03	0.57	1.69	**1.04**	***0.73***
-30^0	-1.41	0.17	-0.03	0.96	0.46	1.98	**0.84**	***1.12***
-20^0	-1.02	-0.46	0.17	0.98	-1.42	1.54	**0.93**	***1.15***
-10^0	0.88	1.38	0.98	0.92	1.36	0.17	**0.95**	***0.44***
0^0	0	-0.5	1.0	1.05	0	0.5	**0.51**	***0.62***
10^0	1.23	0.88	0.40	0.02	0.83	0.34	**0.62**	***0.44***
20^0	1.04	0.36	0.04	0.77	0.21	0.01	**0.41**	***0.42***
30^0	-0.02	-0.41	0.12	1.02	-0.02	2.14	**0.62**	***0.95***
45^0	-0.79	0.16	-1.02	-0.02	0.01	0.97	**0.50**	***0.71***
60^0	1.07	0.24	1.98	0.36	1.29	2.17	**1.19**	***0.80***
90^0	-2.64	-7.08	-4.0	-0.66	-9.33	0.02	**3.96**	***3.66***
Mean	**1.39**	**1.35**	**1.09**	**1.03**	**1.83**	**1.00**	**1.28**	***0.32***
St Dev	***2.21***	***2.36***	***1.64***	***1.30***	***2.85***	***0.80***	**1.86**	***0.75***

Table 5.2 *The localization error in degrees for the input data sample 2 given the source amplitude is 12dB.*

A graphical representation of the error shown in Table 5.2 is presented in figure 5.2

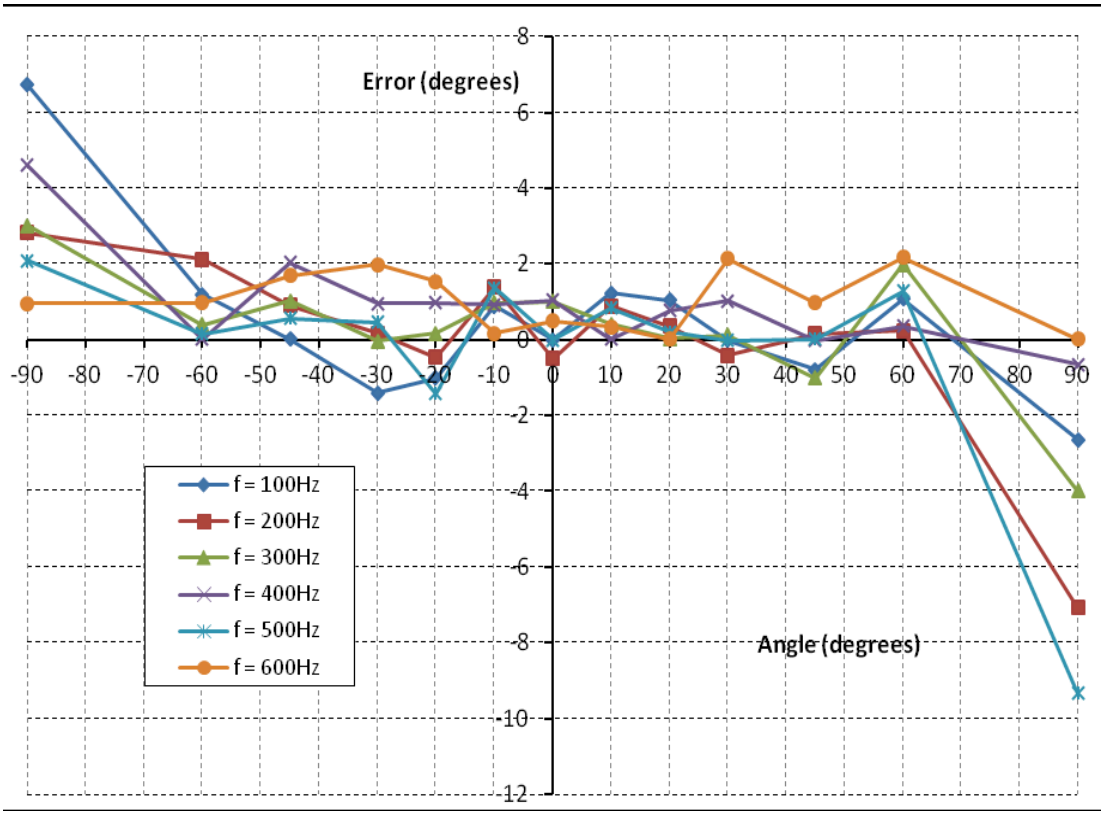

Figure 5.2 ***Response of unimodal audio localization error for sample 2:*** *Graphical representation of audio localization error shown in table 5.2. In this graph the range of error lies between (-10, 8) degrees.*

It can be seen in figure 5.2 that, most of the errors lie in the range (-2^0, 2^0) for sources in the range of (-60^0, 60^0). However, for the range ($\pm60^0$, $\pm90^0$) it varies between (-10^0, 8^0), which is a significant deviation from the mean error. However, compared to audio sample1, a reduction is obtained in the mean error, particularly in the range (-60^0, $+60^0$). Here, the maximum error magnitude is reduced by over two degree. This is attributed to the increase in stimuli intensity resulting from the increased amplitude. There is little change in the ranges (-60^0, -90^0) and ($+60^0$, $+90^0$).

Audio Sample 3:

Source amplitude = 16dB.

Based on the output generated with input sample 3, error obtained during the localization is presented in Table 5.3

Audio Localization Error Chart for Sample 3								
Frequency Vs Angle	**100Hz**	**200Hz**	**300Hz**	**400Hz**	**500Hz**	**600Hz**	**Mean**	***St Dev***
-90^0	2.1	0.80	1.98	3.41	0.83	0.23	**1.56**	***1.16***
-60^0	0.98	1.17	0.98	0.17	-0.66	-0.14	**0.68**	***0.74***
-45^0	-0.88	0.17	-0.44	-1.02	0.17	1.01	**0.62**	***0.76***
-30^0	-0.83	0.17	-0.03	0.0	-0.46	0.98	**0.41**	***0.61***
-20^0	-0.83	-0.46	0.0	0.98	-1.02	0.56	**0.64**	***0.79***
-10^0	-0.88	1.38	0.98	0.92	1.01	0	**0.86**	***0.84***
0^0	0	0.5	-1	0.0	0.0	0.5	**0.33**	***0.55***
10^0	0.5	-0.88	0.40	-0.46	-0.83	0.0	**0.51**	***0.60***
20^0	0.09	0.36	-0.04	0.0	0.21	0.01	**0.12**	***0.15***
30^0	0.0	-0.41	0.12	1.02	-0.02	0.86	**0.41**	***0.56***
45^0	-0.79	0.16	-1.02	-0.02	1.01	0.97	**0.66**	***0.85***
60^0	1.07	0.24	1.98	0.36	1.29	2.17	**1.19**	***0.80***
90^0	-2.64	0.0	-2.02	-0.66	-3.63	0.02	**1.50**	***1.51***
Mean	**0.89**	**0.52**	**0.85**	**0.69**	**0.86**	**0.57**	**0.73**	***0.16***
St Dev	***1.19***	***0.63***	***1.15***	***1.10***	***1.28***	***0.65***	**1.00**	***0.29***

Table 5.3 *The localization error in degrees for the input data sample 3, given the source amplitude is 16dB.*

Graphical representations of errors obtained in Table 5.3 are presented in figure 5.3.

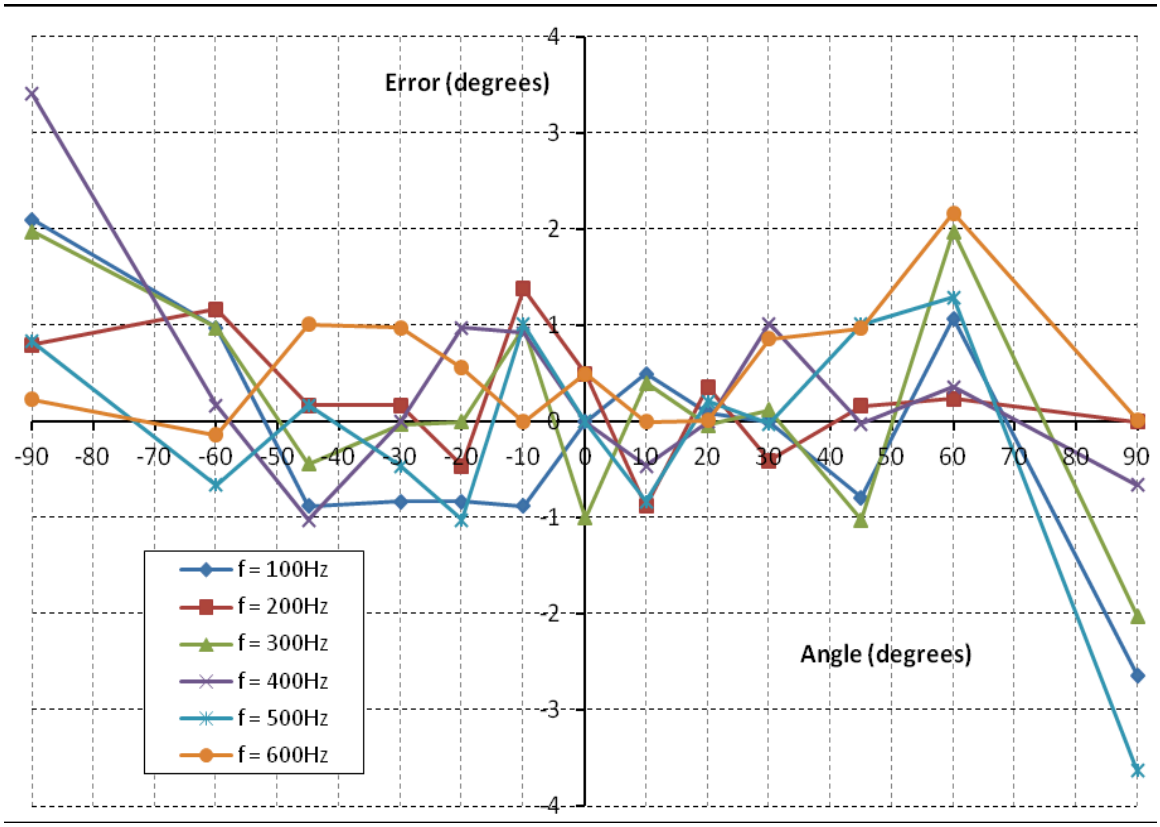

Figure 5.3 ***Response of unimodal audio localization error for sample 3:*** *Graphical representation of audio localization error shown in table 5.3. In this graph the range of error lies between (-4, 4) degrees*

Figure 5.3 shows that errors have been reduced to a range of (-4^0, 4^0). If the boundary errors are excluded, the mean error lies in the range (-1^0, 2^0). This error reduction indicates that the relative accuracy is increased as the amplitude of the stimuli increases. Similarly, as the stimuli frequency decreases, the error also decreases. This contradicts the findings of the first experiment (audio sample 1).

This signifies that although frequency plays an effective role in localizing the source, it is the strength of the stimuli, which is the amplitude in this case, which plays a critical role in determining the localization performance. This behaviour can be observed in all the cases shown.

Audio Sample 4:

Source amplitude = 20dB.

Based on the output generated with input sample 4, error obtained during the localization is provided in Table 5.4.

Audio Localization Error Chart for Sample 4								
Frequency Vs Angle	**100Hz**	**200Hz**	**300Hz**	**400Hz**	**500Hz**	**600Hz**	**Mean**	***St Dev***
-90^0	-1.66	0.89	-1.46	0.59	-0.11	0.0	**0.79**	***1.05***
-60^0	-1.02	1.01	0.98	0.17	-0.64	-0.14	**0.66**	***0.83***
-45^0	-0.77	0.89	-0.44	-1.02	0.17	1.01	**0.72**	***0.86***
-30^0	-0.83	0.64	-0.03	0.0	-0.46	0.98	**0.49**	***0.67***
-20^0	-0.11	-0.99	0.0	0.98	-1.02	0.56	**0.61**	***0.81***
-10^0	0.0	0.38	0.89	0.92	1.01	0.0	**0.53**	***0.47***
0^0	0	0	-0.5	0.0	0.0	0.5	**0.17**	***0.32***
10^0	0.17	-0.11	0.0	-0.46	1.17	0.02	**0.32**	***0.55***
20^0	0.89	0.17	-0.46	0.0	0.07	0.0	**0.27**	***0.44***
30^0	0.16	-0.41	0.12	0.89	-0.02	0.02	**0.27**	***0.43***
45^0	-0.98	0.19	0.0	-0.02	1.01	0.17	**0.40**	***0.64***
60^0	0.89	0.24	1.98	0.07	1.29	1.17	**0.94**	***0.71***
90^0	-1.11	0.0	-1.46	-0.66	-3.63	0.02	**1.15**	***1.35***
Mean	**0.66**	**0.46**	**0.64**	**0.44**	**0.82**	**0.35**	**0.56**	***0.17***
St Dev	***0.79***	***0.56***	***0.94***	***0.61***	***1.29***	***0.46***	**0.78**	***0.31***

Table 5.4 *The localization error in degrees for the input data sample 4, given the source amplitude is 20dB.*

A graphical representation of error obtained in Table 5.4 is presented in figure 5.4.

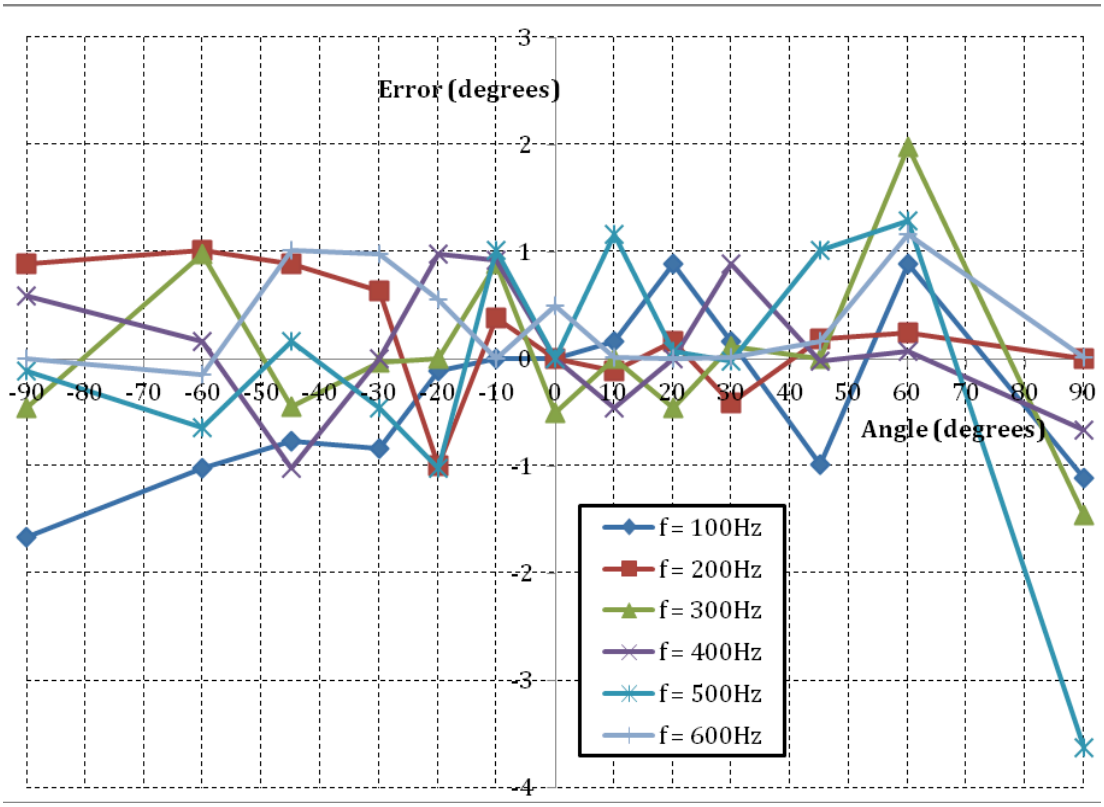

Figure 5.4 ***Response of unimodal audio localization error for sample 4:*** *Graphical representation of audio localization error from table 5.4, featuring relative similarity of each frequency to the target localization. In this graph the range of error lies between (-4, 2) degrees.*

In this sample, the localization error lies between (-4^0, 2^0), which is reduced compared with the previous sample set. Also, the mean error lies in the range of (-1^0, 1^0), which is less than the previous sample. This again signifies the effectiveness of the integration model with the increase in stimuli strength.

Audio Sample 5:

Source amplitude = 22dB

Based on the output generated using input sample 5, error obtained during the localization is provided in Table 5.5.

Audio Localization Error Chart for Sample 5								
Frequency Vs Angle	**100Hz**	**200Hz**	**300Hz**	**400Hz**	**500Hz**	**600Hz**	**Mean**	***St Dev***
-90^0	-0.88	0.17	-0.11	0.59	-1.44	0.0	**0.53**	***0.74***
-60^0	-0.44	0.86	0.12	0.0	-0.88	-0.66	**0.49**	***0.63***
-45^0	-0.83	0.0	-0.44	1.56	0.17	0.98	**0.66**	***0.89***
-30^0	-0.14	0.64	1.02	0.0	-0.88	0.0	**0.45**	***0.66***
-20^0	-0.68	0.64	1.02	0.0	-0.64	0.51	**0.58**	***0.70***
-10^0	0.0	0.38	0.98	0.92	1.01	0.0	**0.55**	***0.48***
0^0	0.0	0.0	0.0	0.0	0.0	0.0	**0.00**	***0.00***
10^0	0.17	-0.11	0.0	-0.46	0.76	0.02	**0.25**	***0.40***
20^0	0.89	0.17	-0.46	-0.14	0.07	0.0	**0.29**	***0.45***
30^0	-0.16	-0.41	0.12	0.89	-0.02	0.02	**0.27**	***0.44***
45^0	-0.98	0.16	0.0	-0.02	1.01	0.17	**0.39**	***0.64***
60^0	0.89	0.24	1.98	0.07	1.29	1.17	**0.94**	***0.71***
90^0	-0.11	0.0	-0.46	-0.83	0.37	0.02	**0.30**	***0.42***
Mean	**0.47**	**0.29**	**0.52**	**0.42**	**0.66**	**0.27**	**0.44**	***0.15***
St Dev	***0.60***	***0.35***	***0.74***	***0.63***	***0.84***	***0.47***	**0.61**	***0.18***

Table 5.5 *The localization error in degrees for the input data sample 5, given the source amplitude is 22dB.*

A graphical representation of error tabulated in Table 5.5 is presented in figure 5.5

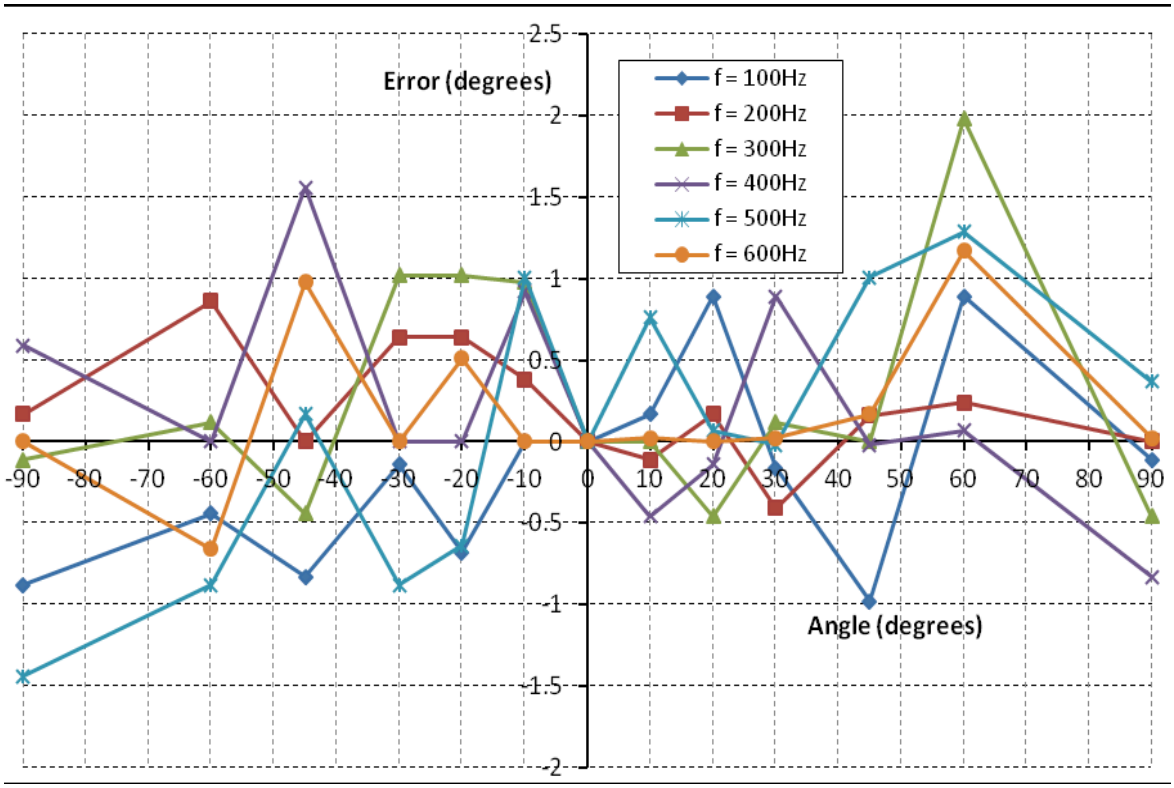

Figure 5.5 ***Response of unimodal audio localization error for sample 5:*** *Graphical representation of audio localization error from table 5.5, featuring relative similarity of each frequency to the target localization. In this graph the range of error lies between (-1.5, 2) degrees.*

In figure 5.5 the localization error range is (-1.5^0, 2^0) and the mean error does not exceed 1^0. This again demonstrates that, localization is improved with increased stimuli strength.

The above graphs show errors obtained during localization of low frequency audio stimuli across variable amplitudes. From the graphs it can be seen that as the amplitude (strength of stimuli) increases, the magnitude of errors between the predicted and actual source location gradually decreases. Considering the entire input space, the error lies within a range of $\pm 10^0$, which gradually decreases with increased stimuli intensity.

The mean and standard deviation of error are now considered based on a sample set for a group of stimuli source stations. In the following three particular source stations (0^0, 45^0, 90^0) are considered, and the mean errors obtained for frequencies 100Hz to 600Hz. Figure 5.6 shows the mean errors obtained during the source location across the amplitude range.

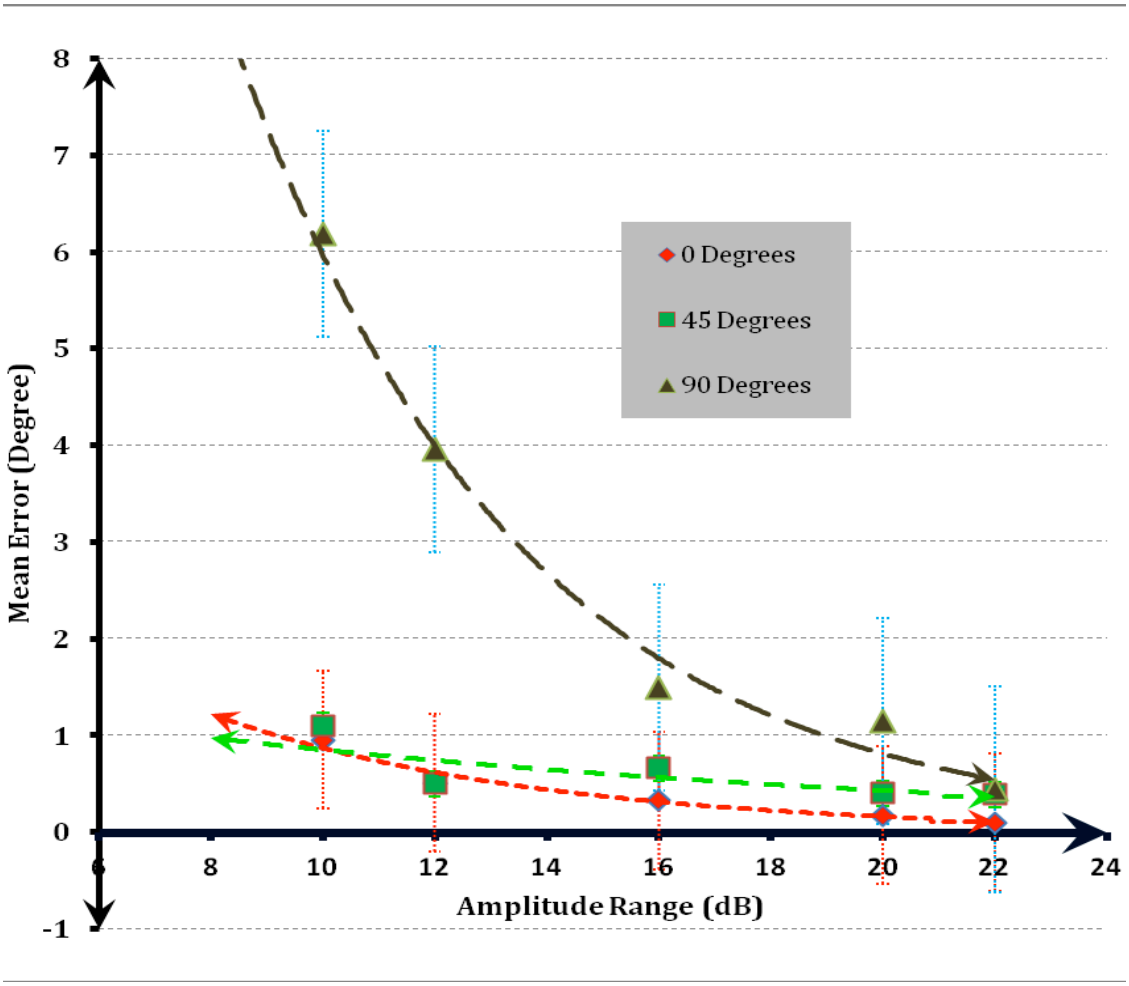

Figure 5.6 ***Mean error graph for a given sample:*** *Representation of audio localization mean error of a source stations (0^0, 45^0, 90^0) for a frequency range (100, 600)Hz.*

In the figure 5.6 the trend line passing through the given series represents the flow of error within the range of amplitudes 8 - 22dB. For 0^0 and 45^0, the mean error is less than 2^0 including the possible deviations. However for 90^0, it is significantly higher; and shows that, with a decrease in amplitude the error increases. Similarly

as the amplitude increases, the mean error decreases which implies that localization is effective for higher order amplitudes.

5.3.2 Unimodal Visual Localization Analysis

In this section different visual stimuli transmitted from the behavioral platform under varied light conditions are used to determine localization performance. The error is processed and analyzed to determine the performance of unimodal visual localization. The collected visual input space is classified into three different types based on the visibility for day and night lighting conditions in the laboratory.

Due to interference (noise) caused by other nearby visual stimuli, the LEDs that emit light from the visual source are affected. Since this interference causes variations in the stimuli strengths that are received at the agent, the quality of the signal is also affected. The quality of the stimuli is quantified based on intensity, which is normalized in the range of 0 to 1.

In the following results, the visual stimuli can be categorized as follows:

Sample 1: Day time conditions (laboratory lights on)

Sample 2: Night time conditions (laboratory lights off)

Visual Sample 1:

Time = Day

Condition = lights on

The error obtained during localization of visual sample 1 is provided in Table 5.6, and the graphical representation of the error is presented in figure 5.7.

Visual Localization Error Chart for Sample 1								
Light Intensity* Vs Angle (degree)	**Set 1**	**Set 2**	**Set 3**	**Set 4**	**Set 5**	**Set 6**	**Mean**	***St Dev***
-30^0	0.85	0.37	0.03	0.54	0.04	-0.64	**0.41**	***0.52***
-20^0	-3.26	-3.67	-2.24	-2.44	-3.44	-3.88	**3.16**	***0.67***
-10^0	1.01	0.53	0.0	0.62	1.59	-0.98	**0.79**	***0.88***
0^0	2.01	2.46	2.46	2.24	1.46	1.57	**2.03**	***0.44***
10^0	0.86	-0.68	0.98	0.0	0.98	2.14	**0.94**	***0.96***
20^0	-3.05	-2.44	-2.44	-1.44	-1.02	-3.05	**2.24**	***0.84***
30^0	-0.44	-0.30	-0.20	0.02	-0.13	0.07	**0.19**	***0.19***
Mean	***1.64***	***1.49***	***1.19***	***1.04***	***1.24***	***1.76***	**1.39**	***0.28***
St Dev	***2.08***	***2.02***	***1.72***	***1.51***	***1.75***	***2.22***	**1.88**	***0.27***

Table 5.6 *The error obtained in localizing the visual stimuli for each of input generated from sample 1. The table also provides the mean and standard deviation for each of the source location and for each of the visual stimuli category.*

The overall pattern of error appeaers similar, irrespective of the type of stimuli. The error range is (2^0, -4^0) and the variation of error for all the stimuli indicates that the output of localization is within the acceptable range (variance of 5^0).

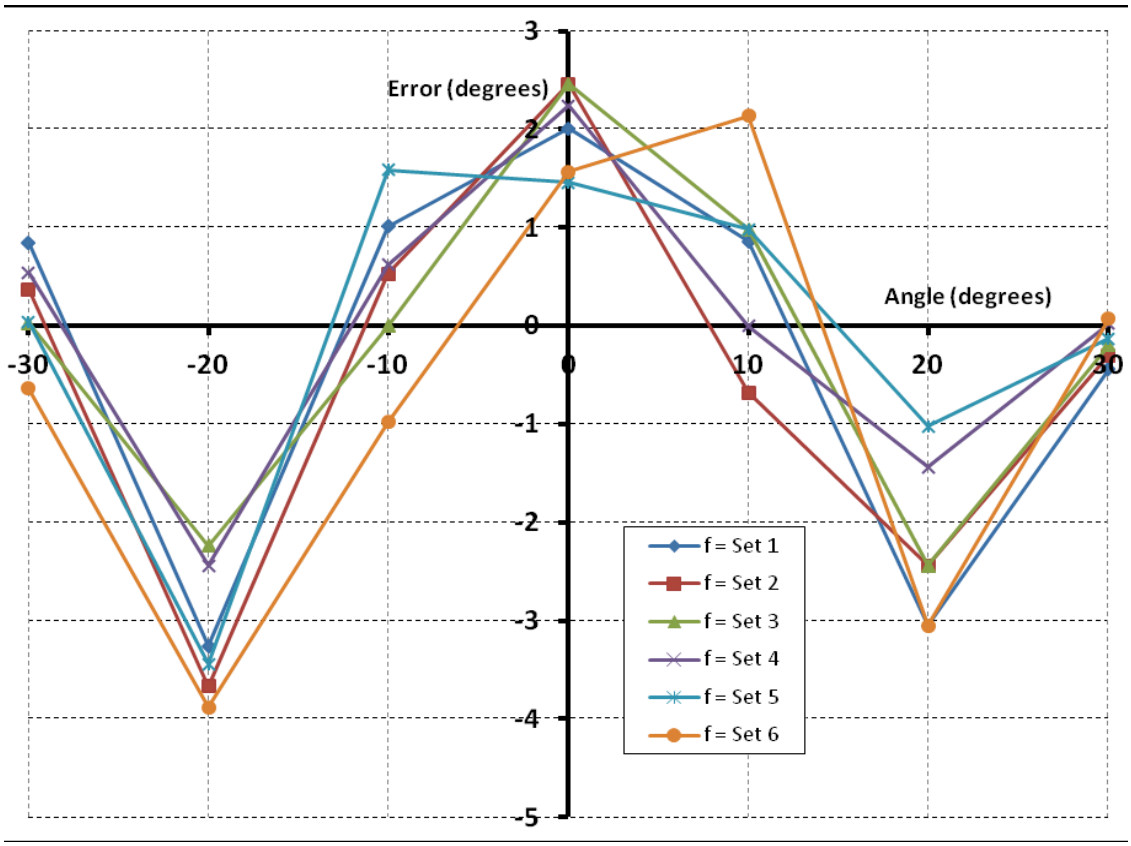

Figure 5.7 ***Response of unimodal visual localization error for sample-1:*** *Graphical representation of visual localization error from Table 5.6, featuring relative similarity of each stimulus to the target localization. In this graph the range of error lies between* $(-4^0, 3^0)$.

Visual Sample 2:

Time = Night

Condition = Lights off

The error determined during localization of visual sample 2 is provided in the Table 5.7, and the graphical representation of the error determined is presented in figure 5.8.

Visual Localization Error Chart for Sample 2								
Light Intensity* Vs Angle (degree)	**Set 1**	**Set 2**	**Set 3**	**Set 4**	**Set 5**	**Set 6**	**Mean**	***St Dev***
-30^0	0.85	0.37	0.03	0.54	0.04	-0.44	**0.38**	***0.45***
-20^0	-0.16	-0.66	0.98	0.0	0.07	-0.41	**0.38**	***0.56***
-10^0	0.21	0.31	0.0	0.20	1.02	0.0	**0.29**	***0.38***
0^0	1.10	0.5	0.0	0.0	0.0	0.02	**0.27**	***0.45***
10^0	0.42	0.12	0.02	0.0	0.46	0.0	**0.17**	***0.21***
20^0	-1.05	0.02	-0.26	0.04	0.0	0.07	**0.24**	***0.43***
30^0	0.36	0.05	-0.20	0.02	-0.13	-0.64	**0.23**	***0.33***
Mean	***0.59***	***0.29***	***0.21***	***0.11***	***0.25***	***0.23***	**0.28**	***0.16***
St Dev	***0.71***	***0.38***	***0.41***	***0.20***	***0.40***	***0.29***	**0.40**	***0.17***

Table 5.7 Visual localization error chart with lights-off condition: *The error obtained in localizing the visual stimuli for each of input generated from sample 2. A graphical representation of this table is provided in figure 5.8 depicting the range of error obtained.*

Figure 5.8 indicates an improvement of the mean error, when compared to the previous sample shown in figure 5.7. The random spikes in the graph are due to

the random selection of data from the input space. However, the mean error lies below one degree. This indicates the improvisation of accuracy in the visual stimuli aspect of localization model.

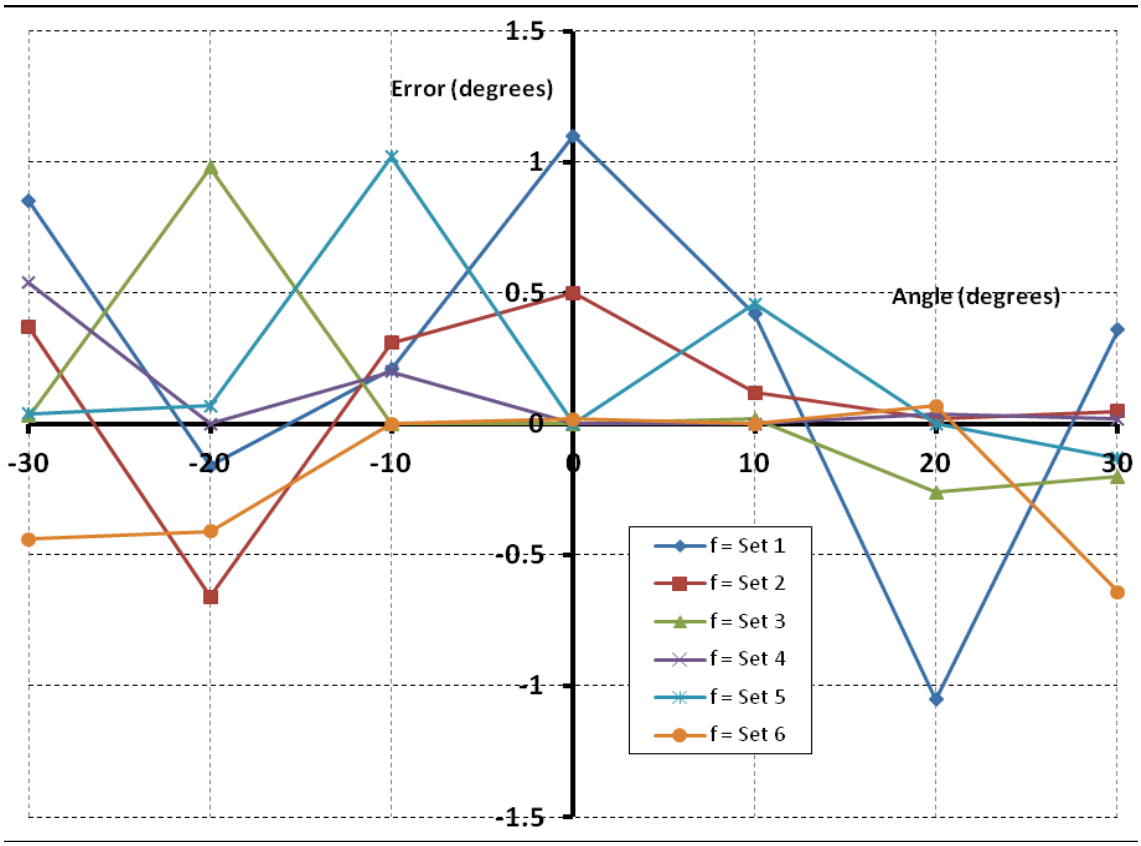

Figure 5.8 ***Response of unimodal visual localization stimuli for sample-2:*** *Graphical representation of audio localization error from table 5.7, featuring relative similarity of each stimulus to the target localization. In this graph the range of error lies between (-1.5, 1.5) degrees.*

The results obtained above are two different samples that are used in obtaining the unimodal visual input data for the experimental investigation. From the above figures 5.7 and 5.8 it is shown that, with an increase in stimuli intensity an improvement in the localization performance is obtained. Hence the graphs signify that the quality of the stimuli influences the accuracy of localization by reducing the error.

5.4 Integrated Experimental Data Analysis

In this section, the multimodal integration model is subjected to testing with the help of a behavioral experimental platform to localize simultaneously generated audio and visual stimuli. The level of performance achieved was determined along with further verification using other inputs in the sub-space. In this section, the multimodal input stimuli collected are used to verify the success by determining the error involved from expected and target output states.

Integrated experimental analysis examines various input states involved in generating the multimodal output, similar to the unimodal analysis. Since a research goal is to verify the enhancement and depression phenomena associated with the integrated output, various cases are demonstrated.

Integration Sample 1

In Table 5.8, a set of multimodal stimuli samples (expressed in degrees) are collected in the order of decreasing intensities of frequencies. As input for this sample, five different multimodal sets of data were created, where:
Set 1 = 500Hz, Set 2 = 400Hz, Set 3 = 300Hz, Set 4 = 200Hz and Set 5 = 100Hz along with visual stimuli in the range of (0.5, 1).

The error in the multimodal localization for sample 1 is given in table 5.8.

Multimodal Localization Error Chart for Sample 1							
Audio Sample (degree) Vs Visual Sample (degree)	**Set 1**	**Set 2**	**Set 3**	**Set 4**	**Set 5**	**Mean**	***St Dev***
-30	0.07	-0.5	0.0	0.0	0.07	**0.13**	***0.24***
-20	1.41	0.04	-0.9	0.0	0.33	**0.54**	***0.83***
-10	1.01	1.07	0.97	0.0	-0.05	**0.62**	***0.57***
0	--	-1.3	-0.04	-1.11	0.04	**0.50**	***0.70***
10	-0.56	--	-0.06	-0.07	0.0	**0.14**	***0.26***
20	-1.02	-0.56	0.04	0.0	0.01	**0.33**	***0.47***
30	0.08	0.89	0.01	0.0	-0.06	**0.21**	***0.40***
Mean	***0.59***	***0.62***	***0.29***	***0.17***	***0.08***	**0.35**	***0.24***
St Dev	***0.92***	***0.91***	***0.54***	***0.42***	***0.13***	**0.58**	***0.34***

Table 5.8 Multimodal localization error chart for sample 1 (multimodal input): *Multimodal localization error determined from the sample 1 with respect to corresponding audio and visual stimuli data.*

Figure 5.9 is a graphical representation of the error table 5.8.

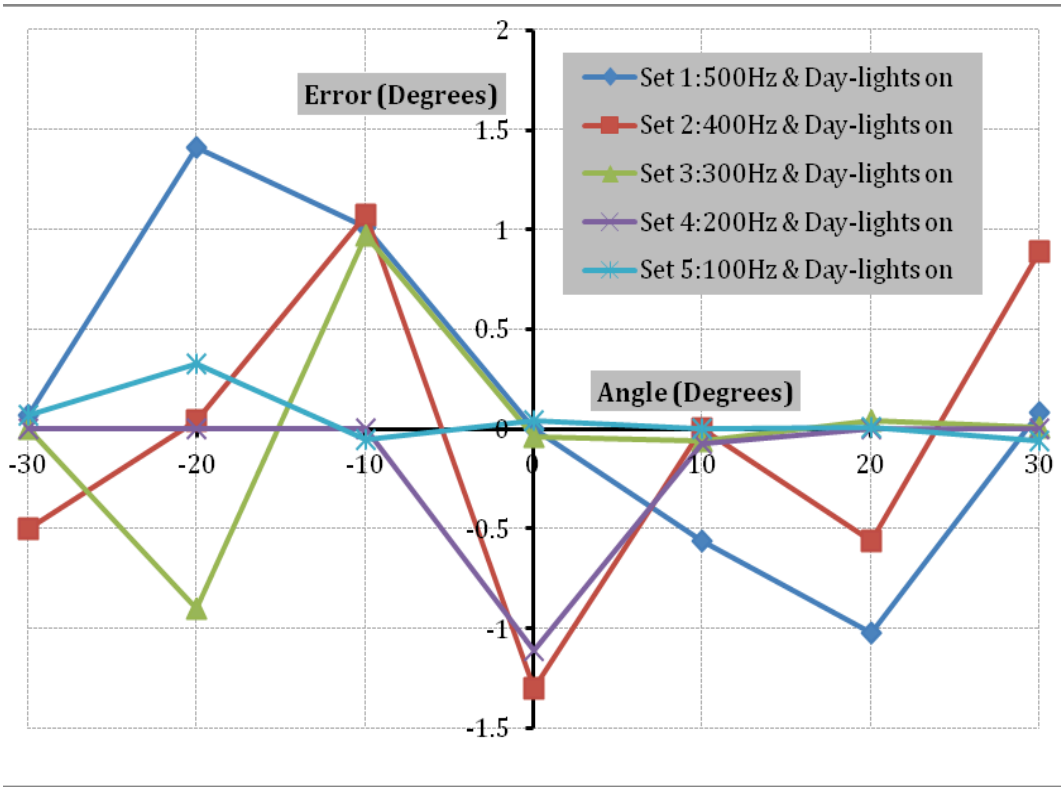

Figure 5.9 ***Response of multimodal neural network integration model error for sample 1:*** *Graphical representation of audio localization error from table 5.8, featuring error obtained during the multimodal localization out of above instances. In this graph the error obtained at the random selected state is plotted.*

In Table 5.8 cells that are empty signify that no output is detected. This results from lack of deterministic states of output stimuli, which can be considered as depression, and will be discussed further in section 5.5. Figure 5.9 is a random selection of inputs selected from the multimodal input space, where audio and visual input is simultaneously transmitted to the integration model. On the graph are plotted the errors that are obtained for inputs which are localized within the range (-30^0, 30^0). From the graph the error of these inputs is in the range (-1.5^0, 1.5^0), while the mean error is less than one degree.

The graph also indicates that as the frequency decreases, the localization improves with error less than $\pm 1^0$. This signifies that the increase in intensity that influences the multimodal localization is effectively adapted in the neural network integration model.

Integration Sample 2

The network was tested by presenting to it both audio and visual data. These samples are a selection of five sets of inputs with frequency ranging from 500 to 100Hz, and fixed visual inputs from a day time (lights on), where the intensity is in the range of (0.5, 1). The multimodal outcomes given in Table 5.9 signify a relatively close localization (error < 2^0) from the input supplied.

Multimodal Error Localization (-30^0)				
Input	**Visual Stimuli**	**Audio Stimuli**	**Multimodal Output**	**Error**
Set 1	-30.85	-26.55	-30.35	0.35
Set 2	-30.37	-28.57	-30.00	0.0
Set 3	-30.03	-29.17	-30.00	0.0
Set 4	-30.54	-29.17	-30.02	0.02
Set 5	-30.04	-29.86	-30.00	0.0

(i)

Multimodal Error Localization (30^0)				
Input	**Visual Stimuli**	**Audio Stimuli**	**Multimodal Output**	**Error**
Set 1	29.36	33.97	30.85	0.85
Set 2	29.70	29.59	30.00	0.0
Set 3	29.30	30.00	30.00	0.0
Set 4	30.02	29.84	30.00	0.0
Set 5	29.87	29.84	30.00	0.0

(vii)

Multimodal Error Localization (-20^0)				
Input	**Visual Stimuli**	**Audio Stimuli**	**Multimodal Output**	**Error**
Set 1	-16.74	-17.34	-17.04	-2.96
Set 2	-16.33	-18.98	-19.00	-1.0
Set 3	-17.76	-19.17	-19.00	-1.0
Set 4	-17.56	-19.89	-20.00	0.0
Set 5	-16.56	-19.32	-19.87	-0.13

(ii)

Multimodal Error Localization (20^0)				
Input	**Visual Stimuli**	**Audio Stimuli**	**Multimodal Output**	**Error**
Set 1	16.95	21.87	20.05	0.05
Set 2	17.56	21.04	20.98	0.98
Set 3	17.56	20.09	20.00	0.0
Set 4	18.56	20.89	20.04	0.04
Set 5	18.98	20.89	20.04	0.04

(vi)

Multimodal Error Localization (-10^0)				
Input	**Visual Stimuli**	**Audio Stimuli**	**Multimodal Output**	**Error**
Set 1	11.01	-8.57	10.26	0.26
Set 2	-10.53	-9.12	10.05	0.05
Set 3	-10.00	-9.12	10.00	0.0
Set 4	-10.62	10.00	10.00	0.0
Set 5	-11.59	10.00	-12.00	2.0

(iii)

Multimodal Error Localization (10^0)				
Input	**Visual Stimuli**	**Audio Stimuli**	**Multimodal Output**	**Error**
Set 1	10.86	10.73	10.00	0.0
Set 2	9.32	11.23	10.56	0.56
Set 3	10.98	10.50	10.00	0.0
Set 4	10.00	10.17	10.00	0.0
Set 5	10.98	10.17	10.00	0.0

(v)

Multimodal Error Localization (0^0)				
Input	**Visual Stimuli**	**Audio Stimuli**	**Multimodal Output**	**Error**
Set 1	2.01	1	0	0.0
Set 2	2.46	0	0	0.0
Set 3	2.46	0	0	0.0
Set 4	2.24	0	0	0.0
Set 5	1.46	0	0.56	0.56

(iv)

Table 5.9 Multimodal localization error chart for sample 2 (multimodal input): *The tables (i)-(vii) depicts the error obtained from multimodal localizations through unimodal data transmitted simultaneously to the agent.*

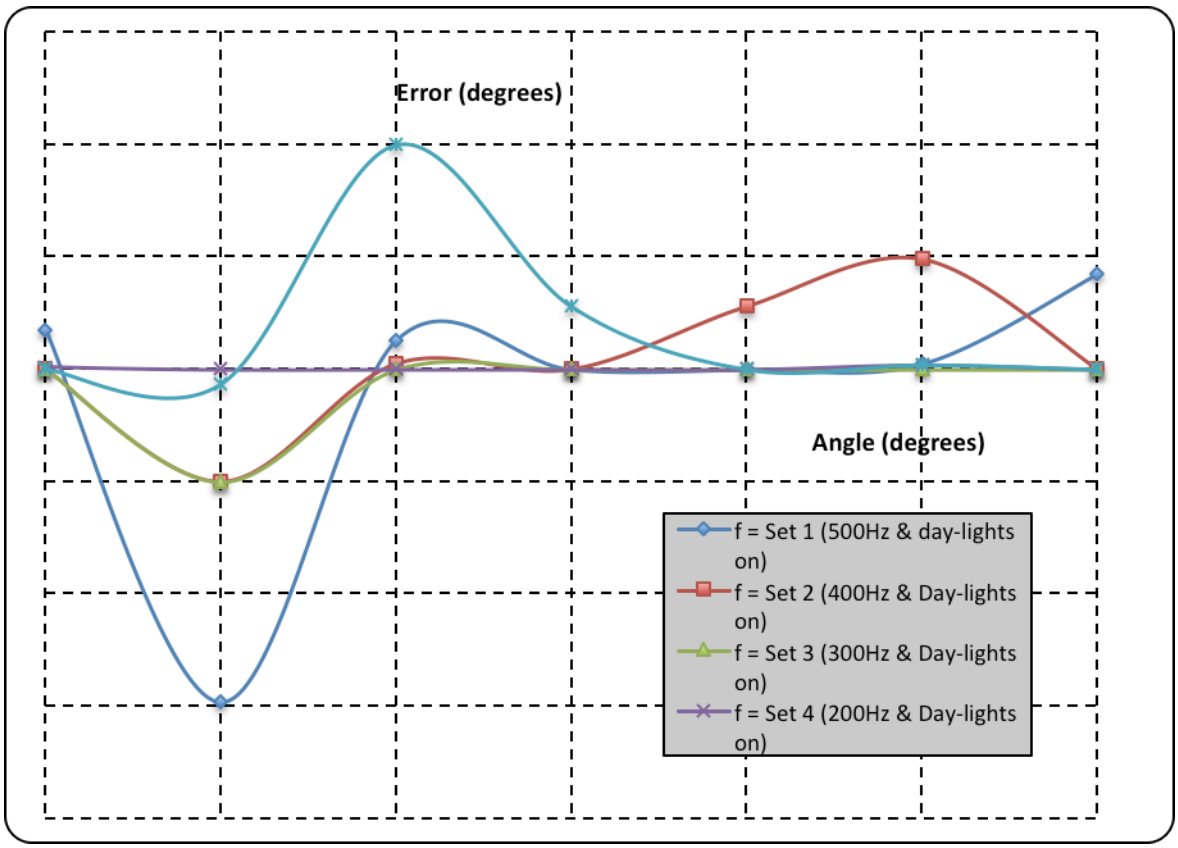

Figure 5.10 ***Response of multimodal neural network integration model error for sample 2:*** *Graphical representation of error from table 5.9, featuring error obtained during the multimodal localization out of above instances. In this graph the error obtained at the random selected state signify the extent of error obtained at particular state. This indicates the efficiency of integration model for multimodal input space.*

Figure 5.10 is a graphical representation of the errors provided in Table 5.9, and indicates the scatter of error obtained during the process of integration for multimodal input cases. The above graph is an example of unimodal stimuli being processed by the integration model, similar to multimodal input. It was observed that most of the error range lies within (-3^0, 2^0), similar to the multimodal input case in previous sample.

Finally, from the integration sample 1 and 2 it was observed that in both samples the maximum error obtained was in the range of (-1.5^0, 1.5^0). Also the concentration of the error was close to the x-axis. This signifies that the integration model is effective with an error less than $\pm 2^0$ for both unimodal and multimodal data samples.

In the next section, the neural network model was subjected to performance tests, based on the output obtained using unimodal and multimodal data. Also, the preliminary experimental analyses that were carried out in the previous chapter are critically evaluated.

5.5 Unimodal Verses Multimodal Performance

From the unimodal experiments for localizing audio and visual stimuli, error levels are obtained for respective cases. During unimodal stimuli analysis it was observed that for auditory experimental data an overall accuracy of 80% is achieved. Similarly, with visual stimuli an accuracy of 90% is achieved, including the variance.

However, the integration model is expected to reach a higher level of accuracy with audio and visual stimuli combined. During the multimodal experimental phase, an estimate of $\pm 5^0$ of variance is considered. This is to comply with the motor commands that are used to generate saccades. During the initial state, though multimodal output is achieved, significant level of error is also generated as shown in figure 5.11.

The data used in the generation of the unimodal verses multimodal performance graph are as follows:

For Audio:

Set 1 = 100Hz, Set 2 = 200Hz, Set 3 = 300Hz, Set 4 = 400Hz, Set 5 = 500Hz

For Visual:

Set 1 = Lights on (Day-Lab), Set 2 = Lights off (Day-Lab), Set 3 = Lights on (Night-Lab), Set 4 = Lights off (Night-Lab), Set 5 = Lights off (Day-Studio)

For Multimodal:

Each set in the multimodal data is the combination of corresponding sets from unimodal audio and visual data, to facilitate a more direct comparison.

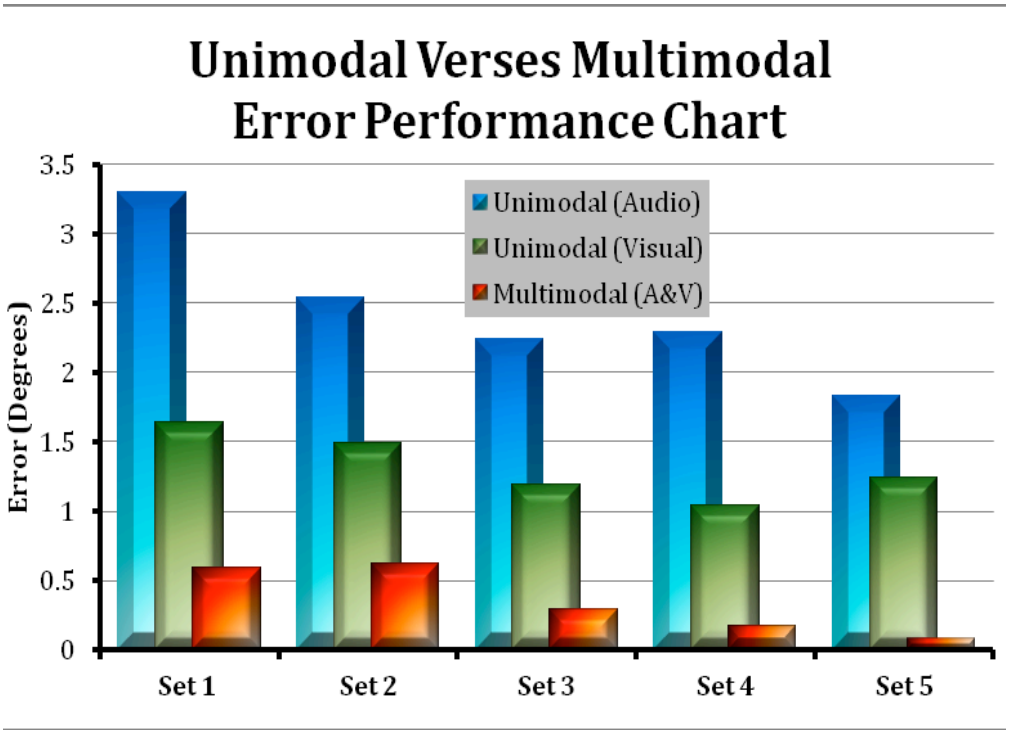

Figure 5.11 ***Error performance chart between unimodal and multimodal integration***: *Error graph of unimodal audio and visual data compared against multimodal integration error.*

The graph represents mean error of unimodal audio and visual data over five different set of inputs against multimodal output generated from the neural network integration model. The selection of input sets is based on increasing order of stimuli strength. From the graph it was evident that the error generated by the multimodal data is significantly less than that of unimodal data. Also there was a gradual decrease in the error, demonstrating the effectiveness of multimodal data. The graph also indicates that multimodal output was more efficient than the unimodal cases with respect to increase in stimuli strength.

In another aspect, the error state observed in figure 5.11 among audio and visual states are varied to greater extent. The audio data set error is significantly greater, compared to visual data sets. This variation could be due to the wide locus (360^0) of audio sensors located at the agent. Due to which the range of stimuli received and localized will entertain intermediate noise causing interference. On the other hand due to narrow visual locus, the chances of interference are comparatively less. But for multimodal case, the overall error is minimized due to the integration aspect that reduces the individual effect, due to the learning aspect induced.

However, it was also observed that all the multimodal output is not completely effective in terms of successful localization of stimuli source, due to the enhancement and depression phenomena. This is demonstrated in the next section.

5.6 Computational versus Neural Network Outcome

In this section, the output generated by both the computational and neural network approaches is discussed. This analysis is carried out in two different ways. Initially, two different samples of the same input are used to generate multimodal output. Later a sample set for a fixed source location such as -30^0 (since variations were observed at this location) was used to generate multimodal results.

In the first instance, a comparison is made between the multimodal outcome of the computational model and the neural network model, described in the previous sections. After careful observation of the output and error generated in the Chapter 4 and Chapter 5, the findings can be summarized as follows:

- **Output:** For a given multimodal input, the output is generated for all cases, irrespective of the strength of the stimuli. This is true of both the computational and neural network models.

- **Error:** For a random selection of inputs, error states are also tabulated in section. In the computational output Table 4.1, it is observed that a maximum error of 23^0 is obtained from the input sample space, which is high. Considering the degree of saccade freedom for object localization (5^0), this error is considered too high. This influences the accuracy of the model.

  On the other hand, for neural network samples the maximum error obtained is -2.96^0. This error is considerably lower when compared with the previous case. Considering the degree of saccade freedom for object localization (5^0), this error is not significant since the ANN integration model error is less than the error degree of saccade freedom for human eye. The model is also much more accurate.

- **Accuracy:** This refers to the correctness of output generated for a given multimodal input. In other words, when there is less than $\pm 2^0$ error obtained from a multimodal output, then it is considered as accurate when compared with computational model. In this context, using the computational model there are few accurate cases. However, with the neural network model, more than half than 75% of the sample set has generated accurate results.

- **Depression and Enhancement:** From the sample space, stimuli exhibiting depression and enhancement phenomena were now considered. With the computational model, out of the accurate outcomes considered from this case, the instances of exhibiting the enhancement phenomena are barely noticeable (the highlighted rows of Table 4.1 and 5.10). This is because the computational algorithm used for integration (weighted arithmetic mean) signifies that the output always lies within the bounds of the given input as discussed in section 4.4.1. However, the chances of depression occurring are high. A case of depression is identified from the Table 4.1 row 25. Even with the presence of maximum intensity levels for either of the stimuli, the

output generated can also be inaccurate if the stimuli are on far apart from one another. This signifies that the output is depressed.

Unlike the computational model, the neural network output has no limitations on the output generated. Hence, the occurrence of enhancement and depression phenomena is due to the stimuli strength. The sample highlighted in red in table 5.17 indicates that the output of that particular state is higher than either of the input stimuli and is correctly identifies the source location. This signifies enhancement in the multimodal output. However, this cannot be completely true, because enhancement and depression phenomena can only be confirmed by measuring the intensity of both input and output stimuli. Based on the increase and decrease of the stimuli intensity, the phenomena can be classified, which is demonstrated in the next chapter.

In another instance, from the available multimodal input space, a fixed set of data was used and is subjected to integration using both the computational and neural network model. Thus, the obtained output was compared, along with error, accuracy, and enhancement and depression phenomena. Table 5.10 shows the input and output for the multimodal test case.

Comparison Table of Multimodal Output						
Visual Stimuli	Visual Intensity	Audio Stimuli	Audio Intensity	Expected Output	Computational Output	Neural Network Output
-30.03	0.90	31.97	0.46	**-30**	**-9.06**	**-30.00**
-16.33	0.82	-19.34	0.44	**-20**	**-17.38**	**-16.33**
-9.45	0.32	10.05	0.41	**-10**	**1.50**	**1.05**
2.46	0.81	6.42	0.41	**0**	**3.79**	**2.40**
10.56	0.14	9.82	0.38	**10**	**10.02**	**10.00**
17.56	0.85	18.96	0.36	**20**	**17.98**	**19.98**
29.7	0.84	30.44	0.35	**30**	**29.92**	**29.92**

Table 5.10 Multimodal input & output table used for test case: *The selected multimodal input stimuli that are used as a unit-test set for verifying performance of the integration model. The output obtained for both computational and neural network models are provided.*

The highlighted orange and blue instances in table 5.10 represent the depression and enhancement in the output, respectively. The error obtained is shown in the table 5.11.

Error Comparison Table of Multimodal Output				
Computational Error	Neural Network Error	Computational Error (%)	Neural Network Error (%)	Variation
-20.94	0.0	69.8%	0%	69.8
-2.62	3.67	13.1%	18.35%	-5.34
11.5	11.05	>100%	>100%	--
3.79	2.40	37.9%	24%	13.9
0.02	0.0	2%	0%	2
2.02	0.02	10.1%	0.1%	10
0.08	0.08	0.2%	0.2%	0
Mean = 5.86	*Mean = 2.46*			

Table 5.11 Error percentage comparison table of multimodal outputs for the test case: *The error percentage generated using the computational and neural network integration models is detailed signifying the variation.*

From the above test case based on the output exhibited in table 5.10 and 5.11 the following observations were made.

- **Output:** Output is generated irrespective of intensity of stimuli. This signifies that the integration models are responsive to at least most of the stimuli.

- **Error:** From the output obtained from both cases, the error present in the output is shown graphically in figure 5.11.

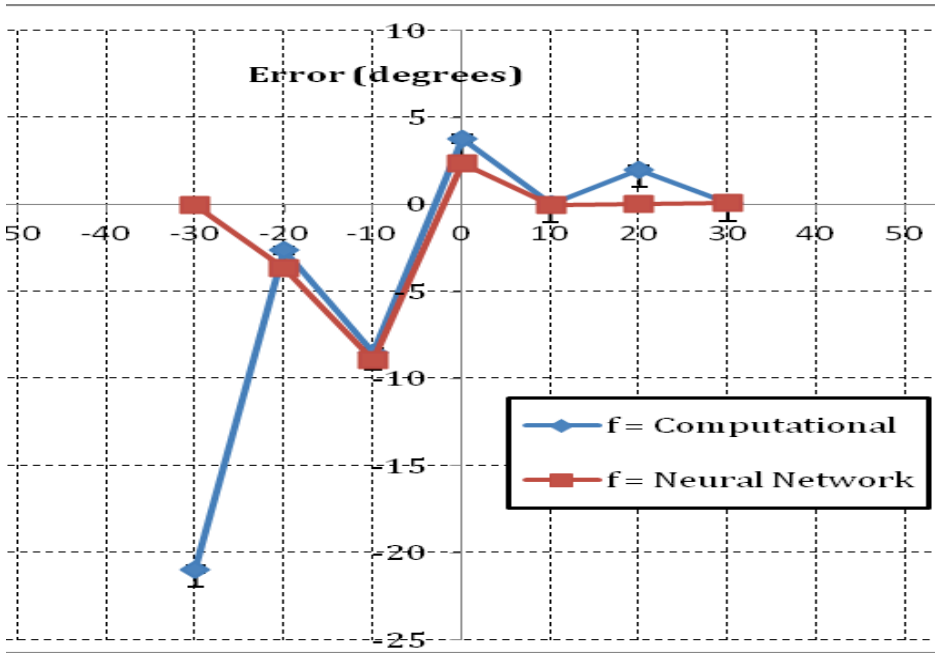

Figure 5.12 ***Error comparison between neural and computational modal outputs for selected input:*** *Graph obtained from projecting the error obtained from integration output of both computational and neural network models*

In both cases, a significant error variation occurred at certain source locations. However, the error with the computational model is particularly pronounced at -30^0. On the other hand, many of the errors appear to be close to x-axis.

- **Accuracy:** Accuracy in this case was measured, taking into account the degree of saccade freedom ($\pm 5^0$) for object localization. From the selected input category, the computational model has successfully achieved 50% accuracy, while the neural network model has achieved 86% accuracy in the generation of output. However, since performance cannot be measured based on limited input space, in the next section a performance analysis is carried out considering the entire stimuli space.

- **Depression and Enhancement:** From the resultant output obtained, in either of the cases the phenomena are observed. As discussed previously, only depression in the output can be observed in the computational model.

The highlighted instance in table 5.20 is an example of stimuli depression. However, due to the huge variation in intensity, it can also be classed as an error unless intensity values are examined. However the next highlighted instance signifies a huge change in the output, irrespective of relative similar intensities. This case is also identified in the neural network model. This instance is a demonstration of depression phenomena.

In the neural network model output, the grey highlighted instance signifies enhancement of the stimuli. The output generated is accurate and also higher then either of the stimuli. This indicates the success of the model in both training and accuracy. However, a later examination of intensity determines the accuracy of the enhancement and depression phenomena.

5.7 Enhancement and Depression Phenomena Evaluation

During the course of the research, variations while integrating audio and visual stimuli were identified and classified accordingly. In this section, a discussion is provided on the enhancement and depression phenomena and their behaviour with respect to the stimuli intensities.

In Chapter 4, the integrated output provided demonstrates the circumstance that lead to enhancement and depression phenomena. In particular, it was observed that the enhancement of the output is obtained in the following case:

- Strong audio and strong visual stimulus (Figure 4.15)

Similarly depression of the output is obtained in the following case:

- Weak audio and weak visual stimulus (Figure 4.16 and 4.17)

In Chapter 5, experimental analysis provided by the integration sample 2 significantly demonstrates the increase in the output (accurate to the required level) resulting from enhancement phenomena. In the output provided in table 5.9,

in most of the cases an enhancement in the output stimuli is observed. However, the highlighted region in the table shows more accurate output due to strong enhancement.

In the computational and neural network model comparison provided in Chapter 5, table 5.10 highlight the enhancement and depression phenomena observed in both the cases. In this example, depression phenomena was demonstrated clearly where the multimodal output was significantly less compared to either of the inputs. However when it comes to accuracy, the above mentioned case was not accurate because the model is expected to generate a null output. Hence the integration model accuracy was reduced (by less than 2^0) in such instances.

In figure 5.12 the phenomena are demonstrated graphically.

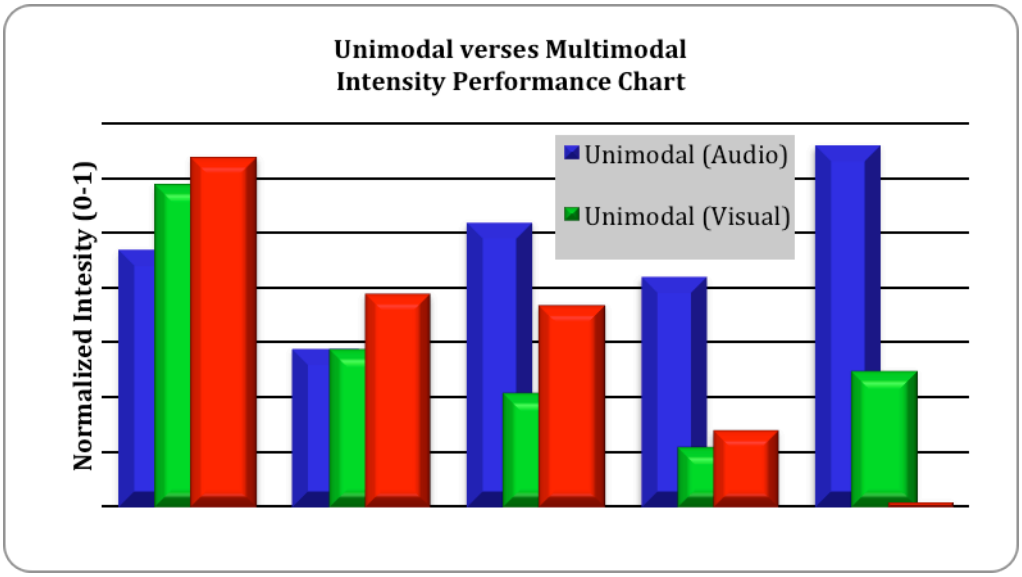

Figure 5.13 ***Intensity graph between unimodal and multimodal output*****:** *Intensity graphs of audio, visual and multimodal output demonstrating intensity verses output.*

In terms of intensity, the graph has generated a mixed pattern for audio and visual cases. In comparison with visual, audio has recorded significant intensity levels. While the visual intensity is concerned it is considerably low. The amount of signal that is taken into account for analyzing the visual stimuli is very sharp and small in many cases (in order to capture the immediate change in visual environment). On

the other hand, multimodal stimuli intensity contains priority-based factors of each of the stimuli and their intensity levels along with localization.

With reference to figure 5.12, in sets 1 and 2, the multimodal intensity is greater than either of the input intensities, signifying the stimuli are from the same direction. However, for the next three sets, there is a gradual drop in the multimodal intensity, even though high unimodal stimuli are recorded. This is due to the stimuli sources being on either side of the reference frame. Set 5 demonstrates depression, where no significant multimodal output is obtained.

Finally, it is concluded that stimuli direction and intensity are the critical factors responsible for the generation of enhancement and depression phenomena. Though the integration output appears to be visually biased, it is actually intensity biased. However, when it comes to action generation, such as saccade generation, priority is given to visual stimuli.

5.8 Summary & Discussion

This chapter describes results that are generated from the audio and visual stimuli integration models developed in chapter 4. In this chapter, both unimodal and multimodal designs are tested using data collected during the initial phase of the project development. This is followed by an analysis detailing the accuracy that was achieved under different conditions, thus quantifying the performance.

Initially unimodal experimental analysis is carried out for both audio and visual data sets. For audio localization, a series of input samples from five different states are fed to the network. Each of these states is verified against the target output and the amount of error generated by each stimulus is tabulated. Generally it is observed that as the frequency of the stimuli increases, the accuracy of localization increases. Similarly with the visual data, where samples of two states (lights-on and lights-off) are provided, it is observed that a visual stimuli increase, multimodal error gets reduced. However, it is observed that as noise in the form of

other interfering light decreases, the localization improves. This is demonstrated with the help of the above-mentioned sample states.

In the next section, multimodal data sets are analyzed in order to determine the success of the neural network integration model. Based on two example instances provided, which obtained from both the unimodal dataset and the multimodal dataset, the output is analyzed for accuracy. Considering the error obtained in both cases, the range lies between (-1.5^0, 1.5^0). This indicates the accuracy of the neural network model in the successful generation of output for both unimodal and multimodal input instances. However, in the next chapter accuracy is demonstrated based on the entire input space to identify the performance of the model.

There was a comparison between the computational model and the neural network model output. Factors such as error, output, accuracy and enhancement and depression phenomena were discussed. Finally it was shown that the neural network model is successful in generating the maximum successful output with greater accuracy and minimal error.

Chapter 6

Conclusions and Recommendations

6.1. Introduction

This chapter provides an overall review of this research project. Conclusions drawn from experimental analysis carried out in previous chapters are used to summarize the research aspects such as research question, project objectives, contribution followed by future recommendations.

This chapter is organized as follows. Section 6.2.1 describes the summary of the project based on the research question. Section 6.2.2 describes the project objectives and how they are achieved during the course of this thesis. Section 6.2.3 describes the contribution and how it is successfully acquired. Later, the chapter is concluded by presenting possible recommendations for enhancing this research into an application.

6.2. Conclusions

6.2.1. Summary of the Project

This section summarizes the main achievements of the research, in terms of the research question and objectives.

The original research question can be re-stated as follows: Is it possible to create a computational architecture inspired by the Superior Colliculus of the mid-brain, using an artificial neural network, which enables the efficient integration of audio and visual stimuli arriving simultaneously at an agent, in order to localize the source of the stimuli? A series of experiments has successfully demonstrated that

the architecture is effective in accurately localizing multimodal stimuli, including those arriving simultaneously at the robot.

In order to achieve this, the research was carried out beyond the original research question, in that the architecture has been shown to be effective at localizing a wide range of input stimuli under different conditions. They include unimodal audio or visual stimuli, with a range of frequencies and intensities. For both the unimodal and the multimodal cases, it has been shown to outperform the purely computational approach tested during the project for comparative purposes.

Along with the research question, the following objectives were defined against which the success of the project can be quantified:

- To understand the biological way of multimodal functionalities of the SC.
- To review the literature on modelling the SC.
- To review different approaches to audio and visual extraction and integration.
- To examine neural network approaches to integration.
- To develop and design an architecture suitable for multimodal integration for a robotic platform.
- To test and evaluate the performance of the architecture.

During the course of the research, all objectives have been successfully achieved. This is explored in detail in the following section.

6.2.2 Objectives Evaluation

Objective:

- To understand the biological way of multimodal functionalities of the SC.

At the beginning of the research, motivated by biological considerations, multisensory integration of audio and visual stimuli within the mammalian nervous system and the brain were investigated within the context of the research question. In particular, the region of the brain called the Superior Colliculus was identified as being responsible for audio and visual stimuli integration. This was explored in detail in order to develop critical and in-depth understanding of the integration process. Chapter 2 of the thesis fulfils this objective. Three distinct areas were investigated, namely biological motivation, neuroscience aspects of the SC, and multimodal behaviour of the SC.

This work established the desirability of stimuli integration, along with the advantages that can be achieved in the context of autonomous intelligent agents that require a source localization capability. A link between the input stimuli and the output motor command, in the form of saccades, was identified that justified the motivation of studying the SC in this project. Neuroscience aspects of the SC described the stimuli flow and structural architecture, which correspond to stimuli transmission and saccade generation.

With regard to multimodal behaviour of the SC, stimuli processing in different regions and the mechanism of integration are discussed. Also, the stimuli combinations explored in this context had provided an insight into the motor commands used for saccade generation. It also provided an understanding of the motor output that is expected from the SC. In addition, stimuli integration was classified and the phenomena of enhancement and depression identified.

Objectives:

- To review the literature on modelling the SC.
- To review different approaches to audio and visual extraction and integration.
- To examine neural network approaches to integration.

The following outcomes were also achieved based upon the literature review:

- A literature review on modelling the multisensory integration based on the SC in the second part of Chapter 2 describes the attempts made in this context. This review helps in identifying the integration process with respect to the required criterion, which is integration for low intensity stimuli.
- In Chapter 2 various approaches that correspond to integration of audio and visual stimuli are reviewed. This review helps in narrowing the approach that is used for the development of the integration model.
- In literature review section of Chapter 2, various computational, probabilistic, neural and applicative approaches are studied to develop a feasible and suitable integration model that can answer the research question. In Chapter 3 a methodology is developed based on the review that can perform audio and visual stimuli integration.

Objectives:

- To develop and design an architecture suitable for multimodal integration for a robotic platform.
- To test and evaluate the performance of the architecture.

The project outcomes that are delivered after the successful development of the integration model are:

- Chapters 3 and 4 describe the design and development of both unimodal and multimodal integration models. During this process, based on the findings of the review chapter, the integration process is designed as a computational model and later developed into a neural network for improved performance. The neural network is trained on a large stimuli space, such that the integration model can be optimized and made more effective with respect to the generation of output i.e., saccade generation.
- Evaluation is critical for the success of any model. However, in this project, a self evaluation criterion was adopted. This criterion evaluates the integration model in two phases. Initially, it is tested with unimodal data and

multimodal data and the output is evaluated. Secondly, it is compared to the computational model using multimodal data. The experimental findings published in Chapters 4 and 5 explicitly signify the success of the integration model in the respective states and confirm the success of the architecture as a multimodal integration model.

6.2.3. Summary of Contribution

The main novelty is the architecture and its ability to handle low intensity audio and visual stimuli and generate efficient and accurate integrated output. During the process, the model also contributes to research into successful reduction of audio and visual dimensional space into an integrated single space.

- The Superior Colliculus inspired dual layered architecture has been developed, where each layer has preprocessed localization data that arrives from corresponding layers to the integration layer simultaneously. This architecture is implemented using a RBF based neural network platform. The model is trained to integrate audio and visual stimuli and generate an integrated output based on the intensity levels of the stimuli. The integration model experimental outcome described in Chapter 4 signifies the success of the proposed architecture. Similarly, the experimental analysis provided in Chapter 5 has demonstrated the performance of the integration model with respect to variable stimuli intensity. This signifies that the novelty of the architecture for successful adaptation towards low-level stimuli is achieved.

- This research is an attempt to investigate multimodal stimuli integration behaviour. During the process, apart from achieving the project objectives, the research has successfully integrated audio and visual stimuli into a single command that is used to generate saccades. On the other hand, this research can also be referred as solution for a dimensionality reduction problem in multimodal context. Transformation of two-dimensional stimuli into a single dimension control signal is accurately achieved using the neural network training process. Therefore this research has contributed to

the successful reduction of audio and visual dimensional space into an integrated single space.

6.3. Recommendations for future work

There are a number of recommendations made as a follow-up to this research. Possible directions are given below:

- It would be useful to extend the scope of the integrated output. This project is intended for generation of horizontal saccade only. However, the introduction of a vertical dimension (level difference) would help in the simultaneous detection of more than one stimulus out of the horizontal plane. This could be used to localize in a two dimensional space. However, the addition of a vertical direction would add complexity and would require different hardware and software solutions. For example audio localization with the current set up only configured in one dimension.
- Another extension of the project could be in the variation of distance between the source and agent. Initially this aspect is overcome by the approximation function used for localization. This function is estimated based on the distance as a variable. However, for future enhancement the function can be extended to operate for any kind of distances. But for such cases, a different kind of experimental setup has to be designed to satisfy the variable distance between source and agent mechanism.
- An important enhancement would be to extend the scope of the integration mechanism by adapting it to all types of input stimuli. One major objective of the project is to investigate the behaviour of the integration stimuli i.e. enhancement and depression phenomena. However, when it comes to a more realistic application:

- Visual stimuli localization becomes more complex, if object identification along with color detection is used, then the chances of recognizing the object increases.
- In the case of audio, rather than simple activation detection, if the sound is distinguished based on strength of the stimuli, along with their time of arrival, then the chances of a more significant audio role in the integration process can be increased. This would improve the overall localization performance.
- The above suggestions can be adapted either before or after integration, depending on the requirements. However if they are adapted before integration, there could be an increase in the time delay between stimuli generation and integration. Hence post-integration is suggested. By doing so, the final integrated output generated can be recognized and the corresponding action can be taken.

- A practical recommendation could be to transform the model into an application that can be used to alert the driver of a vehicle to approaching traffic. When it comes to development of a commercial application such as a driver assistance system, it is necessary that it should be both adaptive as well as effective. For such applications it is critical to have highest possible accuracy. Since the application involves risk to the user, it is suggested that training of the network should be made more efficient by using a bigger training set.
- Another potential application is a self-driven camera (equipped with a mic) that can be used to localize any stimuli within its focus, and later can track the stimuli in the case of a moving source. This concept could also be used in social robot scenario, where a robot interacts with people in public in places such as museums, and hospitals and schools.

Overall, this research project is considered a success in answering the research question and the objectives have been achieved. The research is still in its development state, as far as a reliable application in a real scenario is concerned. However, many of the ideas explored can provide a firm foundation for ongoing and future research in this area.

References

A

Anastasio, T. J., Patton, P. E., Belkacem-Baussaid, K. (2000) "*Using Bayes' Rule to Model Multisensory Enhancement in the Superior Colliculus*". Neural Computation, 12, pp. 1165 – 1187.

Armingol, J. M., Escalera, A., Hilario, C., Collado, J. M., Carrasco, J. P., Flores, M. J., Postor, J. M. and Rodriguez, F. J. (2007) "*IVVI: Intelligent vehicle based on visual information*". Robotics and Autonomous Systems, 55, pp. 904 – 916.

Asif Ullah Khan., Bandopadhyaya T, K., and Sharma, S. (2009) "*Classification of Stocks Using Self Organization Map*". International Journal of Soft Computing Applications, 4, ISSN: 1453-2277, pp. 19 – 24.

B

Beauchamp, M. S., Lee, K. E., Argall, B. D. and Martin, A. (2004) "*Integration of Auditory and Visual Information about Objects in Superior Temporal Sulcus*". Neuron (Cell Press), 41, pp. 809 – 823.

Bellman, R. E. and Rand Corporation. (1957) "*Dynamic Programming*". Princeton University Press. ISBN: 069107951X.

Bennewitz, M., Faber, F., Joho, D., Schreiber, M. and Behnke, S. (2005) "*Integrating Vision and Speech for Conversations with Multiple Persons*". Proceedings of International Conference on Intelligent Robots and System (IROS).

Benediktsson, J. A., Swain, P. H. and Ersoy, O. K. (1990) "*Neural Network Approaches Versus Statistical Methods in Classification of Multisource*

Remote Sensing Data". IEEE Transactions on Geoscience and Remote Sensing, 28(4), pp. 540 – 552.

Bors, A. G. (2001) "*Introduction to the Radial Basis Function (RBF) Networks*". *Online Symposium for Electronics Engineers,* DSP Algorithms: Multimedia, 1(1), pp. 1-7.

Bors, A. G. and Pitas I. (1996) "*Median radial basis functions neural network*". IEEE transactions on Neural Networks, 7(6), pp. 1351 – 1364.

Broomhead, D.S. and Lowe D. (1988) "*Multivariable functional interpolation and adaptive networks*". Complex Systems, 2, pp. 321 – 355.

C

Calvert, G. A. and Thesen, T. (2004) "*Multisensory integration: methodological approaches and emerging principles in the human brain*". Journal of Physiology Paris, 98, Pp. 191 – 205.

Casey, M. C., and Pavlou, A. (2008) "*A Behavioural Model of Sensory Alignment in the Superficial and Deep Layers of the Superior Colliculus*". Proceeding of International Joint Conference on Neural Networks (IJCNN'08), pp. 2750 – 2755.

Casey, M. C. (2009) "*Modelling the Sensory Hierarchy: From Gaze Shifts to Emotions*". Artificial Intelligence and Natural Computation Seminars, Birmingham.

Chan, V. (2009) "*Audio-visual sensor fusion for object localization*". Institute of Neuromorphic Engineer, Article in ine-web, Doi:10.2417/1200906.1640. (Cited on 24/08/2010).

Cheshire Engineering Corporation. (2003) "*Neural Network Technology*". Neuralyst, User's guide, Chapter-3.

Chinmaya Mission. (1983) "*Symbolism in Hinduism"* Chinmaya Mission Publications, Mumbai, INDIA, ISBN: 9788175971493. Pages 338 and 339.

Coen, M. H. (2001) "*Multimodal Integration – A Biological View*". Proceedings of the 15th International Joint Conference on Artificial Intelligence (IJCAI'01), pp. 1414 – 1424.

Cucchiara, R. (2005), "*Multimedia Surveillance Systems*". 3rd International Workshop on Video Surveillance and Sensor Networks (VSSN'05), Singapore, pp. 3 – 10, ISBN: 1-59593-242-92.

Cuppini, C., Magosso, E., Serino A., Pellegrino, G. D. and Ursino, M. (2007) "*A Neural Network for the Analysis of Multisensory Integration in the Superior Colliculus*". Proceedings of Artificial Neural Networks - ICANN 2007, Part 11, 4669, pp. 9 – 11.

Cutsuridis, V., Smyrnis, N., Evdokimidis, I. and Perantonis, S. (2007) "*A Neural Model of Ddecision-making by the Superior Colliculus in an Anti-saccade task*". Neural Networks, 20, pp.690 – 704.

E

Elhilali, M. and Shamma, S. (2006) "*A biologically-Inspired Approach to the Cocktail Party Problem"*. IEEE International Conference on Acoustics, Speech and Signal Processing, 5, pp. 637 – 640.

F

Funk, N. (2003) "A Study of the Kalman Filter applied to Visual Tracking". Edmonton, 7 December.

G

Gilbert, C. and Kuenen, L. P. S. (2008) "*Multimodal Integration: Visual Cues Help Odour-Seeking Fruit Flies*". Current Biology, 18, pp. 295 – 297.

H

Hanheide, M., Bauckhage, C. and Sagerer, G. (2005) "*Combining Environmental Cues & Head Gestures to Interact with Wearable Devices*". Proceedings of 7th International Conference on Multimodal Interfaces, pp. 25 – 31.

Harremoes, P. (2010) "*Information Theory for angular data*". IEEE Information Theory Workshop, ITW2010, pp. 1 – 5.

Hawkins, H. L., McMullen, T. A., Popper, A. N. and Fay, R. R. (1996) "*Auditory Computation*". Springer Handbook of Auditory Research, pp. 334 – 336.

Holmes, N. P. (2009) "*The Principle of Inverse Effectiveness in Multisensory Integration: Some Statistical Considerations*". Brain Topography, 21(3 – 4), pp. 168 – 176.

Huwel, S., Wrede, B. and Sagerer, G. (2006) "*Robust Speech Understanding for Multi-Modal Human-Robot Communication*". 15th IEEE International Symposium on Robot and Human Interactive Communication (RO-MAN 06), UK, pp. 45 – 50.

J

Jolly, K.G., Ravindran, K.P., Vijayakumar, R. and Sreerama, R. K. (2006) "*Intelligent decision making in multi-agent robot soccer system through compounded artificial neural networks*". Robotics and Autonomous Systems, 55, pp. 589 – 596.

Juan, C.H,, Muggleton, N.G., Tzeng, O.J.L., Hung, D.L., Cowey, A. and Walsh, V. (2008) "*Segregation of CIsual Selection and Saccades in Human*". Cerebral Cortex, 18(10), pp. 2410 – 2415.

K

King, A.J. (2004). "*The Superior Colliculus*". Current Biology, 14(9), pp. R335 – R338.

Kohonen, T. (1982) "Self-Organized formation of Topographical correct feature Maps". Biological Cybernetics, 43, pp. 59 – 69.

Koide, Y., Kanda. T., Sumi, Y., Kogure, K. and Ishiguro, H. (2004) *"An approach to Integrating an interactive guide robot with ubiquitous sensors"*. Intelligent Robots and System, IROS'04 Proceedings, 3, pp. 2500 – 2505.

Kyriakos, V. and Jurgen, A. (2007), "*A Biologically inspired spiking neural network for sound source lateralization*". IEEE transactions on Neural Networks, 18(6), pp. 1785 – 1799.

L

Landis, M. F., Crassidis, J. L. and Cheng, Y. (2005) "*Nonlinear Attitude Filtering Methods*". Systems Engineering, Publisher: Citeseer, 30(August), pp. 12 – 28.

Londhe, S. (2008) *"Symbolism in Hinduism"*. A Tribute to Hinduism, Pragun Publications, INDIA, ISBN: 8189920669.

M

Massaro, D. W. (2004) "*A Framework for Evaluating Multimodal integration by Humans and A Role for Embodied Conversational Agents*". In Proceedings of the 6th International Conference on Mulitmodal Interfaces (ICMI'04), pp. 24 – 31.

McAlpine, D. and Grothe, B. (2003) "*Sound localization and delay lines – do mammals fit the model?*". Trends in Neuroscience, 26(7), pp. 347 – 350.

Meredith, M. A. and Stein, B. E. (1986a) "*Visual, auditory and somatosensory convergence on cells in superior colliculus results in multisensory integration*". J. Neurophysiol. 56, pp. 640 – 662.

MobileRobots Inc. (2006) "Performance PeopleBot Operations Manual". MobileRobots Exclusive Advanced Robot Control & Operations Software, Version 3.

Moody J. (1989) "*Fast learning in networks of locally-tuned processing units*". Neural Computation, 1, pp. 281 – 294.

Murray, J., Erwin, H., Wermter, S. (2005) "*A Hybrid Architecture using Cross-Correlation and Recurrent Neural Networks for Acoustic Tracking in Robots"*. Biomimetic Neural Learning for Intelligent Robots, pp. 55-73.

P

Palanivel, S. and Yegnanarayana, B. (2008) "*Multimodal person authentication using speech, face and visual speech*". Computer Vision and Image Understanding (IEEE), 109, pp. 44-55.

Paleari, M. and Lisetti, C. L. (2006) "*Toward Multimodal Fusion of Affective Cues*". Proceedings of International Conference on Human Computer Multimodality HCM'06, pp. 99 – 108.

Pang, K. (2003) "*Self Organizing Maps*". Neural Networks, [Online] (Cited: 21/10/2011).

Park, F. C. and Bahram, R. (1997) "*Smooth Invariant Interpolation of Rotations*". ACM Transactions on Graphics, 16(3), pp. 277 – 295.

Pavon, J., Gomez-Sanz, J., Fernandez-Caballero, A. and Valencia-Jimenez, J. J. (2007) "*Development of intelligent multisensor surveillance systems with agents*". Robotics and Autonomous Systems, 55, Pp. 892 – 903.

Powell, M. J. D. (1987) "*Radial basis functions for multivariable interpolation: a review*". Algorithms for approximation, Clarendon Press, New York, ISBN: 0-19-853612-7.

Q

Quaia, C., Lefevre, P. and Optican, L. M. (1999) "*Model of the Control of Saccades by Superior Colliculus and Cerebellum*". Journal of Neurophysiology, 82(2), pp. 999 – 1018.

S

Schauer, C. and Gross, H. M. (2004) "*Design and Optimization of Amari Neural Fields for Early Auditory – Visual Integration*". Proc. Int. Joint Conference on Neural Networks (IJCNN), Budapest, pp.2523 – 2528.

Smith, L. (2003) "*An Introduction to Neural Networks*". Centre for Cognitive and Computational Neursocience, University of Stirling, (Cited: 20/10/2011).

Srinivas, C. (1993) "*Visual disorders in ancient Indian science (interpretative study)*". Bull Indian Inst Hist Med Hyderabad, 23(2), pp. 101-111.

Stanford, T. R., Stein, B. E. and Quessy, S. (2005) "*Evaluating the Operations Underlying Multisensory Integration in the Cat Superior Colliculus*". The Journal of Neuroscience, 25(28), pp. 6499 – 6508.

Stein, B. E., Huneycutt, W. S. and Meredith, M. A. (1988) "*Neurons and behaviour: the same rules of multisensory integration apply*", Brain Research, 488, pp. 355 – 358.

Stein, B. E., Meredith, M. A., Huneycutt, W. S. and McDade, L. (1989) "*Behavioral indices of multisensory integration: orientation to visual cues is affected by auditory stimuli*", Cognitive Neuroscience, 1, pp. 12 – 24.

Stein, B. E. and Meredith, M. A. (1993) "*The Merging of the Senses*", Cognitive Neuroscience Series. MIT Press, Cambridge.

Stergiou, C. and Siganos, D. (2007) "*Neural Networks*". A report on introduction to Artificial Neural Networks. Vol. 4 [Online]. (Cited: 10 August 2010).

Stiefelhagen, R. (2002) "*Tracking focus of attention in meetings*", International conference on Multimodal Interfaces (IEEE), Pittsburgh, PA. pp. 273 – 280.

Stork, D. G., Wolff, G. and Levine, E. (1992) "*Neural Network lip reading system for improved speech recognition*". Proceedings of International Joint Conference on Neural Networks (IJCNN'92), 2, pp. 289 – 295.

T

Trappenberg, T. (1998) "*A Model of the Superior Colliculus with Competing and Spiking Neurons*". BSIS Technical Report, No. 98-3.

Trifa, V. M., Koene, A., Moren, J. and Cheng, G. (2007) "*Real-time acoustic source localization in noisy environments for human-robot multimodal interaction*". Proceedings of RO-MAN 2007 (IEEE International Symposium on Robot & Human Interactive Communication), Korea, pp. 393 – 398.

W

Waxman, S. G. (2009) Clinical Neuroanatomy 26th Edition. McGraw-Hill Medical Publisher, ISBN: 00771603999.

Wilhelm, T., Bohme, H. J. And Gross, H. M. (2004) "*A multi-modal system for tracking and analyzing faces on a mobile robot*". Robotics and Autonomous Systems, 48(1), pp. 31 – 40.

Wolf, J. C. and Bugmann, G. (2006) "*Linking Speech and Gesture in Multimodal Instruction Systems*". The 15th IEEE International Symposium on Robot and Human Interactive Communication (RO-MAN 06), UK.

X

Xiuju Fu and Lipo Wang. (2003) "*Data Dimensionality Reduction With Application to Simplifying RBF Neural Structure and Improving Classification Performance*", IEEE Transactions on Systems, Man and Cybernetics – Part B: Cybernetics, 33(3), pp. 399 – 409.

Y

Yavuz, H. (2007) "*An integrated approach to the conceptual design and development of an intelligent autonomous mobile robot*". Robotics and Autonomous Systems, 55, pp. 498 – 512.

Z

Zou, X. and Bhanu, B. (2005) "*Tracking humans using Multi-modal Fusion*". IEEE Conference on Computer Vision and Pattern Recognition (CVPR'05), pp. 4 – 4.

Appendix – A

Importance of audio and visual sensors for interaction

Sensory organs in human beings play a vital role when it comes to interaction. Out of them, eyes and ears responsible for audio and visual stimuli processing are considered critical for this research. In the context of vision a Sanskrit (ancient Indian language) saying goes like *"*Sarvendriyanam Nayanam Pradhanam*". According to Ayurveda (ancient Indian medical practice) 'the eyes are the first among different organs of the body when it comes to interacting with the external world' (Srinivas, 1993). In the context of eternal sound which describes the importance of audio stimuli over living beings a Sanskrit saying goes as "**Sisurvethi Pasurvethi…Vethi gaana rasam Phanihi*". Means music (sound) can be felt and enjoyed by kids, animals and even snakes alike. In other words, an audible sound stimulus was always felt effective in grabbing attention when it comes to interaction with kids, animals (mammals) and even animals without ears. According to Sanskrit the mystic sound of 'AUM' was the first generated audio stimuli that echoed the universe in the form of primal energy, which later developed various sounds. (Londhe, 2008) In the book of Symbolism in Hinduism by Chinmaya Mission, page 338 and 339 describes in details about the importance of audio stimuli in both music and life when it comes to interaction (Chinmaya Mission, 1983).

This thesis is the advanced research work carried out to investigate the sound and visual stimuli and their integration based on biological inspiration of the Superior Colliculus and to develop a model that can perform integration mechanism effectively.

'*'--- *are the English version of Sanskrit quotes that are explained with the literal and ethical meaning in a philosophical way which signifies the importance of visual and audio sensors for interaction with environment.*

Appendix – B
List of Publications

Three papers have been published for presenting the initial experimental results and the research concepts developed during the project.

Ravulakollu, K., Knowles, M., Liu, J. and Wermter, S. (2009) "*Towards Computational Modelling of Neural Multimodal Integration Based on the Superior Colliculus Concept*". Innovations in Neural Information Paradigms and Applications, Pp. 269~291, ISBN: 978-3-642-04002-3.

Ravulakollu, K., Erwin, H. and Burn, K. (2011) "Improving Robot-Human Communication by Integrating Visual Attention and Auditory Localization Using a Biologically Inspired Model of Superior Colliculus". Journal of Advanced Material Research, 403 – 408, Pp. 4711 – 4717.

Ravulakollu, K., Liu, J. and Burn, K. (2012) "Stimuli Localization: An Integration Methodology Inspired by the Superior Colliculus for Audio and Visual Attention". Journal of Procedia Computer Science, 13, Pp. 31 – 42.

Towards Computational Modelling of Neural Multimodal Integration based on the Superior Colliculus Concept

Kiran Ravulakollu, Michael Knowles, Jindong Liu and Stefan Wermter
University of Sunderland
Centre for Hybrid Intelligent Systems
Department of Computing, FAS
St Peters Way, Sunderland, SR6 0DD, UK
www.his.sunderland.ac.uk

Abstract

Information processing and responding to sensory input with appropriate actions are among the most important capabilities of the brain and the brain has specific areas that deal with auditory or visual processing. The auditory information is sent first to the cochlea, then to the inferior colliculus area and then later to the auditory cortex where it is further processed so that then eyes, head or both can be turned towards an object or location in response. The visual information is processed in the retina, various subsequent nuclei and then the visual cortex before again actions can be performed. However, how is this information integrated and what is the effect of auditory and visual stimuli arriving at the same time or at different times? Which information is processed when and what are the responses for multimodal stimuli? *Multimodal integration is first performed in the Superior Colliculus, located in a subcortical part of the midbrain. In this chapter we will focus on this first level of multimodal integration, outline various approaches of modelling the superior colliculus, and suggest a model of multimodal integration of visual and auditory information.*

1. Introduction and Motivation

The Superior Colliculus (SC) is a small part of the human brain that is responsible for the multimodal integration of sensory information. In the deep layers of the SC integration takes place among auditory, visual and somatosensory stimuli. Very few types of neurons, such as burst, build up and fixation neurons are responsible for this behaviour [4, 10]. By studying these neurons and their firing rates, integration can be successfully explored. The integration that takes place in the SC is an important phenomenon to study because it deals with different strengths of different stimuli arriving at different times and how the actions based on them are generated. There is evidence that when two different stimuli are received at the same time, the stronger signal influences the response accordingly based on Enhancement and Depression Criteria [3]. A better understanding of multimodal integration in the SC not only helps in exploring the properties of the brain, but also provides indications for building novel bio-inspired computational or robotics models.

Multimodal integration allows humans and animals to perform under difficult, potentially noisy auditory or visual stimulus conditions. In the human brain, the Superior Colliculus is the first region that provides this multimodal integration [23]. The deep layers of the Superior Colliculus integrate multisensory inputs and generate directional information that can be used to identify the source of the input information [20]. The SC uses visual and auditory information for directing the eyes using saccades, that is horizontal eye movements which direct the eyes to the location of the object which generated the stimulus. Before integrating the different modalities the individual stimuli are preprocessed in separate auditory and visual pathways. Preprocessed visual and auditory stimuli can then be used to integrate the stimuli in the deep layers of the SC and eventually generate responses based on the multimodal input.

The types of saccades can be classified in different ways [39] as shown in Figure 1. Most saccades are reflexive and try to identify the point of interest in the visual field which has moved due to the previous visual frame changing to the current one [20]. If no point of interest is found in the visual field, auditory information can be used to identify a source. Saccades are primary actions which in some cases are autonomous and are carried out without conscious processing in the brain. When there is insufficient information to determine the source based on a single modality, the SC uses multimodal integration to determine the output. Saccades are the first actions taken as a result of receiving enough visual and auditory stimuli.